THEORY OF HIGH TEMPERATURE SPIN DYNAMICS

Boris Veniaminovich Fine, Ph.D.
Department of Physics
University of Illinois at Urbana-Champaign, 2000
Anthony J. Leggett / Alexander V. Sokol , Advisors

The problems of high-temperature spin dynamics have practical applications in the fields of nuclear magnetic resonance and inelastic neutron scattering. At the same time. those problems represent an important limit for the study of strongly interacting many-body systems.

In this thesis, we consider systems of interacting spins—both classical and quantum—and develop the quantitative theory of the time-dependent correlation functions characterizing the high temperature spin dynamics.

The original results presented in this thesis include: (I) model-independent analysis of the long-time behavior of the correlation functions of interest, which reveals that that behavior has a universal functional form; (II) model for approximate calculations of the correlation functions of interest; (III) extensive simulations of the classical spin systems performed in order to test the long-time analysis and the approximation technique.

To my parents.

Acknowledgments

The research project presented in this thesis has been started in 1995 under the supervision and with the energetic support of Prof. Alexander Sokol. I am deeply grateful to Sasha for valuable discussions and for many other things he has done to help me.

Since September of 1997, the supervision of my work has been taken over by Prof. Anthony Leggett, from whom I have also enjoyed continuing support. It is my pleasure to thank Tony for numerous discussions, his patient explanations on the subjects related and not related to the scope of this thesis, and his help in editing my manuscripts.

I should also mention that during my work on this project, I have enjoyed, probably, an unusual degree of independence in my research, for which I am very grateful to both Sasha and Tony.

Another impetus for my work came from the enthusiastic encouragement of Prof. Charles Slichter. It is impossible to overestimate the importance of such encouragement, especially when it comes from a renowned scientist to a graduate student. I would also like to thank Charlie for his advice to focus on the problem of NMR free induction decay: The entire content of this thesis grew from my analysis of that problem.

My initial interest in the theoretical issues discussed in this thesis dates back to my years at Moscow Institute of Physics and Technology, where I was introduced to the subject of NMR relaxation by my former research advisor Dr. Vladimir Marchenko, whom I would like to thank for that.

My writings have been much improved by the patient editing of Celia Elliott, and by comments from Dr. Revaz Ramazashvili. I also thank Dr. Klaus Fabricius for supplying me with some of his unpublished numerical results.

Finally, it is an overwhelming pleasure to mention my wife Ada and my son Isaac, who have made an important contribution to this work by making my life enjoyable all that time.

This work has been supported in part from the following sources: the Sloan Fellowship grant of Prof. Alexander Sokol; the MacArthur Chair endowed by the John D. and Catherine T. MacArthur Foundation at the University of Illinois; the Harry Drickamer Research Fellowship from the University of Illinois.

Table of Contents

Chapters

List of Tables

List of Figures

1 Description of the problem

1.1 Introduction

One of the theoretical challenges associated with strongly interacting many-body systems is how to calculate the fast relaxation that takes place on a timescale of the order of the dynamic memory time of individual particles. The challenge here always comes from the simple fact that generic problems of this kind do not have enough small parameters to be solved in a controllable approximation.

In this thesis, we consider systems of interacting spins—both classical and quantum—and develop a theory of the time-dependent infinite temperature correlation functions. The calculation of the correlation functions of our choice belongs to the general class of the fast relaxation problems, because these correlation functions decay on the timescale of the individual spin motion.

A few words about our motivation: Why have we chosen to treat the spin systems? — and why at infinite temperature? The answers to these questions have two closely related aspects — "applied" and "fundamental."

The practical applications of the theory we are pursuing lie primarily in the field of nuclear magnetic resonance (NMR), where the experimental temperatures are almost always much greater than the typical energy of a nuclear spin. The description of the spin-spin relaxation in the solid state NMR is usually formulated in terms of infinite temperature spin correlation functions. The unsettling truth about this subject is that, at present, the accuracy of the NMR experiments measuring the spin-spin relaxation frequently surpasses the accuracy of the first principles theories aimed at calculating the measured quantities.

At the same time, the demand for an adequate theory of the spin-spin relaxation is particularly strong, because NMR is an important source of the microscopic information in condensed matter physics, chemistry and biology. For all those applications, it is a ques-

tion of practical importance how to calculate the result of measurements directly from the microscopic hypothesis.

Another field which uses infinite temperature spin correlation functions is inelastic magnetic neutron scattering. At high temperatures, that technique is not as accurate as NMR, but it can access a wider variety of spin correlation functions.

The fundamental aspect of the spin problems is related to the generic nature of the difficulties we face while trying to solve them. It is,therefore, our hope that the progress in the theory of the many-body spin dynamics can have important implications for similar problems in other fields.

One of the advantages of spin systems in comparison with systems having the translational degrees of freedom is that spin systems are better amenable to numerical investigations, and, therefore, any quantitative theory of spin dynamics can be extensively tested numerically. In addition, the NMR experiments in calcium fluoride (CaF_2), for which the internuclear spin-spin interaction is known from the first principles, provide exceptionally accurate tests of the theory in the regime not accessible to the numerics.

Another important advantage of the spin systems is the possibility of defining the infinite temperature.

In order to illustrate the importance of that limit, we first note that the difficulties associated with the description of the microscopic dynamics are, typically, less severe at low temperatures. The low temperature paradigm is a dilute gas of excitations (eg. magnons, for spin systems). For such a gas, the Boltzmann kinetic equation provides a well-justified description.

At higher temperatures, the dynamics of the system is less dominated by the collective particle motion in the form of propagating waves and more by the motion of individual particles. It is the latter motion that represents a major difficulty at finite temperatures: In condensed systems, each particle, while moving, interacts continuously and simultaneously

with many other particles.

A straightforward way to investigate the properties of the individual particle motion would be to go to the infinite temperature limit. The infinite temperature limit leaves us only with non-trivial dynamics — in contrast to finite temperature problems that may exhibit interference between non-trivial dynamics and non-trivial equilibrium. It is, however, problematic to define the infinite temperature limit for condensed systems with translational degrees of freedom, because the kinetic energy of particles in these systems is not bounded from above. At the same time, the definition of infinite temperature equilibrium in spin systems is very simple: it is the state where all possible orientations of every spin have equal probability.

Finally, we would like to mention that, from a wider perspective, the quantitative description of the fast relaxation should be the first step in solving the more general problem of deriving the statistical description of the many-body systems from the microscopic dynamics. For the latter problem, it is thought that the concept of microscopic chaos has a role to play. In this context, an important result of the present work is that we show how to exploit the assumption of microscopic chaos to extract non-trivial long-time properties of the spin correlation functions.

1.2 General formulation

The general goal of the present work is to understand and to approximate the behavior of the infinite temperature correlation functions defined on an infinite spin lattice as:

$$G(t) = \frac{\langle\ S_0^\mu(t)\ \sum_n \cos(\boldsymbol{q}\cdot\boldsymbol{r}_n)\ S_n^\mu(0)\ \rangle}{\langle\ S_0^\mu(0)\ \sum_n \cos(\boldsymbol{q}\cdot\boldsymbol{r}_n)\ S_n^\mu(0)\ \rangle}, \tag{1.1}$$

where S_n^μ is either the classical projection or the quantum spin operator representing the μth (x,y or z) spin component on the nth lattice site; $\boldsymbol{r}_n$ is the translation vector between the zeroth and the nth sites; and $\boldsymbol{q}$ is a wave vector corresponding to a spatial period com-

mensurate with the lattice periodicity. The notation $\langle ... \rangle$ implies either a classical ensemble average or a quantum-mechanical trace. The lattice can have any Bravais structure in one, two or three dimensions. Each spin on the lattice interacts with a finite number of neighbors according to the Hamiltonian

$$\mathcal{H} = \sum_{k<n} [J^x_{kn} S^x_k S^x_n + J^y_{kn} S^y_k S^y_n + J^z_{kn} S^z_k S^z_n], \tag{1.2}$$

where J^μ_{kn} are coupling constants. These constants must be such that the Hamiltonian (1.2) is invariant with respect to lattice translations.

Formula (1.1) distinguishes the zeroth spin from other spins only for the convenience of the later discussion. We also use the convention that both the Planck constant $\hbar$ and the gyromagnetic ratio of spins are equal to 1. We will also use the variable S without any index to denote the maximum value of one quantum spin, or the length of one classical spin vector.

The above description of the problem is general enough to cover all examples presented below. However, in principle, the theory to be developed in this thesis is applicable to a wider class of spin problems, meaning a more general form of the Hamiltonian with, possibly, several non-equivalent spin species and also more sophisticated lattice structures (in particular, those of higher dimensions).

In the context of inelastic neutron scattering, the correlation functions (1.1) are referred to as intermediate structure factors [1]. If $q = 0$, Eq.(1.1) can also represent the free induction decay in nuclear magnetic resonance (NMR)[2],[3].

Given the Hamiltonian (1.2), the timescale of individual spin motion, referred to below as "fast," "short," or "mean free time," is well-represented by the time τ defined as

$$\tau = \left[S^2 \sum_{n,\mu} {J^\mu_{kn}}^2 \right]^{-1/2}. \tag{1.3}$$

Unless special conservation laws exist, this timescale also characterizes the decay of $G(t)$. This general situation without the separation of timescales is the primary focus of the present work, which, in particular, leaves untouched the widely discussed issue of spin diffusion[4],[5].

(Spin diffusion problems require the conservation of, at least, one component of the total spin.)

As a result of the time reversibility of the spin dynamics, $G(t)$ is an even function of t, which, in particular, implies $\frac{dG}{dt}|_{t=0} = 0$. In general, $G(t)$ can be expanded in even power of t:

$$G(t) = 1 - \frac{M_2}{2!}t^2 + \frac{M_4}{4!}t^4 - ... + \frac{(-1)^n M_{2n}}{(2n)!}t^{2n} + ... \,, \tag{1.4}$$

where the coefficients M_{2n} are called moments.

The infinite-temperature limit offers a unique advantage which will be important for our subsequent treatment. Namely, the correlation function $G(t)$ can be considered as proportional to the polarization of the zeroth spin $\langle S_0^\mu(t)\rangle$ averaged with the initial distribution function (or quantum density matrix)

$$\rho(0) \simeq \exp[\ \beta_0 \textstyle\sum_n \cos(\boldsymbol{q}\cdot\boldsymbol{r}_n)\ S_n^\mu(0)\ ], \tag{1.5}$$

provided the inverse temperature β_0 is very small, and only the first order of β_0 is kept in the expansion of $\langle S_0^\mu(t)\rangle$.

In other words, we are dealing with the decay of the average spin polarization on the zeroth site, given a *weak* initial polarization on each site proportional to $\cos(\boldsymbol{q}\cdot\boldsymbol{r}_n)$.

For the sake of physical interpretation, one can imagine that, at $t < 0$, the Hamiltonian (1.2) was switched off, and the spin system was equilibrated at very high temperature in an external field varying as $\cos(\boldsymbol{q}\cdot\boldsymbol{r}_n)$. Then, at $t = 0$, the environment and the external field were switched off. Simultaneously, the Hamiltonian (1.2) was switched on, and the system started evolving to a new equilibrium, which, to the first order in β_0, corresponds to infinite temperature.

This interpretation is visualized in Fig. 1.1 for classical spins.

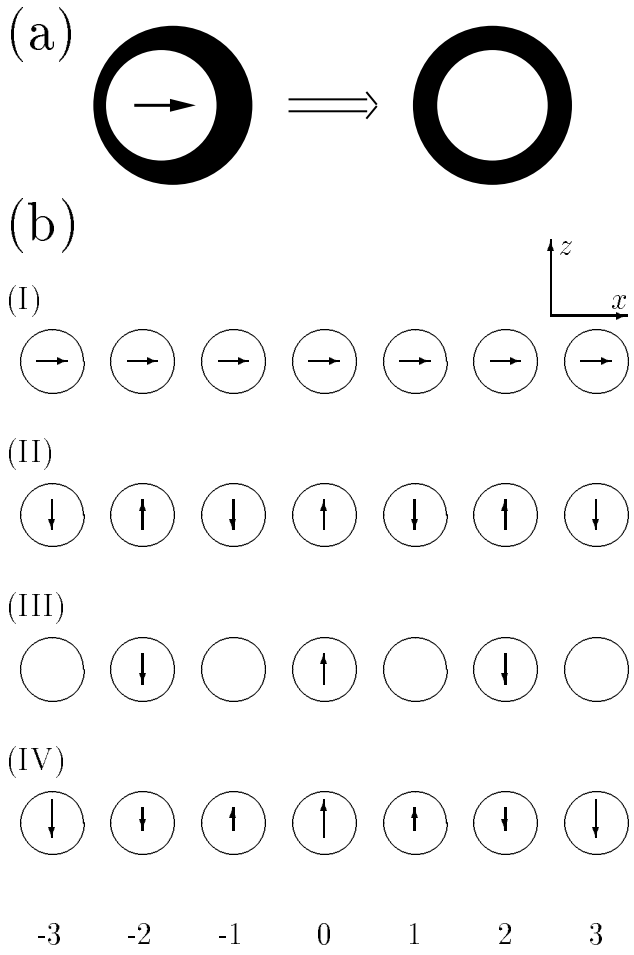

Figure 1.1: These pictures visualize the nonequilibrium problem corresponding to the initial probability distribution (1.5) for classical spins. Picture (a) represents an example of the initial and the final probability distributions of the zeroth spin. The tip of the spin vector moves on a spherical surface shown as a white disk. The thickness of the outer black layer around that disc represents the probability to find the spin oriented in the corresponding radial direction. The arrow in the middle of the white disc indicates the average spin polarization. Thus the problem is one of calculating the time dependence of the average spin polarization, given that the probability density on the spherical surface evolves from a weakly anisotropic distribution (left) to the completely isotropic infinite temperature distribution (right). Picture (b) shows examples of the initial conditions for fragments of infinite spin chains. The arrows indicate the direction and the relative size of the *weak* spin polarization at $t = 0$. The numbers in the bottom line are the indices of the spin sites. Examples (I-IV) correspond to the calculation of the correlation functions of form (1.1), provided (I) $\mu \to x$, $q = 0$; (II) $\mu \to z$, $q = \pi$; (III) $\mu \to z$, $q = \pi/2$; (IV) $\mu \to z$, $q = \pi/3$.

The representation of $G(t)$ in terms of the nonequilibrium decay of certain average spin polarization is quite natural in the context of NMR[6], because the free induction decay is the decay of the nonequilibrium spin polarization in the Larmor rotating reference frame. However, with one recent exception[7], this representation is largely unappreciated in the rest of the spin literature, where the correlation functions (1.1) appear as formal quantities describing inelastic neutron scattering.

The problem formulated in this Section has a long history. Therefore, we chose to postpone the detailed discussion of our theoretical goals until Section 1.7, i.e. after the existing knowledge about the problem is reviewed in Sections 1.3-1.6. That review is organized as follows: Section 1.3 presents the analytically solvable limits; Section 1.4 discusses the problem of exchange narrowing; Section 1.5 summarizes the empirical (experimental and numerical) knowledge about the correlation functions (1.1); and, finally, Section 1.6 contains discussion of previous attempts to find the approximate solution of the problem.

Our original contributions to the subject are mostly exposed in Chapters 2 and 3. However, the theoretical treatment actually starts in Section 1.7 of this Chapter. That Section motivates our theoretical approach and puts the contents of Chapters 2 and 3 in a single perspective. For convenience of discussion, the present Chapter also contains the original results of our own simulations of the classical spin systems. These results are presented Section 1.5 together with other pieces of empirical knowledge.

A large part of the present work has already been published or submitted for publication in physics research journals (Refs.[6], [8], [9]).

1.3 Analytically solvable limits

In this Section, we summarize the existing knowledge of the limits in which the entire form of the correlation functions (1.1) can be obtained analytically. These limits will serve as important reference points in our subsequent treatment of the general case, which does not

admit analytic solutions.

1.3.1 Ising-like case

When, in the Hamiltonian (1.2), all interaction constants J^x_{kn} and J^y_{kn} are set equal to zero, the remaining part has the Ising-like form

$$\mathcal{H} = \sum_{k<n} J^z_{kn} S^z_k S^z_n. \tag{1.6}$$

In this case, any correlation function of form (1.1) can be obtained analytically, because the problem has an infinite number of constants of motion. Those constants of motion are the z-components of spins.

The obvious consequence of the above fact is that the correlation functions (1.1) for the z-components of spins (i.e. $\mu \to z$) do not decay at all.

The general result for $\mu \to x$(or y) and for any $\boldsymbol{q}$ is

$$G(t) = \prod_n \frac{\sin\left[(S+\frac{1}{2})J^z_{kn}t\right]}{(2S+1)\sin\left[\frac{1}{2}J^z_{kn}t\right]} \tag{1.7}$$

In the limit of a large number of neighbors, the right hand side of Eq.(1.7) becomes Gaussian, which is a consequence of the central limit theorem.

Two special cases of formula (1.7) will be used in our subsequent treatment. Namely, for spins 1/2, this formula gives

$$G(t) = \prod_n \cos\left(\frac{1}{2}J^z_{kn}t\right); \tag{1.8}$$

and for classical spins —

$$G(t) = \prod_n \frac{\sin\left(SJ^z_{kn}t\right)}{SJ^z_{kn}t} \tag{1.9}$$

The above result for spins 1/2 and $q = 0$ was first derived by Lowe and Norberg[2].

Because the Ising-like limit will play an important role in our treatment, the derivation of Eq.(1.7) will be given in Section 3.2.1.

An interesting generalization of the Ising-like case is the problem with $S = 1/2, \mu \to x$, $q = 0$ and with a Hamiltonian which is the sum of the infinite-range Ising part and the Heisenberg part[10],[2]. Namely,

$$\mathcal{H} = \sum_{k<n} [J_I S_k^z S_n^z + J_{kn} \boldsymbol{S}_k \cdot \boldsymbol{S}_n], \tag{1.10}$$

where J_I is the interaction constant, which is the same for every pair of spins, and $\{J_{kn}\}$ is the set of Heisenberg interaction constants that can take any values.

It turns out that the solution of this problem is not affected by the presence of the Heisenberg part and is identical to the solution of the pure Ising-like problem. The reason is that the Heisenberg part of the Hamiltonian conserves both the total spin polarization and the energy corresponding to the infinite-range Ising part.

1.3.2 Two spins 1/2

A simple limit, which, however, will play a role in our treatment, is that of two spins 1/2 interacting via the Hamiltonian (1.2). In this case, one can consider $G(t)$ given by Eq.(1.1) only with $q = 0$ or $q = \pi$.

To obtain $G(t)$, one has to solve the two spin problem exactly, which gives the following answer:

For $\mu \to x$ and $q = 0$,

$$G(t) = \cos\left[\frac{1}{2}(J^y - J^z)t\right]; \tag{1.11}$$

and, for $\mu \to x$ and $q = \pi$,

$$G(t) = \cos\left[\frac{1}{2}(J^y + J^z)t\right]. \tag{1.12}$$

It is worth mentioning that the analogous problem for two classical spins does not admit an analytic solution, which defies the common notion that quantum problems are more difficult then their classical analogs.

1.3.3 Spin 1/2 XX chain

The spin 1/2 XX chain chain corresponds to the special case of the Hamiltonian (1.2)

$$\mathcal{H} = \sum_n \left[J S_n^x S_{n+1}^x + J S_n^y S_{n+1}^y \right]. \tag{1.13}$$

In this case, the Jordan-Wigner transformation maps the above spin system to the system of noninteracting lattice fermions[11],[12]. The analytical results of our interest have been summarized in Ref.[13] — they follow from the works of Niemeijer[14] and Katsura *et al.*[15]. These results are:

For $\mu \to z$,

$$G(t) = J_0 \left(2Jt \sin\frac{q}{2} \right), \tag{1.14}$$

where $J_0(...)$ is the Bessel function of the zeroth order.

For $\mu \to x, y$ and arbitrary q,

$$G(t) = \exp\left(-\frac{1}{4} J^2 t^2 \right). \tag{1.15}$$

1.4 Exchange narrowing

The phenomenon of exchange narrowing belongs to a more general class of phenomena collectively referred to as motional narrowing. The term "motional narrowing" means that the resonance lines become very narrow as a result of fast microscopic motion in the system. The term "exchange narrowing" indicates that the motional narrowing is caused by the exchange interaction.

The shapes of the exchange narrowed resonance lines can be obtained as Fourier transforms of certain correlation functions that fall under general definition (1.1).

In the exchange narrowing problems, the exchange interaction is the dominant part of the Hamiltonian, but, by itself, that part cannot affect the correlation function of interest, so that other, much smaller terms in the Hamiltonian become primarily responsible for the

decay of that function. In such a situation, the effect of the exchange term on the correlation function is indirect but still quite dramatic. The fast spin motion induced by the exchange term averages out the direct effects due to the weaker interaction terms. As a result, the correlation function of interest decays much slower than it would do in the absence of the exchange term, and, therefore, the Fourier transform of that function extends over a much narrower interval in the frequency domain — hence the name "exchange narrowing."

The functional form of the resulting slower decay is expected to be nearly exponential, which is a common consequence of the separation of timescales between the fast motion due to the exchange coupling and the slow decay of the correlation function of interest. As we mentioned in Section 1.2, situations with separation of timescales are not the primary focus of this work. However, in the following Chapters we will frequently refer to the limit of exchange narrowing, and, for that reason, below we introduce the results for this problem obtained by Anderson and Weiss[16].

Strictly speaking, those results cannot be considered as rigorous but only as well justified on physical grounds. (See Section 2.3.1 for a relevant discussion.) It should also be mentioned that the example discussed in the end of Section 1.3.1 would contradict Anderson and Weiss's picture of the exchange narrowing, but that example can be considered as an exception from the general rule.

There are two basic setups for the exchange narrowing problem[17], which we call Problem A and Problem B.

Problem A is to find the correlation function (1.1) with $q = 0$ provided the Hamiltonian is

$$\mathcal{H} = \sum_{k<n} [\mathcal{H}_{\rm dip} + J_{kn} \boldsymbol{S}_k \cdot \boldsymbol{S}_n], \tag{1.16}$$

where $\mathcal{H}_{\rm dip}$ stands for the magnetic dipolar interaction, and the second, much stronger term represents the exchange interaction. This formulation is mostly relevant to electron spin resonance (ESR), though it also describes NMR relaxation in solid ^{3}He, where the

internuclear exchange interaction is unusually strong.

Problem B requires two spin species $\boldsymbol{S}$ and $\boldsymbol{I}$ representing electrons and the nuclei respectively. The Hamiltonian of this problem is

$$\mathcal{H} = \sum_{m,n} \boldsymbol{I}_m \boldsymbol{A}_{mn} \boldsymbol{S}_n + \sum_{k<n} J_{kn} \boldsymbol{S}_k \cdot \boldsymbol{S}_n, \tag{1.17}$$

where $\boldsymbol{A}_{mn}$ is the hyperfine coupling tensor.

The correlation function of interest for Problem B is:

$$G(t) = \langle\, I_0^{\mu}(t)\, I_0^{\mu}(0)\, \rangle. \tag{1.18}$$

In this problem, there are no correlations between motions of different nuclear spins. Therefore, any q-dependent correlation function analogous to (1.1) but defined for nuclear spins is equal to the above pair correlation function.

In both Problems A and B, the influence of the exchange interaction on the decay of the correlation functions of interest is indirect, i.e., if only the exchange term is left in the Hamiltonian, those correlation functions would not decay at all.

In Problem A, the above situation is the consequence of the fact that the total polarization of all spins is conserved by the exchange interaction. (According to the non-equilibrium interpretation of Section 1.2, the correlation functions (1.1) for $q = 0$ are proportional to the relaxation of the total spin polarization in the system.) In Problem B, the same situation is caused by the trivial fact that, with only the exchange term left, nuclear spins would not move at all.

Anderson and Weiss have used an intuitively attractive model of fluctuating local fields to obtain the following formula applicable to both Problems A and B:

$$G(t) = \exp\left[-M_2 \int_0^t (t - t')\varphi(t')dt'\right], \tag{1.19}$$

where M_2 is the second moment of $G(t)$, and $\varphi(t)$ is the correlation function of the local fields.

The function $\varphi(t)$ is supposed to decay on the timescale of the order of the inverse constant of the exchange interaction, i.e. much faster than $G(t)$. As a result, $G(t)$ should quickly approach the asymptotic form

$$G(t) = e^{-\xi t}, \tag{1.20}$$

where

$$\xi = M_2 \int_0^\infty \varphi(t')dt'. \tag{1.21}$$

According to Eq.(1.20), the Fourier transform of $G(t)$, which corresponds to the absorption lineshape observable by ESR or NMR, should be Lorentzian with half-width equal to ξ.

In principle, one can obtain the exact theoretical expression for $\varphi(t)$ for both Problems, A and B. However, for Problem A, $\varphi(t)$ has quite a complicated form which does not give much insight into the model. At the same time, for Problem B, the expression for $\varphi(t)$ is very simple and intuitive. For example, if in Eq.(1.18) $\mu \to x$, then $\varphi(t)$ can be written as

$$\varphi(t) = \frac{\langle\ h_m^y(t)\ h_m^y(0)\ +\ h_m^z(t)\ h_m^z(0)\ \rangle}{\langle\ h_m^y(0)\ h_m^y(0)\ +\ h_m^z(0)\ h_m^z(0)\ \rangle}, \tag{1.22}$$

where $\boldsymbol{h}_m$ is the actual local field generated by the electronic spins and acting on the nuclear spins:

$$\boldsymbol{h}_m = \sum_n \boldsymbol{A}_{mn}\boldsymbol{S}_n. \tag{1.23}$$

The theoretical calculation of $\varphi(t)$ belongs to the class of difficult problems without separation of timescales. Anderson and Weiss did not try to perform that calculation. Their goal was a factor-of-two estimate of ξ, which they achieved by substituting a Gaussian ansatz for $\varphi(t)$ in Eq.(1.21).

1.5 Empirical input

The purpose of this Section is three-fold. First, its content should create an overall empirical picture of the behavior of the correlation functions (1.1). Second, the examples presented

here will be used as reference cases for testing the approximate schemes of Chapter 3. Third, this Section is supposed to demonstrate, on empirical grounds, that the generic long-time behavior of the correlation functions (1.1) has the functional form either

$$G(t) \simeq e^{-\xi t}, \tag{1.24}$$

or

$$G(t) \simeq e^{-\xi t} cos(\eta t + \phi), \tag{1.25}$$

where ξ, η and ϕ are some constants about which we can only assert that, in general, the values of ξ and η are of the order of $1/\tau$, where τ is given by Eq.(1.3).

Actually, the special focus on the issue of the long-time behavior is one of the distinguishing features of the present work. Theoretically, this issue will be taken up in Chapter 2. Here we would only like to dispel the false impression that the situation is as simple as that of the damped harmonic oscillator.

The crucial difference between the damped oscillator and our problem is that, in the case of a damped oscillator, there must exist a separation of timescales between the slow oscillator and the quickly equilibrating microscopic motion in the heat bath, which leads to the standard description of the dissipation. In the typical case we consider, there is no separation between the timescale of τ and any other microscopic motion. Moreover, the oscillations in Eq.(1.25) are neither related to a simple rotation nor produced by the equivalent of a simple spring potential. In fact, in Section 1.5.1, we will argue that those oscillations pose a major challenge to the conventional Markovian wisdom.

Before reviewing the experimental and numerical evidence for the long-time behavior (1.24) and (1.25), it should be mentioned that the characteristic decay time of $G(t)$ is expected to be of the order of τ. At the same time, the characteristic long-time behavior does not become pronounced until after several τ, i.e. until $G(t)$ has fallen to a relatively small value. Yet, in order to make definite conclusions about the long-time behavior, one has to go

orders of magnitude below the initial value of $G(t)$. This task is extremely challenging both numerically and experimentally. In particular, it is certainly beyond the reach of inelastic neutron scattering experiments.

We should also mention that this Section does not contain any example of spin 1/2 or any other quantum spin system which would definitely exhibit the monotonic exponential long-time behavior (1.24) characterized by $\xi \sim 1/\tau$. However, it is common knowledge in the field of NMR that such a behavior of the free induction decay is even more frequent than the oscillatory one. The monotonic exponential decay is, in a sense, less surprising, given that, at least, it is expected in situations like that of "exchange narrowing" (Section 1.4), where the separation of timescales is present. In that case, the entire decay is nearly exponential, which is confirmed by experiment[18].

Although the functional forms (1.24) and (1.25) do not describe the initial behavior of the correlation functions, they still reflect the existence of two general regimes — oscillatory and monotonic. The discussion of various factors influencing the competition between the two regimes will be given in Section 3.1. Although placed in Chapter 3, that Section is quite self-contained and, if desired, can be read immediately after the present one.

We now proceed to the discussion of the experimental and numerical data representing the correlation functions (1.1). That discussion will cover (i) NMR free induction decay experiments; (ii) the results of the numerical diagonalization of spin 1/2 chains; and (iii) simulations of classical spin systems.

1.5.1 NMR free induction decay experiments

A typical free induction decay formulation in solids assumes that each nucleus is at rest on its site in the crystal lattice, and the following conditions are fulfilled:

$$\frac{k_B T}{\hbar} >> \Omega >> \frac{1}{T_2} >> \frac{1}{T_1}, \tag{1.26}$$

where T is the temperature of the initial equilibrium distribution, Ω is the Larmor frequency in the static magnetic field, T_2 is the time scale of the nuclear spin-spin interaction, and T_1 is the spin-lattice relaxation time. The spin-lattice relaxation can be neglected, since the time range of interest is of the order of T_2. (the timescale of T_2 corresponds to τ defined by Eq.(1.3).)

Free induction decay is normally described in the Larmor rotating reference frame. In that frame, if the z-axis is chosen along the axis of the Larmor precession, the Hamiltonian of the spin-spin interaction is given by Eq.(1.2) with the restriction that $J^x_{kn} = J^y_{kn}$[10]. Denoting each of these two constants as $J^{\perp}_{kn}$, we thus can write down the most general form of the Hamiltonian for the free induction decay problem

$$\mathcal{H} = \sum_{k<n} [J^{\perp}_{kn}(S^x_k S^x_n + S^y_k S^y_n) + J^z_{kn} S^z_k S^z_n]. \tag{1.27}$$

Even if the full Hamiltonian of the spin-spin interaction contains other bilinear terms, those terms should not be included, because they are are averaged out by the fast Larmor precession. For that reason, the Hamiltonian (1.27) is referred to as a "truncated Hamiltonian."

The free induction decay is measured as the spin response to a $\pi/2$ radio frequency pulse. That pulse can be described as follows: At $t < 0$, the spin system is uniformly polarized along the z-direction. (The Hamiltonian(1.27) conserves the total polarization along that direction.) At $t = 0$, the $\pi/2$ pulse instantaneously turns the equilibrium spin system by 90 degrees, so that immediately after the pulse, all spins are uniformly polarized in the direction perpendicular to the static magnetic field. We set the x-axis of the rotating reference frame to be along the magnetization at this moment of time. After the pulse, the x-component of the magnetization M_x decays to zero as a result of the spin-spin interaction represented by the Hamiltonian (1.27). This process is called free induction decay.

Usually, the free induction decay is presented as a normalized function $G(t) = M_x(t)/M_x(0)$. Since all spins are equivalent, each of them equally contributes to the magnetization. For the purposes of the forthcoming consideration, we express $G(t)$ in terms of the average

polarization $\boldsymbol{m}$ of *one* spin:

$$G(t) = \frac{m_x(t)}{m_x(0)}. \tag{1.28}$$

As explained in Section 1.2, the resulting problem is equivalent to the calculation of the correlation function (1.1) with $\mu \to x$, $q = 0$ and the Hamiltonian (1.27).

For the observation of the free induction decay, the ideal material is calcium fluoride (CaF_2). In fact, there is no material other than CaF_2 where the inter-nuclear spin-spin interaction is so well-known and so well-isolated from other microscopic factors[19] and where, at the same time, the free induction decay is measured with sufficient accuracy.

In CaF_2, the free induction decay is observed on ^{19}F nuclei which have spins 1/2 and form a simple cubic lattice. With a high degree of confidence, one can assume that the experiments in CaF_2 actually measure the correlation functions (1.1) for the ideal problem of a simple cubic lattice of spins 1/2 interacting according to the Hamiltonian (1.27) in which

$$J^z_{kn} = -2J^{\perp}_{kn} \simeq \frac{(1 - 3\cos^2\vartheta)}{|\boldsymbol{r}_k - \boldsymbol{r}_n|^3}, \tag{1.29}$$

where ϑ is the angle between $(\boldsymbol{r}_k - \boldsymbol{r}_n)$ and the z-axis.

We would like emphasize, that, despite all the subtleties associated with the truncation procedure, the magnetic dipolar form of the interaction between the nuclear spins in CaF_2 is essentially known from the first principles, which is very unique, and can be put in contrast, for example, with the exchange interaction between electronic spins. The exchange interaction is usually described by the Heisenberg model representing the entire interaction as two-spin exchange. In principle, however, higher order spin exchange can and should be present in the real materials.

The form (1.29) of the interaction coefficients represents the "truncated" magnetic dipolar interaction. This interaction is what is left from the full Hamiltonian of the magnetic dipolar interaction after averaging over the Larmor precession[3].

We recall that, in the free induction decay formulation, the z-axis does not necessarily

correspond to any of the main lattice directions — this axis coincides with the axis of the Larmor precession, which, in its turn, is set by the direction of the strong external magnetic field. This, in particular, implies that the values of the interaction coefficients strongly depend on the relative orientation of the external field with respect to the lattice.

For example, the truncated interaction of a given spin with its neighbors is strongest, when the external magnetic field is directed along one the main axes of the cubic lattice — for example, [100]. On the other hand, the overall strength of the interaction is maximally reduced, when the external field is directed along one of the main diagonals such as [111]. In that case, the coupling between any given spin and each of its six nearest neighbors equals zero, but the interaction with more distant neighbors remains present.

Figure 1.2, contains three plots of the free induction decay in CaF_2 measured in the high precision experiments of Engelsberg and Lowe[20]. The plots are labeled by the directions of the external magnetic field used to obtain the data.

Each plot in Figure 1.2 exhibits characteristic oscillations quickly approaching the asymptotic form (1.25). In our opinion, the occurrence of those oscillations should be qualified as a very non-trivial fact. Below we shall explain why.

The free induction decay is the decay of the macroscopic magnetization of the nuclear spins under the influence of of local fields fluctuating around zero average value. The Larmor precession has nothing to do with those oscillations, because its frequency is several orders of magnitude greater than the frequency of the oscillations. Neither are those oscillations the result of any other kind of magnetization precession. At the moment when the free induction decay crosses zero, the magnetization of the system is equal to zero in all directions, and then, out of completely unpolarized state the magnetization reappears with the opposite sign.

Such a fact is very hard to understand intuitively. Normal intuition, which is supported by numerous examples of the Markovian limit, would suggest that, even on a non-Markovian

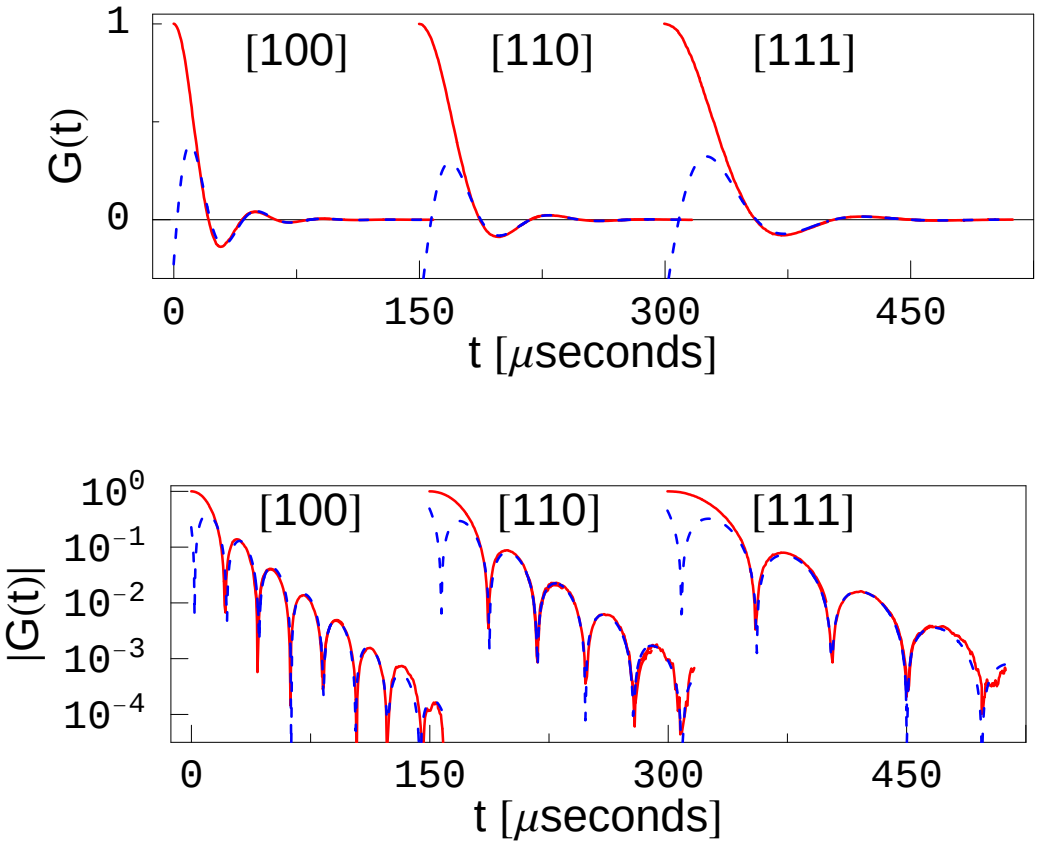

Figure 1.2: Free induction decay in CaF_2. The top and the bottom frames contain identical pieces of data presented on direct(non-logarithmic) and on logarithmic scales respectively. Because $G(t)$ changes sign, the logarithmic plots present the absolute value of $G(t)$. The solid red lines represent the experimental data of Engelsberg and Lowe [20]. The blue dashed lines represent long-time fits of the form (1.25). Each plot is labeled by the direction of the external magnetic field. The time origins of the [110] and [111] plots are shifted by 150 and 300 microseconds respectively.

timescale, the system should not evolve away from equilibrium. The value of the macroscopic magnetization can be considered as a direct measure of the deviation from equilibrium. Therefore, if one further insists that the zero value of magnetization corresponds to equilibrium, it is very difficult to explain how the system recovers a nonequilibrium macroscopic magnetization after the free induction decay crosses zero.

The mechanism and the physical picture underlying the oscillations of the correlations functions (1.1) will be discussed in Chapters 2 and 3.

1.5.2 Numerical diagonalization of spin 1/2 chains

The second piece of empirical knowledge used in our work comes from the paper of Fabricius, Löw, and Stolze[13], where they presented the results of numerical diagonalization of chains (rings) of sixteen spins 1/2 coupled by a nearest-neighbor interaction of the form (1.2), with the restriction $J^x_{n,n+1} = J^y_{n,n+1}$.

These chains are known as XXZ chains. Three correlation functions of the form (1.1) have been presented in Ref.[13], and are reproduced in Fig. 1.3.

It is an interesting open question to what extent the the spin 1/2 XXZ chains with $J^z_{n,n+1} \neq 0$ display generic properties, because, on one hand, they are known to be integrable, but, on the other hand, if this is attempted, the actual solution is so complex that the explicit form of the correlation functions of interest has never been obtained.

As far as infinite temperature correlation functions are concerned, the numerical study of these chains[13],[5] did not reveal anything qualitatively unusual. Therefore, for now, since not much data on the long-time behavior of the correlation functions (1.1) exists, it is reasonable to take the data on the spin 1/2 XXZ chains as a strong hint for the generic nature of Eq.(1.25). However, in the future, if more evidence for the long-time behavior (1.24,1.25) in generic spin systems emerges, the logic can be turned around, and the existence of such behavior in the spin 1/2 XXZ chains can be considered as a piece of evidence proving that

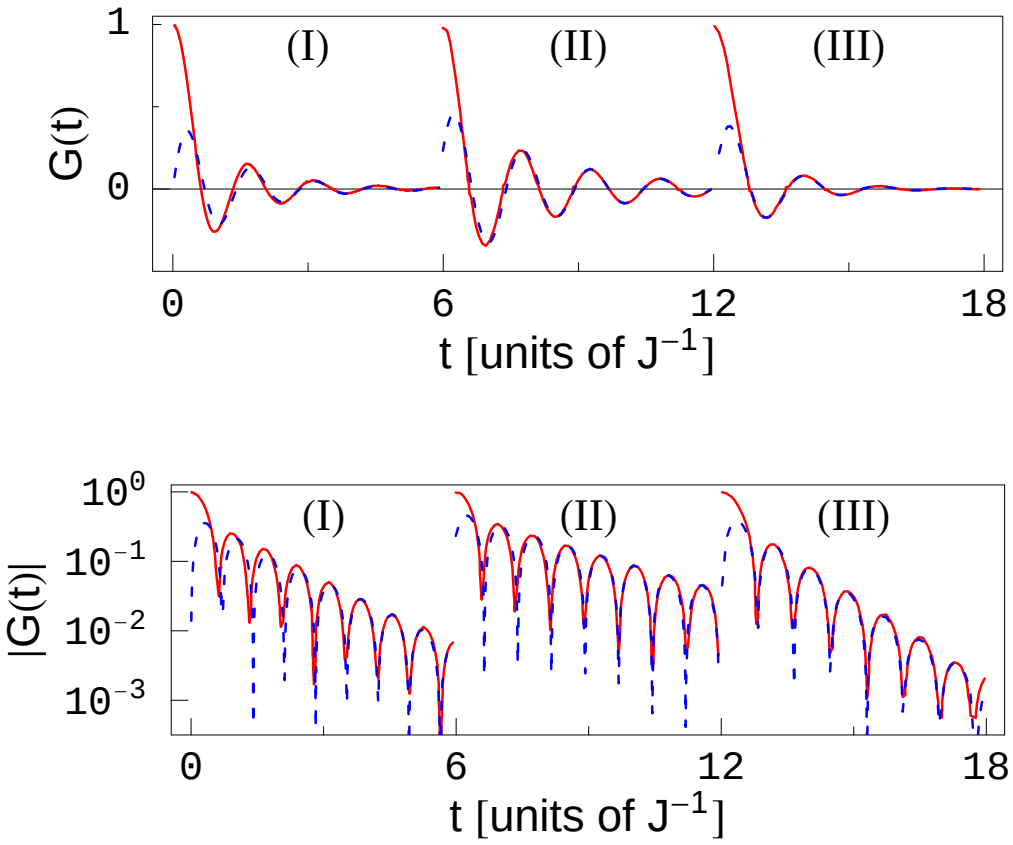

Figure 1.3: Intermediate structure factors for spin 1/2 XXZ chains. The top and the bottom sets of plots contain identical pieces of data presented on direct(non-logarithmic) and on logarithmic scales respectively. Because $G(t)$ changes sign, the logarithmic plots present the absolute value of $G(t)$. The solid red lines represent the numerical results of Fabricius *et al.*[13]. The blue dashed lines represent long-time fits of the form (1.25). Each of those correlation functions is characterized by the following parameters entering Eqs.(1.1, 1.2): $q = \pi$ (in the units of inverse chain spacing), and $J^x_{n,n+1} = J^y_{n,n+1} = J$, where J is an auxiliary variable. Other parameters are: (I) $J^z_{n,n+1} = J$, any value of μ; (II) $J^z_{n,n+1} = J\cos(0.3\pi)$, $\mu \to z$; (III) $J^z_{n,n+1} = J\cos(0.3\pi)$, $\mu \to x$. The time origins of plots (II) and (III) are shifted by 6 and 12 time units respectively.

the properties of those integrable chains are, at least, partially generic.

1.5.3 Numerical simulations of classical spin systems

Motivated by the spin 1/2 problems and by the theory to be presented in Chapter 2, we have performed numerical simulations of classical spin systems [9]. The simulations generated a wide spectrum of data covering different dimensions, interactions and wave vectors — all entirely consistent with the long-time behavior (1.24, 1.25). The results of these simulations have also been an important driving force behind the final development of the computational scheme introduced in Chapter 3.

The simulations have been limited to the nearest-neighbor interaction of the form

$$\mathcal{H} = \sum_{k,n} [J^x S_k^x S_n^x + J^y S_k^y S_n^y + J^z S_k^z S_n^z], \tag{1.30}$$

which is a special case of the Hamiltonian (1.2).

Before proceeding with the description of the simulations, it should be mentioned that, for the Heisenberg interaction in classical spin systems, the long-time properties have previously been studied numerically for the infinite temperature pair-correlation functions $\langle S_k^x(t) S_k^x(0) \rangle$ by Müller [21] and by Gerling and Landau[22]; and for the q-dependent correlation functions (1.1) with small wave vectors by Bonfim and Reiter[23]. Those works have mostly been motivated by the problem of spin diffusion, which, as we mentioned in Section 1.2, implies the separation of timescales and thus lies outside of the primary scope of the present work. For the the classical spin systems, the long-time behavior of the fast-decaying q-dependent correlation functions that we consider has never been addressed.

Simulations.

We computed the correlation functions of interest directly, i.e. by evaluating the RHS of their equilibrium definition (1.1). For that purpose we simulated the microscopic dynamics

of *equilibrium* spin systems. (It is, in fact, the only part of this thesis where the definition (1.1) is used directly instead of its non-equilibrium equivalent introduced in Section 1.2.)

Our computational strategy was similar to that of Müller[21]. Namely, we did not deal with very large systems but, instead, performed an ensemble averaging over a large number of finite, but not too small, lattices having periodic boundary conditions. The finite size effects were then controlled by varying the size of the lattice.

For a given lattice size, many computational runs have thus been performed. Each of them started from completely random initial orientations of spins (corresponding to the infinite temperature) and generated the evolution of the system over a time interval two orders of magnitude longer than the mean free time τ (see Table 1 for specific numbers). The correlation functions were then obtained by evaluating the RHS of Eq.(1.1) for each run and then averaging over different runs.

The following algorithm has been used in order to simulate the evolution of the system.

At each time step, the spins were advanced sequentially in such a way that, if the spin number k interacted with the spin number n, and the kth spin was advanced first, then the new coordinates of the nth spin were computed based on the local field created by the already advanced kth spin.

The procedure for advancing a given (kth) spin to the next point along the discrete time grid consisted of two steps.

Step 1: The coordinates of the kth spin were changed by $\delta \boldsymbol{S}_k$ according to the straightforward discretization of the equations of motion, i.e.

$$\delta \boldsymbol{S}_k = [\boldsymbol{S}_k \times \boldsymbol{h}_k]\, \delta t, \tag{1.31}$$

where $\boldsymbol{h}_k$ was the local field equal to $\sum_n^{\text{n.n.}} [J^x S_n^x \hat{\boldsymbol{e}}_x + J^y S_n^y \hat{\boldsymbol{e}}_y + J^z S_n^z \hat{\boldsymbol{e}}_z]$ (sum over the nearest neighbors of the kth spin); and δt was the discretization time step.

Step 2: The higher order errors that changed the length of the spin vector were eliminated. This was done by contracting the spin component perpendicular to the local field, so that it

took the absolute value it had before Step 1.

The whole manipulation could not change the spin projection parallel to the local field and, therefore, the energy of interaction of that spin with its neighbors. Since the next spin was advanced in the newly updated local field, the energy of the whole system was conserved exactly during the entire integration. Apart from insuring meaningful behavior of the computed trajectories, the exact conservation of energy substantially improved the convergence of the algorithm in respect to the limit $\delta t \to 0$.

In our simulations, the discretization time steps (given in Table 1) were admitted as sufficient when their further reduction appeared to have no effect on the computed correlation functions. We also checked that the averaging over a larger number of much shorter runs led to results consistent with the longer runs we used.

The time lengths of the runs indicated in Table 1 were chosen to optimize the resulting efficiency of averaging: too short runs (of the order of the time length of the computed correlation function) did not make many independent contributions to the correlation functions, while too long runs did not improve the quality of the averaging proportionally to their length.

Results.

The results of our simulations for different dimensions, interaction constants, and wave numbers are presented in Fig. 1.4, together with the long-time theoretical fits based on either Eq.(1.24) or (1.25). Since we aimed at demonstrating the exponential character of the long-time behavior, it was natural to use a logarithmic scale for $G(t)$. However, because in the half of the cases, $G(t)$ was also oscillating, we chose to show the logarithmic plots for the absolute value of $G(t)$, which explains the cusps in the left column of plots in Fig. 1.4. Those cusps correspond to the points where $G(t)$ crosses zero. The reason that the cusp minima do not reach $-\infty$ is that a discrete grid was used.

The selection of parameters for the simulations was subject to certain practical constraints: The computed correlation functions could be considered reliable only within quite a limited range along both the t- and $\mathrm{Log}(G(t))$- axes. Therefore, we avoided correlation functions that reached too-small values too fast, or, on the contrary, decayed too slowly.

The values of q corresponding to the longer periods on the lattice are, naturally, more sensitive to finite size effects. From such a perspective, $q = 0$ (which, in the sense of the lattice period, is better thought of as $q = 2\pi$) corresponds to the shortest possible period equal to the lattice spacing and is the most suitable value for the simulations. For this reason, q was chosen to be zero in six of eight examples presented in Fig. 1.4.

Since the long-time behavior of the correlation functions was only marginally accessible with our computational resources, we present the results in substantial detail, thus making clear the uncertainties associated with insufficient ensemble averaging and finite size effects. Each of the correlation functions presented in Fig. 1.4 was computed four times: two statistically independent averaging results for each of two different lattice sizes. "Two statistically independent averaging results" means that, in each case, the same number of sample runs was performed but two statistically independent sets of random numbers were used for setting the initial orientations of spins. Each frame in that figure thus contains a superposition of four plots. The time interval where those plots do not deviate from each other can be considered as representing the limit of infinite lattice size with sufficient ensemble averaging.

The finite size effects are not evident in any of the examples shown in Fig. 1.4 — in every case, the plots representing different simulation outcomes do not deviate from each other before the statistical fluctuations for each of the two lattice sizes become apparent.

Our experience indicates that further improvement in the accuracy of the computed correlation functions would simultaneously require a finer discretization, much more extensive ensemble averaging and, probably, larger system sizes, i.e. much greater computational effort.

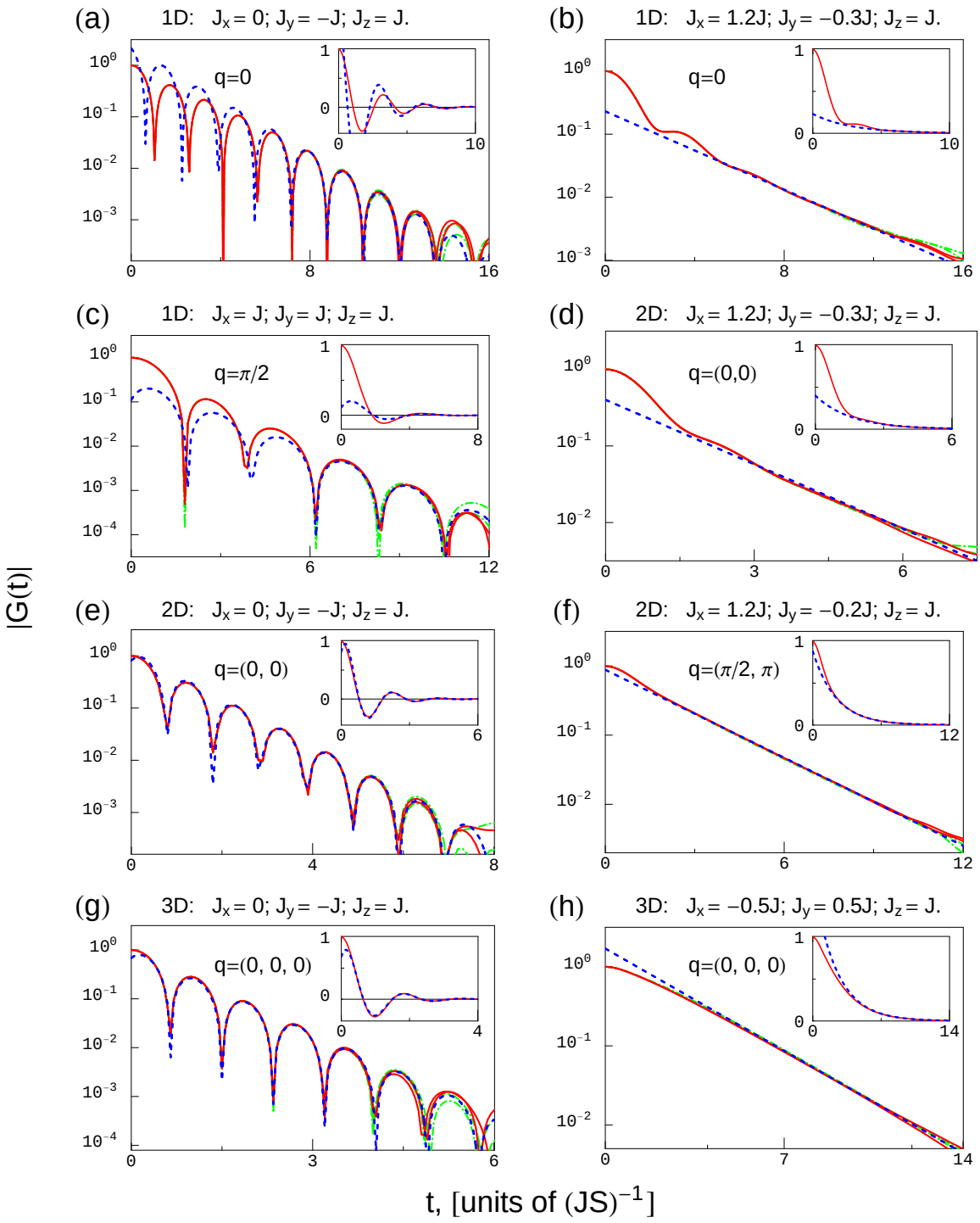

Figure 1.4: Correlation functions $G(t)$ of the form (1.1) with Hamiltonian (1.30) for 1D chain, 2D square lattice, and 3D cubic lattice of classical spins. The simulation results are presented by almost indistinguishable superposition of data for two lattice sizes, and each size is represented by two statistically independent averaging results; therefore, two solid red lines for the larger size (Size 1) and two dash-dotted green lines for the smaller size (Size 2). The spread of the four lines indicates the computational uncertainty — it becomes visible only in the lower right corner of each frame. The dashed blue lines are the long-time theoretical fits of form (1.24) or (1.25). The numbers relevant to each data set are given in Table 1.

Frame label	Lattice dimensions Size 1	Size 2	Number of runs	Time length of each run, $[(JS)^{-1}]$	Discretization time step, $[(JS)^{-1}]$	Long-time fit (time units - $[(JS)^{-1}]$)
(a)	19	15	500000	320	0.02	2.25 exp(-0.585 t) cos(1.93 t + 0.31)
(b)	19	15	500000	320	0.02	0.23 exp(-0.357 t)
(c)	40	24	160000	320	0.02	0.30 exp(-0.588 t) cos(1.46 t - 1.19)
(d)	10 × 10	7 × 7	60000	100	0.0025	0.40 exp(-0.645 t)
(e)	10 × 10	7 × 7	80000	170	0.01	1.20 exp(-1.031 t) cos(3.06 t - 0.82)
(f)	12 × 8	8 × 4	60000	100	0.0025	0.88 exp(-0.488 t)
(g)	5 × 5 × 5	4 × 4 × 3	80000	170	0.005	1.00 exp(-1.299 t) cos(3.70 t - 0.82)
(h)	5 × 5 × 5	4 × 4 × 3	80000	170	0.005	1.70 exp(-0.426 t)

Table 1.1: Simulation parameters and long-time fits corresponding to the plots presented in Fig. 1.4. The numbers in the right four columns characterize each of the four data sets superimposed in the corresponding frame.

Summarizing the evidence, we observe that, with the marginal exception of Fig. 1.4(d), in every other case presented there is an interval, covering at least one decade of the values of $G(t)$, where the simulation results agree with the long-time fits (1.24) or (1.25). We would also like to point out that, while in all cases the exponential behavior becomes pronounced quite early, the long-time exponents in Figs. 1.4(e,g) describe almost the entire correlation functions.

It is thus safe to conclude that our numerical results lend strong support to the idea expressed in Chapter 2, that a discrete spectrum of well-separated exponents describes the long-time behavior of the correlation functions considered, with the slowest of those exponents responsible for the asymptotic functional form given by Eq.(1.24) or (1.25). It is also very likely, though slightly less reliable, that in the examples presented, our simulations revealed the slowest exponents. The reservation here is for the possibility that even slower exponents could enter the long-time expansion of $G(t)$ with anomalously small coefficients.

1.6 Previous works

In this Section, we describe previous theoretical attempts to find an approximate solution to the problem of NMR free induction decay. To the best of our knowledge, the theoretical situation with free induction decay is entirely representative of the general problem formulated in Section 1.2. At the same time, the calculation of the free induction decay is the most direct practical application of the theory to be exposed in this thesis.

It should be mentioned from the very beginning that the present review is selective and somewhat personal. For a complementary recent review, we can refer the reader to the book of Brian Cowan [19].

The first theoretical works dealing with the high temperature spin dynamics appeared in the context of NMR very soon after the discovery of that phenomenon.

In 1946, Bloch proposed a description of the NMR relaxation processes in terms of the set of simple phenomenological equations now well known as the Bloch equations[24]. Although the Bloch equations could be formally written for both solids and liquids, it was immediately clear that these equations can provide a quantitative description only for liquids. In solids, the Bloch equations would imply the simple exponential decay of the free induction decay, which is in apparent contradiction to the empirical data presented in Section 1.5.1. The wide use of the Bloch equation, however, coined the name "T_2-relaxation", which, in particular, refers to the spin-spin relaxation in solids.

In 1948, Bloembergen, Purcell and Pound gave the first qualitative analysis and estimates of various factors affecting the NMR relaxation[25].

The above work was followed by the famous Van Vleck paper of 1948, where he introduced a rigorous formulation of the NMR lineshape theory in solids in terms of the moment expansion[10]. In practice, however, the amount of computational effort required for computing the higher order moments grows exponentially with the moment number, and, even with the present day computational resources, it is not feasible to compute all moments nec-

essary for the accurate reconstruction of the NMR absorption lineshape due to the magnetic dipolar interaction.

In 1953, Anderson and Weiss developed a very intuitive theory of exchanged narrowed lines (see Section 1.4). They considered a model according to which every spin was moving under the action of randomly fluctuating local fields. Using that model, they derived formula (1.20), which indicated that the correlation functions of their interest should decay nearly exponentially. In addition, they related the constant of the exponential decay with the integral of the correlation function of the local field (Eq.(1.21)).

An important condition of validity of the Anderson and Weiss' treatment is that a given spin exerts no influence on the fluctuations of the local fields driving that spin. Such an assumption appears to be adequate, when the spin rotates more slowly than the local field fluctuates, which is the case for the exchange narrowing problem. However, it does not admit any obvious generalization to the problems of our interest, where both the local fields acting on a given spin and that spin itself evolve on the same timescale, and, moreover, the fluctuations of those local fields are being affected by the object of their action.

The next important step was made by Lowe and Norberg in 1956, when, in one paper[2], they (i) showed theoretically that the absorption lineshape problem in the frequency domain is equivalent to the free induction decay problem in the time domain; (ii) confirmed the above theoretical statement experimentally; and (iii) proposed the first approximate scheme for the calculation of the free induction decay. The outcome on their calculation very closely reproduced their own experimental data in CaF_2 (see Fig. 1.5(a)).

The formalism employed by Lowe and Norberg was reminiscent of the perturbation schemes in the interaction representation of quantum mechanics. As an equivalent of the noninteracting limit, they used the Ising-like case discussed in Sections 1.3.1 and 3.2.1. The Hamiltonian (1.27) was decomposed as the sum of an Ising-like part and a Heisenberg part, and the Heisenberg part was treated as a perturbation, even though, strictly speaking, it

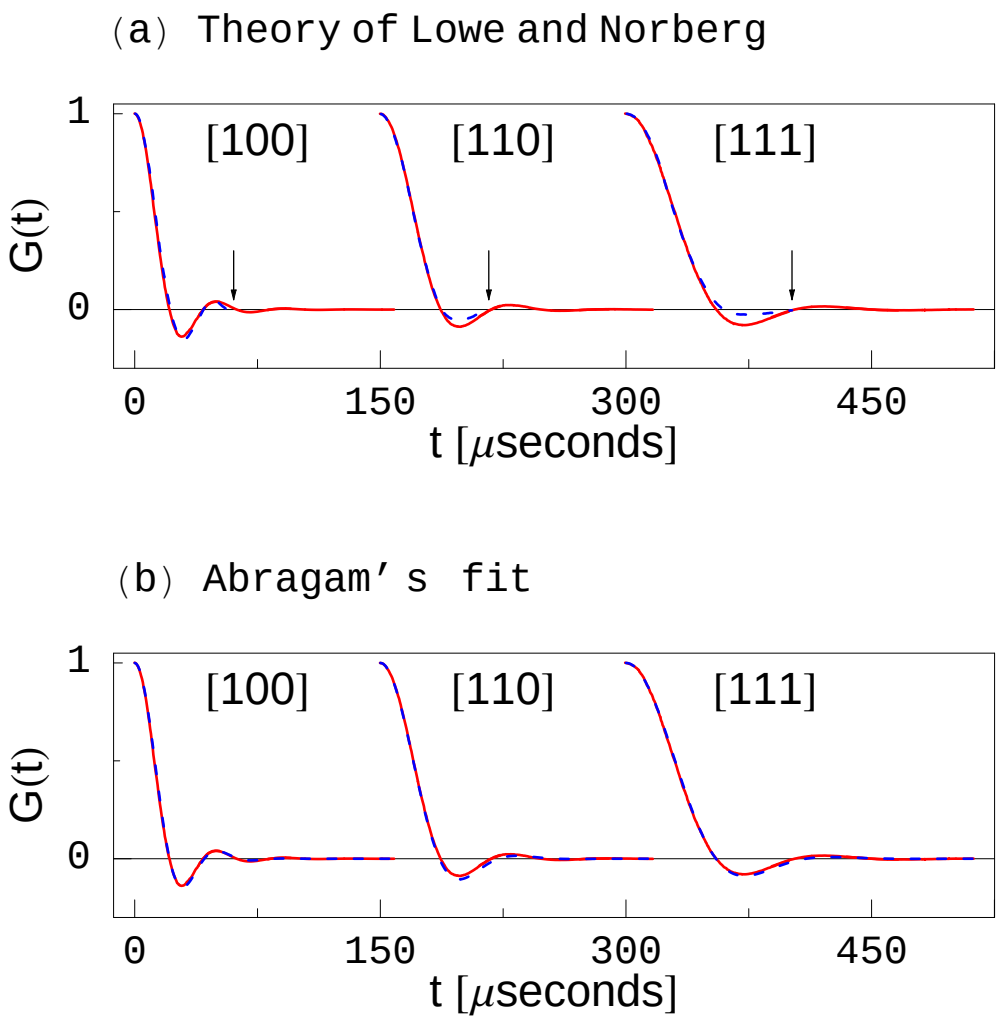

Figure 1.5: Comparison of the free induction decay experiments in CaF_2 with the theory of Lowe and Norberg[2] and with Abragam's fit (1.32). Solid red lines represent the experiment of Engelsberg and Lowe[20], and dashed blue lines represent the results of the calculations. Arrows in figure (a) indicate the end of the theoretical curve (see the text).

was not small. The final approximation went to the fourth order in the above perturbation scheme, which actually required a fair amount of analytical calculation.

It should be mentioned that the theoretical curves in Fig. 1.5(a) are cut at the the time points indicated by arrows, because beyond those points the theoretical expression of Lowe and Norberg would lead to erratic fluctuations of large amplitude, which is neither physical nor consistent with the experiment.

With all the above reservations, the kind of agreement between the theory and the experiment shown in Fig. 1.5(a) should be considered as an impressive success of the theory. And yet, the approximation of Lowe and Norberg has been strongly criticized by Abragam in his classical NMR textbook[3].

Abragam pointed out that there is neither a rigorous mathematical proof nor a physical argument explaining why Lowe and Norberg's approximation should work better then any other scheme that just matches the second and the fourth moments of the free induction decay. In that situation, he argued, the simplicity should become the main criterion for the choice of the approximation scheme.

To illustrate the above point, Abragam proposed a fitting function of the form

$$G(t) = \exp\left(-\frac{1}{2}a^2t^2\right)\ \frac{\sin(bt)}{bt}, \tag{1.32}$$

where the parameters a and b were obtained from the knowledge of the exact theoretical values of the second and the fourth moments. The results of the Abragam's fitting produced somewhat better agreement with the experiment than the calculation of Lowe and Norberg. Those results are reproduced in Fig. 1.5(b).

Postponing the discussion of the Abragam's objections until Section 1.6, here we just mention that his fitting function has no chance to approximate the free induction decays in the monotonic (non-oscillating) regime exemplified in Section 1.5.3. At the same time, there is no clear criterion for the values of the coupling constants in the Hamiltonian (1.2) that would assure *a priori* that the behavior represented by the Abragam's function is adequate.

As far as the approximation scheme of Lowe and Norberg is concerned, then, to the best of our knowledge, it has never been applied beyond the free induction decay problem in CaF_2. Although we did not experiment with that scheme either, we suspect that, as with Abragam's fit, the outcome of the calculation would be disappointing in the range of the Hamiltonian parameters which corresponds to the monotonic free induction decay.

Subsequent attempts to develop quantitative methods for the problem of the free induction decay focused on finding simple approximation schemes that would embrace both oscillatory and monotonic regimes and/or were based on physical arguments.

Before proceeding with the discussion of those attempts, it should be mentioned that, for all post-Lowe-and-Norberg works, the comparison of the theoretical and experimental plots for the free induction decay in CaF_2[2],[20] has become the most important and, in many cases, the only test of the theory. It is, therefore, not surprising that later work came under pressure to surpass the quality of agreement between the calculation of Lowe and Norberg and the experiment. As a result, most of those works contained explicit or implicit adjustments to the CaF_2 data. This introduces a degree of uncertainty in the evaluation of the theoretical progress in the field, because even minor adjustments to the experiment compromise CaF_2 as the main testing ground of the theory.

With such a perspective, we now turn to several widely used formal techniques that have been applied to the free induction decay problem.

One such a technique is based on the memory function formalism. In the context of the free induction decay, it was first applied by Tjon[26] in 1965, and then refined by Parker and Lado[27] in 1973. That technique is based on the equation

$$\frac{dG(t)}{dt} = -\int_0^t F(t')G(t-t')dt', \tag{1.33}$$

where $F(t)$ is called the memory function. Equation (1.33) can be considered as a straight-

forward generalization of the standard Markovian equation

$$\frac{dG(t)}{dt} = -\lambda G(t), \tag{1.34}$$

where λ is the rate constant. The Markovian limit implied by Eq.(1.34) requires that the rate of change $\frac{dG}{dt}$ at time t cannot be affected by the values of G at the previous moments of time. On the contrary, Equation (1.33) allows some memory effects. According to that equation, $\frac{dG(t)}{dt}$ depends on $G(t-t')$, and the function $F(t')$, which is expected to be bell-shaped, controls such a memory, hence its name — "memory function." The Markovian equation (1.34) can be restored in the limit of the fast decay of $F(t')$, i.e. when $F(t') \to \lambda\delta(t')$, where $\delta(t')$ is the conventional delta-function. In the opposite limit of the very slow decay of $F(t')$, i.e. when $F(t') \to \omega_0^2$ (ω_0^2 is just some constant), the solution of Eq.(1.33) has the form $\cos(\omega_0 t)$.

In principle, for any function $G(t)$, one can find a memory function $F(t)$ that would fit Eq.(1.33). Therefore, it is not immediately obvious how the introduction of an unknown function $F(t)$ can help in computing $G(t)$. The philosophy of this approach is based on the fact[27] that estimates of the ratio of M_4/M_2^2 for memory functions of very different problems fall in the range between 3 and 4, which seems to suggest that there exists a universal shape of the memory function, and that that shape is not too different from Gaussian. That hope, however, has not come true.

For CaF_2, the Gaussian shape of the memory function was tested by Tjon [26] in 1966, and he discovered that it does not work well, unless the second moment of the Gaussian is adjusted directly to the experiment. Later, Parker and Lado found [27] that a more sophisticated form of the memory function can work even better in CaF_2, but that also required fitting several parameters of their functional form directly to the experiment.

In 1969, Borckmans and Walgraef approached the free induction decay problem by the diagram resummation technique[28],[29] developed by Prigogine and coworkers[30],[31]. In the framework of that technique, they encountered severe computational difficulties and were

not able to obtain a good quantitative description of the entire free induction decay in CaF_2.

However, they were first to make the strong claim that the free induction decay in CaF_2 must have the long-time functional form (1.24, 1.25), and such a functional form can be *derived* (our emphasis) based on the formalism they use. The claim of their theory has been subsequently strengthened by the fact the long-time functional form (1.25) has, indeed, been observed in the later version of the CaF_2 experiments[20], though with parameters that were up to 45% different from the predictions of Borckmans and Walgraef.

In our opinion, the treatment of Borckmans and Walgraef fell short of being a derivation. In fact, below we shall argue that the scheme they used is not adequate for the analysis of the long-time behavior.

We recall that even though the technique used by Borckmans and Walgraef is more sophisticated then the memory function approach, it describes the long-time behavior of the free induction decay by an equation identical with Eq.(1.33) of the memory function formalism. One can solve that equation by the method of the Laplace transform, which leads to the following expression:

$$\tilde{G}(s) = \frac{G(0)}{s + \tilde{F}(s)}, \tag{1.35}$$

where s is the variable of the Laplace transform, and $\tilde{G}(s)$ and $\tilde{F}(s)$ are the Laplace transforms of $G(t)$ and $F(t)$ respectively.

It is not difficult to see that, under very general conditions (eg. when $F(t)$ is Gaussian), $G(S)$ has a discrete set of poles, and, therefore, the pole closest to the imaginary axis ultimately controls the long-time behavior of $G(t)$, which means that that behavior must have the exponential functional form (1.24) or (1.25).

The proof of Borckmans and Walgraef essentially consisted of exploiting the above fact in conjunction with several arguments that the shape of $F(t)$ should not differ much from Gaussian. Those arguments included (i) mentioning the fact that, for the problem of free induction decay in CaF_2, the moment ratio M_4/M_2^2 for $F(t)$ is 3.24, which is close to 3

(the value for the Gaussian shape); and (ii) reference to the numerical computations (not presented in Ref.[29]). In Ref.[28], they also asserted that a non-Gaussian shape of $G(t)$ would change the parameters entering Eqs.(1.25) but not the long-time functional form itself.

It is this last assertion that we put in doubt. If one takes that assertion to the extreme then, actually, every function in the world should have the long-time behavior (1.24) or (1.25), because a memory function can be constructed for every function, and, according to that assertion it does not matter whether the memory function is Gaussian or not. One can thus ask: Where, in that argument, is the place for algebraically decaying functions or for those functions that do not decay at all?

A closer examination of the issue reveals a very simple answer: The long-time behavior of $G(t)$ depends crucially on the long-time behavior of the memory function $F(t)$. If the long-time decay of $F(t)$ is slower than exponential, then it is easy to verify by direct substitution in Eq.(1.33) that $G(t)$ cannot decay exponentially either. Technically, the issue boils down to the fact that, when the long-time decay of $F(t)$ is slower than exponential, the Laplace transform of $F(t)$ is likely to have a branch cut passing through $s = 0$.

Therefore, the only thing Eq.(1.35) does is that it reformulates the difficult problem of the long-time behavior of $G(t)$ in terms of an even less tractable problem of the long-time behavior of $F(t)$, for which the crude simulations or knowledge of the ratio M_4/M_2^2 are not sufficient. Even if that ratio is equal to 3 exactly, the long-time behavior of such a function can be anything one can wish. With the same degree of rigor, one could try to predict the long-time behavior directly from the knowledge of M_4/M_2^2 for $G(t)$.

Continuing our review we now turn to the 1975 work of Engelsberg and Chao[32], where they approached the free induction decay problem using the Green's functions formalism, which led them to a continuous fraction expression for the free induction decay. The technical complication of their method was that it required the knowledge of the higher moments (M_6

and M_8), and it appeared that the quality of the agreement with the CaF_2 experiments was very sensitive to the minute changes in the values of those moments — changes that fell within the limits of the theoretical uncertainty of those values. Within that uncertainty, they did make some adjustments to the CaF_2 experiments and thus obtained very good agreement between theory and experiment. It seems though, that the agreement would be less perfect but still good if no adjustments were made.

Importantly, however, Engelsberg and Chao went beyond CaF_2. They applied the same scheme to the radically different situation of the exchange-narrowed NMR lines (Problem B in Section 1.4), and found very good agreement with the experiments in rutile and perovskite materials[18].

While that agreement certainly strengthens the base of their approximation scheme, it should be mentioned that there is a certain degree of coincidence in that agreement. In a sense, they tried to bypass the task of calculating the electron spin correlation function $\varphi(t)$ given by Eq.(1.22). Engelsberg and Chao used only the second, the fourth and the sixth moments of the exchange narrowed lines in order to obtain the linewidth of those lines, which is, otherwise, given by Eq.(1.21). Knowledge of the above moments implies knowledge of the second and the fourth moments of $\varphi(t)$. Since, apart from the knowledge of moments, the scheme of Engelsberg and Chao does not rely on any other input about the electron spin system, it follows that it should give the same answer for any form of the electron spin-spin interaction, provided that interaction leads to the same values of the second and the fourth moments of the correlation function $\varphi(t)$. However, the exchange interaction has the peculiar property that it conserves the total spin polarization in the system, and, although, in the case considered, this does not prevent $\varphi(t)$ from decaying, it makes the long-time portion of that decay significantly slower. This leads to an atypically large value of the time integral of that function. For interactions other than the exchange one, the value of the integral, and, therefore, the value of the linewidth would be smaller than the result of Engelsberg and

Chao, by at least 30%.

The continuous fraction approach to the free induction decay was further developed by Jensen[33] in 1995. His continuous fraction expression is more sophisticated than that of Engelsberg and Chao. He obtained it as a result of explicit manipulation of the Green's functions, which gave him a better control over the contribution from various terms in the Hamiltonian. In particular, he explicitly exploited the fact the the interaction coefficients of the magnetic dipolar Hamiltonian have alternating signs, which helps by canceling out certain intractable terms. Jensen's scheme contains a minor adjustment to the CaF_2 experiments, which sets certain parameters that would not be changed if the scheme is to be applied to other problems with the same interaction. However, so far, it was only applied to the free induction decay in the exotic material ^{13}C-diamond, for which no good quality experimental data have been obtained yet.

In our opinion, Jensen's scheme looks very promising, and at present it is one of a few good choices for calculating the free induction decay. It is, however, unclear, how well it can perform beyond the case of the magnetic-dipolar interaction.

In 1976, Becker, Plefka and Sauermann[34] (BPS) have developed an equation-of-motion method for the hierarchy of spin correlation functions. They proceeded with a scheme that expressed the derivatives of the two-spin correlation functions in terms of the three-spin correlation functions. The three-spin correlation functions were then factorized in such a fashion that the the system of equations became closed.

The above procedure is, of course, quite standard, apart from the factorization recipe, for which there could be many variations. The BPS factorization was reasonably well justified, and the result turned out to be in very good agreement with the CaF_2 experiment.

We are somewhat biased to view the work of BPS as significant because, in that work, they obtained an integral equation that turned out to be identical to the one we derived later[6] from quite different considerations and with somewhat different ingredients. An analogous

equation is also known to be popular in theory of simple liquids[35]. That equation will play an important role in our treatment, and, for that reason, it will be introduced later in Chapter 3 (Eq.(3.22)).

Here we only mention that the scheme of BPS was tailored specifically for the magnetic dipolar interaction, but, otherwise, contained no explicit adjustments to experiments. However, they have presented the test only for CaF_2 and only for the [100] direction of the external field, in which case the agreement was exceptionally good. From our experience, the agreement between their scheme and the experiments for two other field direction ([110] and [111]) would also be good but notably less impressive.

Each of the approximate theories mentioned so far could be characterized as formal in the sense of being not a physical model. Bringing physical arguments into the picture was, in fact, not a trivial task. As was explained in Section 1.5.1, the oscillatory character of the free induction decay is not very compatible with a simple physical intuition.

A focused effort to introduce the physical interpretation into the problem was made by Lundin and Provotorov[36] in 1976. Their analysis was strongly affected by the success of Abragam's fit (1.32). They attributed the term $\frac{\sin(bt)}{bt}$ in Eq.(1.32) to the contribution from the "cell" containing six nearest neighbors of a given spin, and the term $\exp(-\frac{1}{2}a^2t^2)$ to the statistically independent contribution from all other neighbors.

The original treatment of Lundin and Provotorov did not provide a recipe for calculating the contribution from the "cell" — this was the subject of 1984 work of Lundin and Makarenko[37]. The later work was corrected, and its approximate scheme was somewhat revised, by Lundin[38] in 1992. Another variation along the same line was introduced by Shakhmuratov[39] in 1991.

The above mentioned works contain many useful physical insights, and, in fact, our theoretical treatment in Section 3.2.1 will have a few ingredients resembling the treatment of Shakhmuratov. However, even though the physical arguments invoked by the above authors

were legitimate, the problem with their treatment was in attaching numbers and functional forms to those arguments. The gaps in their treatment could be exposed if one tries to answer the question: What would change if the relative sign of the flip-flop term and the Ising terms in the Hamiltonian was not negative (as is the case for the truncated magnetic dipolar Hamiltonian (1.27)) but positive? On one hand, their treatment should apply to this case, but, on the other hand, it appears to be extremely difficult to reconcile their analysis and their calculational schemes with the fact that, in comparison with the negative relative sign, the actual behavior the free induction decay should change dramatically from oscillating to monotonic.

We would also like to comment that, in our opinion, the very idea of explicit discrimination between the effects due to the direct interaction with the nearest neighbors (the "cell") and effects due to the interaction with other neighbors did not prove to be very productive. In fact, the contribution from the out-of-cell spins became an ambiguous feature of those theories, and, at the same time, that feature does not appear to be crucial for the resulting approximations.

Concluding our review, it is fair to summarize by saying that none of the theories discussed in this Section has cleared the barrier after which it could be routinely used for the quantitative predictions of free induction decay.

1.7 Outline of a new theoretical approach

The philosophy of our treatment is that, as far as the correlation functions (1.1) are concerned, the task of explaining and the task of quantitative prediction are not identical: The task of explaining is relevant to the universal properties of those functions, while the accurate quantitative prediction of each function necessarily reproduces certain nonuniversal features. Below we shall explain such an attitude and demonstrate that it can be productive for both explanations and quantitative predictions.

We start from asking the question: What, in the first place, makes us think that, for the class of the problems we consider, a simple "first principles" approximation can substitute for the exact solution for the purposes of quantitative predictions?

The answer to that question is certainly linked to the elusive constraint that the correlation functions (1.1) should behave "physically", which brings us back to the issue of the physical arguments raised by Abragam in his criticism of the Lowe and Norberg's approximation (see Section 1.6).

What can the physical arguments give us? If we associate the term "physical" with the term "universal", then, in fact, the most reliable universal consequence of our intuition is *not* the selection of a simplified model (such a selection is not unique for the problem of interest), but the mere fact that, unless the special conservation laws exist, the correlation functions (1.1) should decay on the timescale τ given by Eq.(1.3): they should not bounce back to the initial value, they should not asymptotically approach any non-zero value — they should just decay.

In essence, the above statement is equivalent to Boltzmann's assumption of "molecular chaos." That assumption stipulates that the fast decay of the microscopic dynamical correlations guarantees consistency between the exact dynamical evolution of a macroscopic system and the statistical thermodynamic description of the same system.

In that context, any approximation scheme that leads the decay of $G(t)$ on the timescale of τ can be called "physical."

Is there anything universal or "physical" in the behavior of the correlation functions (1.1) beyond just the fact that they decay fast?

Chapter 2 of this thesis presents a strong case in favor of a positive answer to the above question. The issue taken up in Chapter 2 is that the correlation functions (1.1) not only decay fast but that, after a time of the order of several τ, they approach the universal functional form (1.24) or (1.25). That Chapter contains an important conjecture about the

extreme Markovian properties of many-body dynamical problems, which we call *Conjecture I*. The scope of that Conjecture certainly extends far beyond the spin problems we consider.

After the validity of the long-time behavior (1.24,1.25) is shown in a model-independent way, any approximate scheme can rely on such a result rather than derive it, which changes the status of such a scheme from an uncontrollable extrapolation in the time domain to something more similar to interpolation. In fact, "interpolation" is the key concept characterizing our approach to the quantitative predictions of the correlation functions (1.1).

Before turning to our computational procedure, let us first return to the issue of "universality vs. non-universality."

It is generally accepted that for small lattices containing a few spins, the correlation functions (1.1) are not expected to exhibit universal properties. In particular, the statement that those functions decay irreversibly without bouncing back at later times is apparently wrong for a-few-spin quantum systems, where the discreteness of the frequency spectrum will ultimately lead to the refocusing of the correlations. At the same time, the values of the first few moments controlling the initial behavior of the correlation functions (1.1) for small lattices are the same as for infinite lattices. (Those values depend only on the interaction of a given spins with a finite number of surrounding spins.)

From the above fact, we deduce that the initial behavior of the correlation functions for the infinite lattice of spins is *not* universal, because the same behavior is exhibited by a small lattice. Another, probably, more fundamental reason for the non-universality of the initial behavior will be given in Sections 2.3.5 and 2.3.6.

Combining the above statement with our analysis of the long-time behavior, we thus formulate the paradigm of our computational approach:

The correlation functions (1.1) initially exhibit a non-universal behavior characteristic of a few-body systems and then approach the universal long-time behavior (1.24) or (1.25) intrinsic to many-body systems. Computational efforts should thus be focused on getting

accurate results for an extended initial time interval of the order of several τ (given by Eq.(1.3)). By the end of that interval the long-time behavior (1.24) or (1.25) is supposed to become dominant. Therefore, the correlation functions should then be continued using the long-time functional form (1.24) or (1.25).

The above description is illustrated in Fig. 1.6. As we indicate in that figure, the behavior of $G(t)$ at the beginning of the "extended initial time interval" can be typically obtained just from the knowledge of the second and the fourth moments of $G(t)$. It is the remaining part of that interval that poses a major challenge for the computational schemes.

In principle, that remaining part can be obtained by computing higher moments or by numerical calculations for finite but not too small lattices. If such a computation is possible, then it should certainly be chosen as a preferred method. However, for three dimensional lattices of quantum spins with a long-range spin-spin interaction (eg. magnetic dipolar interaction), such a direct approach is certainly not feasible, which leaves approximate schemes as the only option.

This brings us to the discussion of the principles upon which the approximation for the "extended initial time interval" should be constructed.

As must have become evident from our discussion in Section 1.6, first principles approximate schemes are easy to criticize. Even when an approximation without a small parameter claims that it has no numbers adjusted to an experiment, then, it necessarily contains some assumptions which are not controlled quantitatively. If the whole work is devoted to the explanation of one known experimental or numerical result, then it is natural that from the long list of plausible assumptions, the authors would not choose those that lead to noticeable disagreements with the data. For the works discussed in Section 1.6, such assumptions are commonly made in the form of certain functional dependences that enter the approximation scheme.

Apart from rigorous derivation, the only logical way to counter the above criticism is

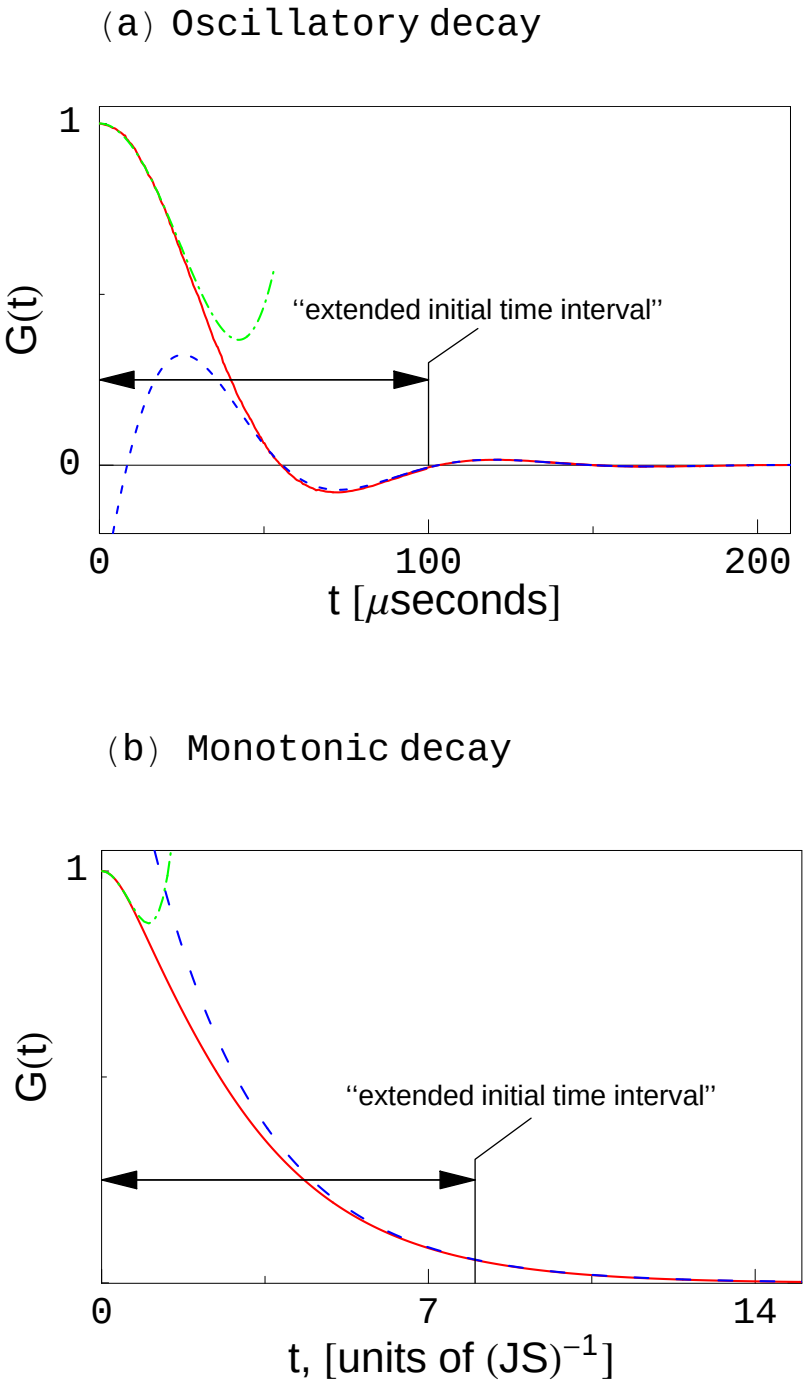

Figure 1.6: These pictures illustrate the fact that the knowledge of the long-time functional form has practical value: When that functional form is known, all one needs to find is a good approximation for the "extended initial time interval." The solid red lines represent the actual data: plot (a) corresponds to Fig. 1.2([111]), and plot (b) — to Fig. 1.4(h). The dashed blue lines represent the long time fits (1.24) or (1.25). The dash-dotted green lines indicate how much of the initial behavior can be determined rigorously by the expansion $1 - M_2 t^2/2! + M_4 t^4/4!$.

to show that the same approximation recipe works well for many different pieces of reliable data. After that one can point out that such a recipe is a continuous function of the interaction coefficients. Therefore, if there is an extended mesh of reference cases, for which the approximation recipe works well, then for other cases the same recipe can be considered as an interpolation between the reference cases.

As we mentioned before, our perception is that not every detail of the initial behavior of the correlation functions (1.1) is universal and, therefore, not everything in this behavior requires a fundamental explanation. In particular, our understanding of the subject will not suffer, if certain details characterizing the initial behavior are derived not from a laborious theoretical calculation but from the observation of the mathematical pattern exhibited by the experimental or numerical data.

Provided that such an interpolation scheme can be found, the criticism of implicit or explicit adjustments to the data becomes redundant. In the end, what will matter is just the predictive power of that scheme.

In this work, we take the first step towards finding a perfect interpolating procedure. Namely, in Chapter 3, we have developed a kinetic model, which embraces almost all analytic limits for correlation functions of the form (1.1) and thus can be considered as an interpolation between those limits. Away from those analytic limits, the model reproduces the functional form of the long-time behavior given by Eq.(1.24) or (1.25).

We have tested this model on many examples and, in most cases, found good agreement with experimental and numerical data distributed over a wide range of Hamiltonians and wave vectors.

At the moment, our ongoing project is to improve performance of that model even further on the basis of an extensive analysis of the whole body of classical and quantum data.

Let us mention at this point that we consider bringing the classical spins in the picture as an important achievement of this work. The discussion of the behavior of the correlation

functions (1.1) for quantum systems frequently involves reference to dephasing or decoherence and thus creates an impression that the theoretical difficulty of the problem is essentially quantum. However, the universality of the long-time behavior (1.24, 1.25) indicates that the problem is equally difficult for both classical and quantum systems, and the difficulty is essentially dynamical. The dynamical relaxation at constant energy, which is another name for the problem we consider, need not be called dephasing or decoherence — it has analogs in classical systems. For the problems considered in this work, the difference between quantum and classical problems is not qualitative but quantitative, i.e. qualitatively the same regimes are characterized by somewhat different numbers.

Summarizing this Section, we would like to list three important features that distinguish the present work from all previous ones:

1. We analyze the universal long-time behavior separately from the issues associated with effective approximations to entire correlation functions (1.1).

2. Instead of attempting to reproduce the behavior of one or a few known correlation functions, we propose an approximate scheme for all correlation functions of the form (1.1) and for the whole class of Hamiltonians (1.2).

3. We use rich empirical material generated by our simulations of the classical spin systems, and also by the numerical diagonalization of spin 1/2 chains[13]. That material was not available to the previous authors.

2 Long-time relaxation on a spin lattice as a manifestation of chaotic dynamics

2.1 Preliminary remarks

In the present Chapter, we develop a theoretical framework for treating the long-time behavior of correlation functions of the form (1.1). The main theoretical result of this Chapter has already been introduced in Section 1.5 on purely empirical grounds. This result is:

[For convenience of discussion, we just reproduce a part from Section 1.5.]

The generic long-time behavior of the correlation functions (1.1) has one of the following two functional forms: either

$$G(t) \simeq e^{-\xi t}, \qquad \text{(same as Eq.(1.24))}$$

or

$$G(t) \simeq e^{-\xi t} cos(\eta t + \phi), \qquad \text{(same as Eq.(1.25))}$$

where ξ, η and ϕ are some constants about which we can only assert that, in general, the values of ξ and η are of the order of $1/\tau$, where τ is given by Eq.(1.3)

It follows from the empirical evidence given in Section 1.5, and it will follow from our theory, that $G(t)$ approaches the asymptotic form (1.24) or (1.25) after a time of the order of several τ, i.e. sufficiently fast.

It is important to realize that, if the above functional form of the long-time behavior is, indeed, generic (i.e. independent of the specific details of interaction), then this property is very likely related to the randomness generated by the spin dynamics. At the same time, as we have already discussed in Section 1.5, the problem cannot be reduced to the Markovian paradigm of "a slow variable interacting with a fast equilibrating background" — the decay (1.24) or (1.25) occurs on the fastest natural timescale of the problem. Therefore, whatever

is the ultimate explanation of that behavior, it will certainly be a step beyond the standard theory of Brownian-type motion.

Some of the existing approximate schemes would predict this kind of long-time behavior[28],[38],[6 However, as exemplified by our discussion of the method of Borckmans and Walgraef (Section 1.6), all these schemes struggle to achieve an effective approximation for the entire evolution of $G(t)$, of which the long-time part is not the most prominent one. As a result, the long-time functional dependence becomes a side effect of quite crude and uncontrollable assumptions adopted only for the sake of simplicity. Therefore, the long-time predictions of those theories remain doubtful.

As a historical remark indicating the non-trivial character of the long-time behavior (1.24), (1.25), we would like to mention that, when Abragam proposed his empirical formula (1.32), that formula has not been criticized on the ground that it predicts the wrong long-time behavior. This fact just illustrates that the decay of $G(t)$ was generally expected to be fast but not with a universal asymptotic functional form.

Before proceeding further, it is necessary to clarify our use of term "generic" with respect to the long-time behavior of the correlation functions (1.1).

In Section 1.3, we discussed several cases when the entire evolution of the correlation functions (1.1) could be obtained analytically. In all those cases, the long-time functional form was not that of Eqs.(1.24,1.25). However, in every instance, the system had non-generic conservation laws. For example, analytical results in the Ising-like case (Section 1.3.1) could be obtained only because the z-components of spins were constants of the motion. Therefore, our reference to "generic long-time behavior" can be, to some extent, understood as implying the exclusion of systems with non-generic conservation laws.

However, a closer examination of the issue reveals that the line between "generic" and "non-generic" systems is not so easy to draw. The situation with the 1/2 XXZ chains

discussed in Section 1.5.2 is an example of such a difficulty. For those chains, the distinction between "generic" and "non-generic" actually depends on what property of the system is being addressed.

As we shall also see, even within the framework of our "generic" treatment it is possible to have situations where, instead of a single exponent, the long-time behavior is accidentally characterized by two or more exponents.

We thus define our "generic long-time behavior" as follows:

Let assume that, according to the Hamiltonian (1.2), each spin directly interacts with N_0 neighbors, and, therefore, this Hamiltonian is completely characterized by the values of $3N_0$ interaction coefficients —three coefficients J^x, J^y and J^z per each neighbor. If, we restrict the values of those $3N_0$ interaction coefficients to a finite interval and, from that interval, randomly pick the value of each coefficient, then, what we mean as generic is that, with probability 1, the long-time behavior of the correlation functions (1.1) will have the functional form either (1.24) or (1.25).

The above definition implies that there can be infinitely many exceptions not exhibiting the long-time behavior (1.24, 1.25) — we cannot name all of them — but the overwhelmingly general rule is still given by Eqs.(1.24, 1.25).

As another preliminary remark, we would like to mention that, based on the theory presented in this Chapter, one can only obtain the functional forms (1.24, 1.25); the theory does not give recipes for the calculation of the parameters entering Eqs.(1.24, 1.25). At the same time, the theory does not contain a rigorous mathematical proof of that behavior. In fact, this Chapter consists mostly of the long chain of qualitative arguments. The question can thus be asked: What can such a long treatment give in comparison with the empirical picture already known from Section 1.5?

The answer to the above question is that we hope deeper understanding can be gained

from such an analysis. That analysis is, in fact, completely independent of the empirical picture of Section 1.5. That picture could but did not emerge two decades ago, because understanding of the matter was lacking and nobody tried to look at the long-time properties of the fast-decaying correlation functions (1.1). It was the theory presented in this Chapter that motivated us to perform the simulations of the classical spin systems, and without those simulations, the empirical picture would be much less convincing.

From a practical perspective, the assumption of the long-time behavior (1.24,1.25) plays an important role for the approximate scheme developed in Chapter 3, which, actually, generates the parameters of the long-time behavior (1.24,1.25).

It would, however, be extremely uncomfortable if, in Chapter 3, we used the long-time functional forms (1.24,1.25) on purely empirical grounds without answering the following questions:

Why is the long-time regime universal?

What makes that regime different from the initial regime?

Why does it have such a functional form?

How should the apparent time-irreversibility of Eqs.(1.24,1.25) be reconciled with the time-reversibility of the underlying microscopic dynamics of a perfectly isolated system?

What mechanism is responsible for the oscillations in Eq.(1.25)?

Why are Eqs.(1.24,1.25) primarily relevant to the q-dependent correlation functions (1.1) and not to the pair correlation functions?

What makes the situation at finite temperatures less transparent than at infinite temperature?

The theory developed in the present Chapter allows us to give substantive answers to each of the above questions. Those answers will be summarized in the concluding Section of this Chapter.

One more preliminary comment should be made on our use of the term "chaos."

The reference to "chaos" in this work is very appropriate, because we deal with the randomness generated by the deterministic dynamics in a regular spin system. However, the place of our terminology in the spectrum of specific definitions of "chaos" must be clarified[40].

What we below call "chaos" is a concept stronger than Boltzmann's "molecular chaos," because "molecular chaos" only postulates the irrelevance of fast decaying correlations to slow observables, while in this work we address precisely the issue of how those fast correlations decay. At the same time, our assumptions of chaos are formulated mostly in terms of the motion of a single particle, which is consistent with, but less restrictive than, the mathematical definition of chaos related to the exponential instabilities of trajectories in the phase space of the entire system. In particular, our treatment will not be altered if the assumed single particle properties result from taking the thermodynamic limit in systems which do not quite comply with the mathematical definition of chaos.

We should also mention that there are apparent parallels between our treatment and the mathematical theory of Policott-Ruelle resonances in classical chaotic systems[41]. However, we are not aware of any definite mathematical result applicable to our problem, especially in the quantum case. One of the advantages of the approach we use is that it allows the quantum case to be addressed directly, i.e. without any reference to the classical limit.

In the quantum context, the reference to chaos is frequently associated with the Wigner-Dyson statistics of energy levels. The connection between that property and the subject of this work is not straightforward, and we do not speculate on it. We can only mention that the spin 1/2 XXZ chains discussed in Section 1.5 do not exhibit Wigner-Dyson statistics but nevertheless show the long-time behavior (1.25).

We conclude this Section with an outline of the rest of this Chapter.

In the following Sections, we provide a number of arguments asserting that, as a result of the chaotic mixing generated by spin dynamics, the long-time properties of the correlation functions (1.1) can be deduced from the problem of correlated diffusion in a finite volume. As in a typical diffusion case, the solution of the correlated diffusion problem can be decomposed in terms of the discrete set of the eigenfunctions multiplied by time-dependent exponentials (determined by the corresponding eigenvalues), and the term having the smallest constant of the exponential decay finally controls the long-time behavior. However, in contrast with conventional diffusion, the correlated diffusion can generate eigenvalues having both real and imaginary parts. Therefore, the dominating term can oscillate.

Below, the theory is developed according to the following plan: First, in Section 2.2, we introduce the classical case but then digress and, in Section 2.3, analyze one rarely discussed piece of empirical knowledge related to the Markovian description. This analysis generates *Conjecture I*, on which the rest of the theory is built. Section 2.3 is quite long, but, in fact, reading only the formulation of *Conjecture I* is sufficient to proceed to Sections 2.4 and 2.5. In Section 2.4, we return to the treatment of classical spins and, in Section 2.5, extend that treatment to quantum spins. Although the classical limit of the quantum problems will not be taken, the treatment of quantum spins will be developed by analogy with that for classical spins. Therefore, reading the classical section is essential to understanding the quantum section. Finally, we discuss the limits of the theory in Section 2.6.

2.2 Classical spins — long-time assumption

We shall treat the classical case from the viewpoint of the nonequilibrium interpretation presented in Section 1.2 and illustrated in Fig. 1.1. Our attention will be focused on the one-particle probability distributions of the spin orientations.

The evolution of each classical spin vector can be represented as the trajectory of its tip on a spherical surface. Describing the ensemble of all possible trajectories of a given spin,

we assume chaotic mixing of the following kind:

On the scale characterized by the mean free time τ given by Eq.(1.3) and by the corresponding mean free path (of the order of the radius of the sphere), (i) each trajectory loses the memory of its initial position; (ii) the set of all possible trajectories starting from any arbitrary small surface element disperses over the entire spherical surface in a random manner; and (iii) the statistics of the trajectory patterns of this set becomes representative of the statistics of the whole ensemble of one-spin trajectories.

The estimate of the mean free time in the above assumption by formula (1.3) is how the infinite temperature condition enters our treatment. At finite temperatures, the mean free time should be longer, and may even become infinite, because of the equilibrium correlations between the orientations of different spins.

Our assumption of chaotic mixing does not require that the statistical properties of every one-spin trajectory be representative of the properties of the whole ensemble. This detail signifies the difference between mixing and ergodicity. Following Krylov[42], we assume that ergodicity is not a necessary condition for relaxation to the equilibrium.

If a point-like particle moves under similar conditions on an infinite plane, it would be appropriate to apply the theory of Brownian motion on a scale much greater than the mean free path, so that after a time much greater than the mean free time the probability distribution approaches the solution of the diffusion equation. The problem is that in our case the typical mean free path is of the order of the size of the sphere. Therefore, we are interested in an accurate description on the scale of the order of the mean free path and smaller.

We now turn to a general discussion that motivates one additional assumption.

2.3 Markovian description for the ensembles of trajectories

The standard microscopic theory of Brownian motion is Markovian, i.e. it employs processes possessing no memory of the past state. It is always emphasized (at least in the physics literature) that such a description is justified only on a timescale much greater than the mean free time.

Contrary to the above point, we shall argue that, as far as ensemble averaging is concerned, the adequacy of the commonly accepted Markovian descriptions typically propagates to much shorter time scales, and it is only the initial short-time behavior of a typical theoretical quantity that is not Markovian.

In the rest of this section, we first clarify the above statement and then explain why it does not contradict the theoretical, experimental, or numerical facts. We then proceed with formulating a stronger statement, which we call *Conjecture I*. Finally, we link *Conjecture I* to concepts known from the mathematical theory of chaos.

2.3.1 Exponential decay

The inapplicability of the Markovian description to short (ballistic) timescales is frequently demonstrated by presenting an example of the nearly exponential decay exhibited by an autocorrelation function having the general form

$$R(t) = \langle X(t)X(0)\rangle. \tag{2.1}$$

This function characterizes the equilibrium fluctuations of some variable X in some macroscopic system (not specified here). The variable X should evolve much slower than the rest of the variables describing the same system. In equilibrium, $\langle X\rangle = 0$, which implies that $R(\infty) = 0$.

An example of such a situation relevant to the subject of this work is the exchange narrowing problem[16][17]. In that case, X corresponds to the total spin polarization, which

is conserved by the dominating exchange part of the Hamiltonian.

The following assumptions in respect to $R(t)$ are usually appropriate (at least the "usual wisdom" suggests so):

Assumption 1: The equilibrium correlation function $R(t)$ can be equivalently considered as characterizing the relaxation of the slow average quantity $\langle X(t)\rangle_{\rho_R(0)}$ starting from a very small initial value $\langle X(0)\rangle_{\rho_R(0)}$ and decaying to the equilibrium zero value. The notation $\langle\rangle_{\rho_R(0)}$ implies that the averaging should be taken over all possible evolutions of the entire system weighed by the probability of the initial conditions given by the distribution function denoted here as $\rho_R(0)$. The small deviation of $\rho_R(0)$ from the equilibrium distribution function should be proportional to $X(0)$.

As explained in Section 1.2, as far as the infinite temperature spin correlation functions are concerned, this kind of property can be obtained from the high-temperature expansion. In a general context, the equivalence between the correlation function of equilibrium fluctuations and the law of relaxation was first explicitly postulated by Onsager[43].

Assumption 2: On the long timescale, the relaxation of the slow quantities can be represented by Markovian first order rate equations, which can include only slow variables. These equations have to be linearized in terms of the small deviations from equilibrium.

Assumption 3: There are no other slow variables that can affect $\langle X(t)\rangle$.

Given the above assumptions, the only Markovian rate equation that can be written is

$$\frac{dR}{dt} = -\gamma R, \tag{2.2}$$

where the new constant γ is the decay rate defined by this equation. Assuming $R(0) = 1$, the solution of Eq.(2.2) is $R(t) = \exp(-\gamma t)$.

It is, usually, at this point that the inapplicability of the Markovian description to short timescales is illustrated by pointing out that, on one hand, the Markovian approximation gives $\frac{dR}{dt}|_{t=0} = -\gamma$, but, on the other hand, the time reversibility of the underlying dynamics

guarantees that $\langle X(t)X(0)\rangle = \langle X(-t)X(0)\rangle$, which means $R(t)$ is an even function of time and, therefore, $\frac{dR}{dt}|_{t=0} = 0$.

The above contradiction does not invalidate the Markovian description, because, *a priori*, that description does not claim to provide the exact derivatives corresponding to the short-time fluctuations around the average long-time behavior. However, it is rarely emphasized that, in principle, there are two pictures of the short-time behavior of $R(t)$ that can be consistent with the long-time Markovian approximation: (a) smooth approach of $R(t)$ to the Markovian prediction or (b) persistent short-time fluctuations of $R(t)$ around the average Markovian behavior. Both pictures are illustrated in Fig. 2.1.

Although, at first sight, it might seem that picture (b) better corresponds to the spirit of the Markovian approximation, the fact is: Whenever a theoretical attempt is made to embrace both the short- and the long-time behavior of $R(t)$, it results in picture (a). Moreover, we are not aware of any experiment or numerical calculation reliably showing the persistent short-time fluctuations of a correlation function around the average long-time behavior, provided that behavior is *correctly* predicted from a Markovian description.

Below, we illustrate the assertion made in the previous paragraph by showing that the assumption of smooth approach to Markovian behavior is the only one that is necessary in order to obtain the Green-Kubo formula [44] for the calculation of the constant γ entering Eq.(2.2).

The smooth approach to Markovian behavior shown in Fig. 2.1(a) implies that the deviation of $R(t)$ from the Markovian prediction occurs only around $t = 0$, and then the exact first time derivative of $R(t)$ approaches the value of $(-\gamma)$ within a short time interval, over which the value of $R(t)$ itself can change only insignificantly, and, after that, $R(t)$ follows the Markovian solution without any fluctuations. Within the same time interval, the second time derivative of $R(t)$ should change dramatically from a certain value characteristic of the short timescale to the value complying with the smooth and slow Markovian behavior.

Such a picture gives a recipe for the calculation of γ consisting of the following steps: (i) Write the exact expression for the second derivative of $R(t)$ (ii) Perform the time integration of that expression until the value of the integral stops changing significantly on the fast timescale of the problem. The saturation value of that integral becomes the first derivative with which the correlation function enters the Markovian regime. This value should be equated to $(-\gamma)$. In order to present the result in a familiar form, we note that $\langle \ddot{X}(t)X(0)\rangle$ (the exact expression for the second time derivative of $R(t)$) can be transformed to $-\langle \dot{X}(t)\dot{X}(0)\rangle$[45]. Therefore,

$$\gamma = \int_0^\infty \langle \dot{X}(t)\dot{X}(0)\rangle dt. \tag{2.3}$$

The infinite upper limit of this integral should be understood in an approximate sense — it implies an upper cutoff which is much longer than the characteristic time of the fast environment but much shorter than $1/\gamma$. In the context of statistical physics, Eq.(2.3) is best recognizable as the Green-Kubo formula, though its resemblance with the "golden rule" of second order perturbation theory is not a coincidence.

It turns out that one can easily find an ansatz of the form $R(t) = \exp(-a(t))$, where the function $a(t)$ quickly approaches γt, but, at the same time, $\frac{dR}{dt}|_{t=0} = 0$, and initially, the second time derivative of $R(t)$ follows $-\langle \dot{X}(t)\dot{X}(0)\rangle$. Such an ansatz is given by the formula:

$$R(t) = \exp\left[-\int_0^t (t-t')\langle \dot{X}(t')\dot{X}(0)\rangle dt'\right]. \tag{2.4}$$

In the context of the exchange narrowing problem, this formula was first obtained by Anderson and Weiss[16] on the basis of a Gaussian random noise model.

Fast decaying correlation functions like $\langle \dot{X}(t)\dot{X}(0)\rangle$ are usually difficult to compute, but they can be either reasonably approximated or, sometimes, extracted from experiment. Extensive experience with the Green-Kubo formula leaves no doubt that it is a reliable quantitative recipe provided the long-time Markovian assumptions are adequate. It is, however, clearly seen from the above discussion that, if the assumption of smooth approach to the

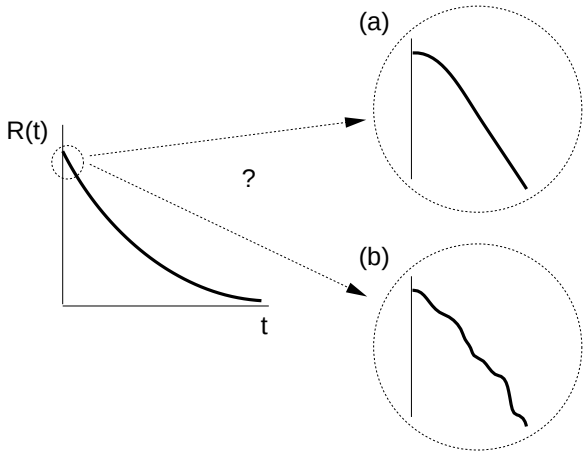

Figure 2.1: This picture represents the correlation function $R(t)$ introduced in the text and, by magnifying the short timescale, shows two short-scale pictures compatible with the long-time Markovian description, namely: (a) smooth approach to the Markovian behavior with no further fluctuations and (b) persistent fluctuations around the average Markovian behavior. It is argued in the text that picture (a) is the one that corresponds to the reality.

Markovian behavior is incorrect, then the Green-Kubo formula should be abandoned. In a typical discussion of this formula, it is not that assumption but the equivalent property of the convergence of the integral in Eq.(2.3) that is emphasized. We stress the smoothness of the correlation functions in the Markovian regime because this is apparently more than granted by the standard physical Markovian arguments, and, therefore, if correct, represents a a stronger property that can be used elsewhere.

2.3.2 General argument

Now we present a general intuitive argument that indeed, as the above treatment suggests, there should be no persistent short-time fluctuations of the correlation function $R(t)$ around the exponential Markovian behavior.

Let return to Assumption 1 made in Section 2.3.1, which postulated that $R(t)$ can be treated as a relaxation function.

A subtlety associated with that assumption is that, on the one hand, it is given in terms of the quantity $\langle X(t)\rangle_{\rho_R(0)}$ requiring the averaging over the ensemble of the sample evolutions of the entire system, but, on the other hand, the same quantity is equally expected to represent just one sample evolution of the macroscopic system in the sense of a real experiment, in which the initial conditions are randomly set in compliance with the initial probability distribution $\rho_R(0)$, and then the value of $X(t)$ is measured. This can only be true, if $X(t)$ is — or can be considered as — either the sum or the average of infinitely many equivalent contributions from statistically independent parts of the system.

Such a condition is, normally, fulfilled for any quantity accessible by a macroscopic measurement. For example, in the exchange narrowing problem mentioned earlier, the prototype of the variable X is the spin polarization of the entire system, in which case the equivalent contributions come from the individual spin polarizations.

In the following, we assume that the variable X is decomposable as stated above, i.e.

$$X(t) = \sum_m \tilde{x}_m(t), \tag{2.5}$$

where $\tilde{x}_m(t)$ denotes one of many equivalent contributions to $X(t)$. Therefore, the correlation function $R(t)$ can be rewritten as

$$R(t) \simeq \langle \tilde{x}_m(t)\rangle_{\rho_R(0),m}, \tag{2.6}$$

where the additional average is taken over all trajectories $\tilde{x}_m(t)$ during the same sample evolution of the entire system.

In Section 2.3.1, the variable X was assumed to be the only slow variable characterizing the large system — therefore, the dynamic evolution of the variables $\tilde{x}_m$ is supposed to exhibit fast fluctuations representative of the short (ballistic) timescale of the problem. We reformulated the problem in terms of variables $\tilde{x}_m$ because we would like to analyze the elementary random contributions underlying the Markovian approximation for $R(t)$.

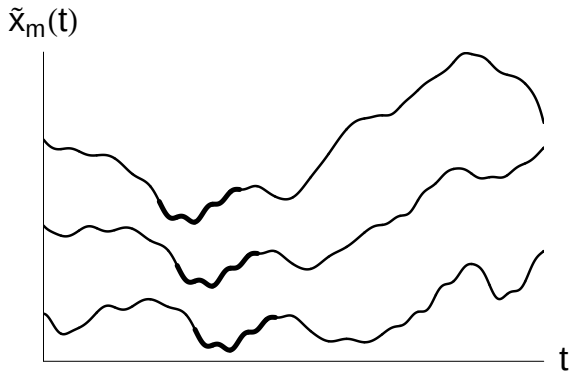

Figure 2.2: This picture illustrates the argument made in the text that identical short-time pieces can appear in different trajectories of variable $\tilde{x}_m$. The three trajectories shown in this picture have one identical piece – the thicker part of each trajectory line. These trajectories have been displaced along the vertical axis to make them distinguishable. In this picture, the identical pieces are shifted in time by an interval which is shorter than the time length of each piece. In general, the time shift between the identical pieces can be both very short and very long.

Considering the ensemble averaged quantity $\langle \tilde{x}_m(t) \rangle_{\rho_R(0),m}$, it is important to realize that any violent short-time event experienced by one trajectory $\tilde{x}_m(t)$ can be experienced simultaneously by many other trajectories. Moreover, another set of trajectories $\tilde{x}_m(t)$ can also go through an identical short-time event, shifted in time by an interval much shorter or much longer than the scale of this short-time event itself (see Fig. 2.2 for the illustration). In other words, any given short-time event can start at any given moment of time. Therefore, in order for the short timescale to be pronounced after averaging over all trajectories, it is necessary that not only the short-time events were present in each trajectory but also the probability of those events must fluctuate on the same short timescale.

As an extreme alternative, one can consider the case when the probability of a given short-time event is time independent. In that case, the contribution of such a short-time event to the ensemble average will also be time independent, no matter how violent that

event may be.

We now focus on the later stages of the nonequilibrium evolution, meaning that the value of the time variable in Eq.(2.6) is greater than the characteristic mean free time for the variables $\tilde{x}_m$. At this stage, the short-time fluctuations of the probability of a given short-time event, if they persisted, would certainly represent a peculiar and counterintuitive effect, showing that the system did not lose the memory of the initial conditions. In order to see that, one has to realize that the probability weight of each trajectory exhibiting a given short-time event depends only on the initial conditions from which the trajectory started at the beginning of the nonequilibrium evolution. The occurrence of the above probability fluctuation would mean that a very long time after the nonequilibrium evolution started, the system somehow "remembers" that the fluctuation of the probability of a given short-time event should start at a certain moment and not at any subsequent one. But those two moments are different only by the virtue of the fact that they are separated by different intervals from the moment when the nonequilibrium evolution started.

In fact, it is quite obvious that the situation should be exactly opposite to the one described in the previous paragraph. Namely, with nearly the same probability, any given short-time event can occur starting at two different moments of time separated by any not too long interval. The rationale for such an assertion is that the probability of any short-time event is determined by a very large number of random contributions from uncorrelated trajectories. Being an extremely well averaged quantity, the above probability does not fluctuate. The reason why it changes at all is that, as long as the slow variable $X(t)$ has a non-zero value, $\langle \tilde{x}_m(t) \rangle$ also has the non-zero value. Therefore, there is a slightly greater probability (proportional to the above time dependent average) that the short-time events start from the positive rather than from the negative value of $\tilde{x}_m$.

It should also be taken into account that even if the fluctuation of the probability of a specific short-time event accidentally occurs, then there are many different short-time events

to be averaged over, and it is very unlikely, that the probability fluctuations for all of them happen at the same time and affect the average in the same direction.

Our conclusion for this part is: After not too short a time from the moment when the nonequilibrium evolution started, the contribution of any short-time event occurring in the trajectories $\tilde{x}_m(t)$ to the ensemble average (2.6) repeats itself continuously, being only slowly modulated by the probability of that event, and, therefore, no manifestation of the short timescale is seen after averaging.

To make the above statement complete, one would certainly have to answer the question: What is the difference between the initial probability distribution $\rho_{_R}(0)$ and the probability distributions at later times that explains why the short-time deviation of $R(t)$ from the slow Markovian behavior occurs only around $t = 0$? This question will be addressed in Sections 2.3.5 and 2.3.6 in a more general context.

2.3.3 One-dimensional Brownian motion

In order to bring the discussion one step closer to the forthcoming description of the spin problems, we now present the standard one-dimensional diffusion of Brownian particles in a fashion similar to the treatment of the exponential decay in Section 2.3.1. The difference between the two cases is that, instead of one slow variable, the treatment of diffusion requires a continuum of slow variables.

In the problem of Brownian motion[46][44], the Markovian timescale should be associated with a slow change in the position coordinate $x(t)$ of a Brownian particle. The drift of Brownian particles is, usually, characterized by the correlation function

$$B(t) = \langle x^2 \rangle - \langle x(t)x(0) \rangle. \tag{2.7}$$

We consider the problem as if many Brownian particles move simultaneously, and the average is taken over all of them.

In order to proceed with the Markovian description, it is necessary to introduce spatial coarse-graining with the size Δ_x of the coarse-grained subvolumes (linear intervals in this case). This size is much greater than the mean free path of the Brownian particles. The slowly changing particle populations in each subvolume become the primary variables of the Markovian description. It is then assumed that the Markovian equations should only describe the direct exchange of particles between adjacent subvolumes, which gives

$$\frac{\partial f(t, x_{(i)})}{\partial t} = W \sum_j (f(t, x_{(j)}) - f(t, x_{(i)})), \tag{2.8}$$

where $f(t, x_{(i)})$ is the nonequilibrium fraction of the particle population in subvolume number i; the sum over j includes only the subvolumes adjacent to the ith subvolume; and W is the rate of transitions across the boundary of two adjacent subvolumes. There are two additional assumptions behind Eq.(2.8). Namely: (a) every Brownian particle is always affected by the same equilibrated environment; and (b) the transitions in both directions ($(i) \to (j)$ and $(j) \to (i)$) are equivalent. The continuum limit of the description represented by Eq.(2.8) yields the standard diffusion equation:

$$\frac{\partial f(t, x)}{\partial t} = D \, \frac{\partial^2 f(t, x)}{\partial x^2}, \tag{2.9}$$

where the diffusion coefficient $D = W\Delta_x^2$.

The solution of Eq.(2.9) allows $B(t)$ to be calculated, which gives

$$B(t) = Dt. \tag{2.10}$$

According to the general recipe preceding Eq.(2.3), the Green-Kubo expression for the diffusion coefficient can be obtained by equating the first time derivative of the Markovian result for $B(t)$ to the saturation value of the integral of the exact second time derivative of $B(t)$. As in the earlier example in Section 2.3.1, the second derivative of $B(t)$ can be presented as $\langle v(t)v(0)\rangle$, where $v(t) = \frac{dx(t)}{dt}$. Therefore, the expression for the diffusion coefficient becomes

$$D = \int_0^\infty \langle v(t)v(0)\rangle \, dt. \tag{2.11}$$

Thus we have again illustrated the general statement that the assumption of the smooth approach to the Markovian behavior is sufficient in order to obtain the standard Green-Kubo results for the parameters describing the Markovian approximation.

Finally, we mention that the argument given in Section 2.3.2 to explain the smooth approach to the Markovian behavior could also be rephrased for the problem of Brownian motion. We do not do it, because it would not add anything conceptually different from the content of Section 2.3.2.

2.3.4 Conjecture I

The preceding discussion motivated the postulate that whenever a kind of Markovian description is assumed to be adequate for long space- and timescales, the functional form of the correlation functions obtained in the framework of such a description also applies to the short timescale, with the only exception being an initial time interval of the order of the mean free time. As far as the corresponding relaxation process is concerned, it is difficult to embrace that postulate without concluding that, after a certain time from the beginning of the nonequilibrium evolution, not only the resulting Markovian functional form but the Markovian rate equations themselves apply to the short timescales, and, if necessary, the spatial coarse-graining for the Markovian description can also be chosen very fine.

Making one step from the above seemingly formal observation, we now introduce a stronger statement:

Conjecture I: After the memory of the initial probability distribution is lost in the relaxation process corresponding to the decay of the second order correlation function of equilibrium fluctuations in a very large system, a kind of randomness subsequently propagates to very short space and time scales. That randomness is such that, considering the nonequilibrium behavior of the *ensemble averaged* quantity of interest at later times, it is appropriate to invoke a Brownian-like Markovian description, which is consistent with the long-time

Markovian assumptions, but, at the same time, based on a very fine coarse-graining with the scale much smaller than the scale of the ballistic behavior of the particles composing the large system. (The precise meaning of the "Brownian-like Markovian description" will be clarified in Section 2.4 in the system-specific context.)

Two closely related aspects make the above conjecture different from the previous treatment: First, it does not require the quantity of interest to evolve much more slowly than a typical microscopic variable. Second, it does not call for the long-time Markovian description to be developed first and then extended to the short timescales — it only requires the long-time Markovian assumptions to be consistent with the resulting description.

The last circumstance makes *Conjecture I* complementary to the long-time assumption of chaotic mixing for the classical spin trajectories on a sphere (Section 2.2). As we mentioned in Section 2.2, it is impossible to construct a self-contained long-time description on the spherical surface because of the physical absence of distances much greater than the mean free path. (The mean free path in our spin problem is of the order of the radius of the sphere). However, if the spherical surface is coarse-grained in very fine elements, then, locally, those elements can be considered flat. It is, therefore, natural to assume, that the random properties on the very fine scale in the case of random motion on the spherical surface are not qualitatively different from the case of Brownian motion on the infinite plane. Therefore, the rate equations similar to those used in Section 2.3.3 can be introduced on the spherical surface. An analogous situation will characterize the quantum case in Section 2.5.

Before we proceed with the specific description of our spin problems, the issue of the difference between the initial probability distribution and the distribution which supports *Conjecture I* must be addressed. We do this in Sections 2.3.5 and 2.3.6.

2.3.5 Local phase space picture for hyperbolic-like systems

In this part, we introduce a complementary line of argument involving the hypothesis that the many-body system addressed by *Conjecture I* is a chaotic hyperbolic system [41]. The connection between *Conjecture I* and the hypothesis of hyperbolicity is not an obvious one. We believe that hyperbolicity is not a necessary condition for *Conjecture I*, and we do not even speculate whether the hyperbolicity is sufficient to prove *Conjecture I*. However, the origin and the limits of *Conjecture I* become more transparent when discussed in the context of hyperbolic systems.

The following discussion deals with an abstract many-body Hamiltonian system, about which it is no longer assumed that it exhibits separation between slow and fast motions. For consistency of language, the Hamiltonian system in question is assumed to be very large but finite. As a prototype of such a system, we keep in mind the lattice of interacting classical spins introduced in Section 1.2. It is not known whether that spin system is, actually, hyperbolic. But, as a compensation, our handling of the hyperbolicity requirements is minimally restrictive and, in that sense, maximally realistic.

In the many-body phase space of a Hamiltonian system, the phase volume is conserved under dynamical evolution. When the whole system shows chaotic mixing, it means that any continuous set of points initially occupying a small part of the phase space would eventually be distributed over the whole phase space — subject to the energy conservation constraint. (This property is consistent with the mixing we assumed in Section 2.2 for the individual particle trajectories but somewhat more restrictive.) A volume-preserving continuous procedure of spreading the above set of points is to expand a part of this set in certain (stable) directions and contract it in other (unstable) directions, keeping the volume unchanged. At a given point of the phase space, the stable and unstable directions can be obtained by linearization of the equations of motion in the vicinity of that point. Assuming that the dynamical evolution insures such an expansion-contraction (hyperbolic) property for most

points and most directions in the phase space, the initially compact small volume will be spread over the phase space as a continuous random pattern of very thin cells. The longer the time allowed for this process, the smaller the initial volume which can be chosen, and, therefore, the smaller the ultimate transverse size of the thin cells becomes. This transverse size corresponds to the contraction directions of the phase space. It characterizes the scale of dynamically developed randomness and thus underlies the propagation of the Markovian assumptions to very short scales.

At the same time, if a smooth not-too-fast varying probability distribution is assigned within the initial small volume, such a distribution will be stretched over much larger phase space, and, therefore it will become nearly flat along the longitudinal (expansion) directions of the above cells. This extreme smoothness of the random pattern along the expansion directions makes the integrated average over large subvolumes behave in the same way as the average over much smaller subvolumes, and, therefore, allows the Brownian-like description for the long space and time intervals to be extended to much shorter intervals.

The last point underscores an important difference between the mathematical theory and the present physical analysis. While the mathematical theory struggles for the rigorous derivation of the long-scale properties from its understanding of the local phase space dynamics, we assume that the whole physical experience of dealing with the long scales is correct and compatible with the local expansion-contraction picture. It turns out that, on the basis of such an approach, we can treat situations that are accessible neither by the rigorous mathematical analysis nor by the conventional "physical" Markovian approximation.

We can now explain why *Conjecture I* distinguishes the initial and the long-time behavior of the correlation functions.

From the viewpoint of the contraction-expansion picture described above, the small parameter implicitly underlying *Conjecture I* is the ratio of the characteristic scales of the many-body probability distribution along the contraction and expansion directions in the

many-body phase space. Such a small parameter develops dynamically and cannot be present in the initial probability distributions of the nonequilibrium problems corresponding to calculations of second order correlation functions.

The above point can be illustrated by the example of the correlation function $G(t)$ given by Eq.(1.1) for the classical spins, in which case the initial probability distribution $\rho(0)$ is given by Eq.(1.5).

According to Eq.(1.5), the probability of initial polarization of each spin is completely independent of the polarizations of its neighbors, which means that $\rho(0)$ can be factorized in terms of the distributions describing each spin separately. This factorization essentially implies that a single scale (that of the initial one-spin distribution) characterizes the many-spin distribution along all directions of the phase space. That scale corresponds to the radius of the sphere on which the one-spin distribution is defined. (The explicit form of this distribution is given in Section 2.4.) Thus, as always happens with well-defined initial conditions of many-body problems, the initial distribution (1.5) is not complex enough to discriminate between the contraction and expansion directions intrinsic for the many-body phase space of a given dynamical problem. Therefore, some time ($\sim \tau$) is required before the chaotic pattern possessing the necessary small parameter is established.

We thus expect that a many-spin distribution consistent with *Conjecture I* has the following property: The nonequilibrium correction to the equilibrium probability that a given spin has a certain orientation is strongly dependent on the polarization of the neighbors of that spin — a small variation in the coordinates of the neighbors will give another nonequilibrium correction supposedly uncorrelated with the original one. However, if this variation is intentionally directed exactly along the expansion direction, then the two probability corrections will be almost equal. The last two statements do not contradict to each other, because it is improbable by random variation of the neighbor coordinate to pick an exact expansion direction in the many-body phase space — a randomly chosen direction has projections along

both the expansion and the contraction directions.

The property described in the previous paragraph has the following consequence: When, in the regime corresponding to *Conjecture I*, coarse-graining with a characteristic size much longer than the contraction scale of the true many-spin distribution is introduced along the spin axes, the many-spin probability distribution redefined in the coarse-grained sense can be factorized in terms of the individual spin distributions.

Besides clarifying the status of the "usual" initial conditions, the expansion-contraction picture also helps to understand what happens if one reverses the exact dynamics of a system which before such a time reversal was well in the regime describable by *Conjecture I* [47]. In the case of classical spin problems, time reversal means that the orientations of all spins should be instantaneously changed to the opposite ones, or, equivalently, one can think that, in the phase space of the problem, the directions of all spin axes are reversed. In other problems, there are also phase space axes that change the direction. If, at the moment of time reversal, the probability distribution in the many-body phase space has a pattern conforming with the expansion and contraction directions intrinsic for a given dynamical problem, then, in respect to that pattern, all formerly stable directions suddenly become unstable, and all formerly unstable directions become stable. As a result, the ratio of the characteristic scales along the contraction and expansion directions becomes large instead of being small, implying an "anti-Markovian" regime.

2.3.6 General scope of Conjecture I

Returning to the argument given in Section 2.3.2, it is important in general, — and for the treatment of the quantum case in particular — that the argument is not limited to the case when the trajectories in question describe a subsystem within a chaotic Hamiltonian environment. In general, this argument applies when the ensemble of trajectories represents the behavior of a subsystem subjected to the influence of an external environment which

follows continuous dynamics and has a continuous distribution. As long as that external influence satisfies the long-time assumption of mixing for a given ensemble of the subsystem trajectories (meaning an assumption similar to the one made in Section 2.2), the argument does not exclude a non-chaotic or non-Hamiltonian environment, and neither does *Conjecture I*.

In the case of a non-chaotic or non-Hamiltonian environment, the extreme stretching of the subsystem-plus-environment probability distribution (similar to the one described in Section 2.3.5) should also underly *Conjecture I*, though, in such a case, it is more difficult to visualize the small parameter. Nevertheless, it is clear that *Conjecture I* becomes applicable after the probability distribution develops the complexity intrinsic to a given dynamics. An initial distribution like the one given by Eq.(1.5), in which the variables belonging to the subsystem in question (one of those spins, in our case) are factorized from the variables describing the environment, has no chance to be complex enough.

Finally, we note that the possibility of finer and finer coarse-graining postulated by *Conjecture I* does not have an apparent limit as long as the long-time assumption of chaotic mixing formulated in Section 2.2 remains applicable to smaller and smaller initial sets of trajectories and extends over longer and longer times. We shall return to the issue of limits in Section 2.6.

2.4 Classical spins — continued

Conjecture I can now be applied to our problem in the following way.

Let us assume that, on the spherical surface corresponding to the nth spin, we trace a large number of sample trajectories of that spin. Different sample trajectories of the nth spin correspond to different realizations of the dynamical evolution of the entire system, and the initial conditions for each such a realization are chosen in accordance with the initial probability distribution (1.5). We thus have a large number of sample points moving

simultaneously on the spherical surface.

Now let us coarse-grain the spherical surface in sufficiently fine elements. The greater the target accuracy of the calculation, the finer the coarse-graining should be. The large number of sample trajectories should guarantee that, at any moment of time, there are enough sample points in each coarse-grained subvolume (surface element, in this case) to give an accurate representation of the probability to find a point in this subvolume.

The probability distribution of the sample points on the nth sphere is initially close and expected to remain close to the uniform distribution corresponding to the infinite temperature equilibrium. We denote the small deviation from the uniform distribution as $f_n(t, x_n)$, where x_n stands for two standard spherical angles θ_n and φ_n, chosen such that in Eq.(1.5), $S_n^\mu = S\,\cos\theta_n$. The expansion of $\rho(0)$ in powers of β_0 gives

$$f_n(0, x_n) \simeq \beta_0 \cos(\boldsymbol{q} \cdot \boldsymbol{r}_n)\; S\,\cos\theta_n. \tag{2.12}$$

We now recall, that, in Section 2.2, we have already introduced the notion of the mean free path of a typical sample point on the above spherical surface.

When the coarse-grained scale is smaller than that mean free path, the influx and outflux events for the subvolumes along a given trajectory of that point will be correlated in time in a way primarily dependent on the velocity of that point. However, for a given subvolume, there should be many sample points entering and leaving with a given velocity, and, in equilibrium, the non-Markovian influx and outflux events should be perfectly balanced by the exact dynamics of the system. The slight imbalance between the influx and the outflux events is what governs the nonequilibrium evolution in that subvolume.

The property that underlies *Conjecture I* can now be reformulated as follows: At the later stages of the evolution of the ensemble, there are no important correlations between the sample points that are responsible for the imbalance of the influx and outflux events for a given coarse-grained subvolume at the given and at previous moments. The time interval

between the two moments in question can be substantially shorter than the time required for a sample point to cross that subvolume.

In the regime describable by *Conjecture I*, the nonequilibrium population of sample points in a given subvolume becomes a "slow" variable. As explained in Section 2.3.4, we must now treat the problem as if the populations of the sample points in each subvolume on each spin sphere are represented by Brownian particles with mean free path much smaller than the size of that subvolume. In other words, we have to imagine that the mean free path of the sample points is much smaller than it actually is.

If the nth spin was in an equilibrium environment, then the description presented in Section 2.3.3 could be adopted, and the continuum limit of such a description would lead to a standard diffusion equation similar to Eq.(2.9). However, in our case, the environment, which means spin distributions on the neighboring lattice sites, is slightly out of equilibrium.

At the level of the rate equation (2.8), the leading order effect caused by the nonequilibrium environment is that the transition rate from one subvolume to another becomes slightly different from the transition rate in the opposite direction. In that case, the *equilibrium* fractions of particles in the two subvolumes respond to the violation of the balance of the transition rates and create the additional particle flux between those subvolumes. Below, we proceed directly to the continuum description, which takes into account the effect we just described.

In order to avoid unnecessary details, we adopt a schematic notation, which makes all quantities look one-dimensional, but imply the proper number of dimensions and the proper covariant form of the differential operations. In such a notation, the linear response formula for the probability flux on the nth site can be written as

$$\begin{aligned} j_n(t,x_n) &= -D_n(x_n)\frac{\partial f_n(t,x_n)}{\partial x_n} \\ &\quad + \sum_k \int_{V_{x_k}} K_{nk}(x_n,x_k) f_k(t,x_k) dx_k, \end{aligned} \tag{2.13}$$

where $D_n(x_n)$ is the diffusion coefficient (actually, tensor) corresponding to the standard diffusion in the equilibrium environment; $K_{nk}(x_n, x_k)$ is the kernel of the term representing the linear flux response on the nth site to the slight deviation from the equilibrium distribution on the kth site (this response is analogous to Ohm's law); and V_{x_k} stands for the entire space of variables characterizing the kth site.

The probability density f_n and the probability flux j_n must satisfy the continuity equation

$$\frac{\partial f_n(t, x_n)}{\partial t} = -\mathrm{div}[j_n(t, x_n)], \tag{2.14}$$

which completes the description of the nth site. In general, pairs of equations (2.13, 2.14) should be written for each lattice site, and together they form a closed set of integro-differential equations.

Although introduced above as a natural development of the previous treatment, the integral term in Eq.(2.13) represents quite a dramatic step in the extension of the Brownian-like formalism beyond the limits of the conventional Markovian approximation. This term should absorb the seemingly intractable dynamical correlations between different spins. An intuitive picture behind such a representation of the correlations is the following:

The nonequilibrium probability of a certain orientation of the kth spin creates a preferred direction of the local field by which the kth spin affects the nth spin. The preferred direction of the local field means the preferred direction in which the tip of the spin vector moves on the spherical surface. The subtlety here is that the direction in which the additional flux becomes non-uniform and, therefore, causes a change in the particle populations, is not the one that corresponds to the precession around the preferred direction of the local field but the perpendicular one. The rotation of the equilibrium uniform distribution of particles does not change the particle population on any part of the spherical surface. At the same time, the drift in the perpendicular direction changes the projection of the nth spin on the local field, and, therefore, it also changes the energy of that spin, and thus makes two opposite directions non-equivalent. One can think that the resulting effect is similar to the friction

experienced by a precessing gyroscope in a viscous medium: the torque created by the friction tends to turn the gyroscope axis in the direction opposite to the precession axis. From that analogy, one can see that the effect of "friction" would depend on the angle between the spin vector and the preferred direction of the local field, which makes the resulting particle flux non-uniform and, therefore, capable of changing the particle populations on the spherical surface. (An additional insight into the subject can be gained from Chapter 3.)

Our speculation is that the energy lost by the equilibrium spin fraction in the above process is transferred to the very complex many-spin correlations, to which the chosen coarse-graining is insensitive. Those correlations represent the equivalent of the "heat bath" in our Brownian-like description. The same energy is then transferred back to the coarse-grained description via the fluctuations, which underly the the standard gradient part of the diffusive flux.

Consistently promoting a Brownian-like description, it is necessary to assume that the response of one slow variable (the population of a given subvolume) to the deviation of another slow variable from the equilibrium can be caused not only by the direct interaction between those variables but also by the indirect effects mediated by the "heat bath" of the many-spin dynamical correlations. This means that there can exist a nonzero kernel $K_{nk}(x_n, x_k)$ coupling the nth and the kth spins, even though those spins do not interact directly. Another kernel not to be neglected is $K_{nn}(x_n, x'_n)$. In general, it is only reasonable to expect that when the distance between the spins becomes much greater than the radius of interaction the indirect effects become insignificant.

The evaluation of $D_n(x_n)$ and $K_{nk}(x_n, x_k)$ from the knowledge of the Hamiltonian (1.2) is not attempted in this work, and, in fact, we are not sure if such a task is achievable — the absence of a self-contained long-scale description on a sphere precludes us from applying a straightforward generalization of the Green-Kubo recipe (2.11). Nevertheless, as we show below, it is possible to come to very definite conclusions about the time-dependences of the

resulting solutions.

When two distributions $f_n(0, x_n)$ on different sites can be transferred to each other by a symmetry transformation, the dynamic evolution induced by the Hamiltonian (1.2) retains that equivalence. Thus those two sites can be characterized by the same probability distribution in the diffusive regime.

It turns out that, in the nonequilibrium problem corresponding to the calculation of any correlation function of the form (1.1), all probability distributions $f_n(t, x_n)$ are equivalent to each other. This helpful state of affaires is due to the fact that the irreducible representations of the group of the lattice translations have the form $\exp(i\boldsymbol{q} \cdot \boldsymbol{r}_n)$, where, as in our problem, vectors $\boldsymbol{q}$ are commensurate with the lattice periodicity.

The symmetry argument can be illustrated using the examples presented in Fig. 1.1(b). In that figure, all spins are explicitly equivalent in example (I). It is also quite obvious that the probability distributions corresponding to the alternating spin sites in example (II) are just mirror reflections of each other. In the other two examples, one would have to imagine that the probability distribution of each spin is the real part of a complex-valued function which is the same for all spins up to the helically arranged complex phase.

It thus follows that, in our problem,

$$f_n(t, x_n)|_{x_n = x_0} = \cos(\boldsymbol{q} \cdot \boldsymbol{r}_n) f_0(t, x_0) \tag{2.15}$$

Given the above relationship one can easily obtain from Eqs.(2.13, 2.14) that

$$\frac{\partial f(t,x)}{\partial t} = \frac{\partial}{\partial x}\left(D(x)\frac{\partial f(t,x)}{\partial x} - \int_{V_{x'}} K(x,x') f(t,x') dx' \right), \tag{2.16}$$

where the newly introduced distribution function $f(t, x)$ is equivalent to $f_0(t, x_0)$ with index 0 dropped, and

$$K(x, x') = \sum_k \cos(\boldsymbol{q} \cdot \boldsymbol{r}_k) K_{0k}(x, x'). \tag{2.17}$$

Equation (2.16) represents correlated diffusion on a spherical surface. Like an ordinary diffusion equation, this equation has a set of solutions of the form $f^\lambda(t, x) = e^{-\lambda t} u_\lambda(x)$,

where λ is one of the eigenvalues of the integro-differential linear operator acting on $f(t,x)$ in the right-hand side of the equation, and $u_\lambda(x)$ is the corresponding eigenfunction.

Unlike a typical diffusion problem, however, the eigenvalues of our problem can have both real and imaginary parts. This property originates from the fact that, in general, the kernel $K(x,x')$ is expected to have no symmetry with respect to interchange of the variables x and x', and, as a result, the integro-differential operator we deal with is non-Hermitian. The asymmetry of the kernel $K(x,x')$ can be traced back to the asymmetry of the kernels $K_{0k}(x,x')$ entering Eq.(2.17). Although it is impossible to separate different factors influencing the kernels $K_{0k}(x,x')$, it is, at least, clear that those kernels are strongly affected by the direct spin-spin interaction (1.2). That interaction is asymmetric in the sense that, in general, the kth spin with orientation x' creates on the zeroth site a local field, which is different from the local field created on the kth site by the zeroth spin with some arbitrary orientation x.

Since we deal with a finite volume (meaning spherical surface), the eigenfunctions $u_\lambda(x)$ necessarily form a discrete set and generate a corresponding discrete set of eigenvalues. Although the eigenvalues of our problem can be complex (in which case only the real part of the solution should be taken), we still assume that the underlying dynamics of the spin system guarantees that the real parts of all eigenvalues are non-negative

In order to obtain $G(t)$ from the above description, one has to average the μth polarization of the zeroth spin over the solution of Eq.(2.16). Therefore,

$$G(t) \simeq \int_{\text{sphere}} \cos\theta \; f(t,\theta,\varphi) \sin\theta \; d\theta \; d\varphi, \tag{2.18}$$

where we returned to the spherical variables $\{\theta,\varphi\}$ introduced earlier (with index n dropped). As a result, the generic long-time behavior of $G(t)$ is given by Eqs. (1.24,1.25) – it is controlled by the eigenvalue that has the smallest real part among those, whose respective eigenfunctions $u_\lambda(\theta,\varphi)$ give nonzero contribution to the integral in Eq.(2.18).

The alternatives to the long-time behavior (1.24, 1.25), which we left out as "non-generic",

correspond to the following possibilities: (i) the system does not experience chaotic mixing sufficient to justify the diffusion description (2.13, 2.14); (ii) within the diffusion description, the expansion of $G(t)$ contains more than one eigenvalue with the smallest real part (complex conjugates do not count).

Although in this work we do not suggest a recipe for the calculation of $D(x)$ and $K(x,x')$, we expect the characteristic scale of all quantities to be given by the appropriate combination of the mean free time and the radius of the sphere. In particular, both differential and integral terms in Eq.(2.16) should have the same order of magnitude. With this, we can make the following simple estimate of the time after which the exponential dependence (1.24) or (1.25) actually becomes pronounced.

It presumably takes a time of the order of the mean free time to reach the Markovian regime describable by Eq.(2.16). In the Markovian regime, both the slowest exponent ξ entering Eqs.(1.24, 1.25) , and the difference between ξ and the second slowest exponent should be of the order of the inverse mean free time, implying that it will take another time of the order of the mean free time before the contributions from the faster exponents become suppressed. Therefore, the behavior of $G(t)$ should approach asymptotic form (1.24, 1.25) after a time of the order of several mean free times, i.e. sufficiently fast.

It is important for the above estimate that the differential term in Eq.(2.16) guarantees that the eigenfunction $u_\lambda(x)$ corresponding to the slowest exponent does not have spatial derivatives much greater than the inverse radius of the sphere. The initial probability distribution (2.12) is also characterized by the same scale, and it is very unlikely that $f(t,x)$ will become much more non-uniform during the initial non-Markovian stage of the ensemble evolution. Therefore, if, in the Markovian regime, $f(t,x)$ is expanded in terms of $f^\lambda(t,x)$, the coefficient corresponding to the slowest term should not be anomalously small, and in fact can very well be of the order of unity.

In the context of experimental or numerical verification of the long-time behavior (1.24,

1.25), the estimate just given should be complemented by reasonably good luck. For example, if the difference between the slowest exponent and the second slowest exponent equals one third of the slowest exponent, then the two exponents still compete over a quite extended time interval, and by the time the faster of those exponents becomes completely suppressed, the overall value of the correlation function has become too small to be obtained from experiments or from numerical calculations.

2.5 Quantum spins

Generalization of the previous treatment to quantum spins requires one modification, namely, instead of trajectories of the tip of the classical spin on a sphere, we consider trajectories in the space of parameters describing the density matrix of a quantum spin.

As straightforward as the above approach might seem, it is not how Markovian assumptions are usually introduced in quantum problems. Usually, Markovian assumptions are based either on the classical limit of the quantum problem, or on classical models for the occupation numbers of the quantum states (eg. Ising model). Both of those approaches are deficient because of the lack of invariance with respect to the transformations of the Hilbert space of the quantum problem. Sometimes (not in our case), such a deficiency appears to be unimportant, but it always makes the discussion of compatibility of the Markovian assumptions with the exact dynamics of the problem intractable even at the level of posing the problem. If the Markovian assumptions are to be discussed in a situation where their extreme implications are expected to be quantitatively adequate, it is crucially important to have those assumptions grounded on the well-defined notion of trajectories consistent with the symmetry of the Hilbert space.

Below, in order to be specific, we limit our treatment only to spins 1/2. We also assume that the spin system is very large but finite, and, therefore, the number of states in the quantum basis is also finite.

The 2×2 density matrix of a given spin 1/2 can always be obtained by averaging over the full many-body density matrix. Already an ensemble average, the one-spin density matrix is expected to show, not a random behavior, but, in our case, a rapid relaxation toward the 2×2 unit matrix corresponding to the infinite temperature equilibrium. Therefore, in order to identify the underlying chaotic trajectories, we have to trace back the quantum mechanical and statistical averaging.

We propose a description that treats different spins by using different basis sets of the many-body wave functions. Considering the nth spin, we adopt an interaction-like representation for the basis wave functions: First, at $t = 0$, for the whole system excluding the nth spin, we choose a complete orthogonal set of wave functions $\{\Psi_{n\alpha}(0)\}$ enumerated by an index α. Each wave function $\Psi_{n\alpha}(0)$ is such that every spin has a definite projection on the axis μ entering Eq.(1.5). (The spins are weakly polarized along that axis at $t = 0$.) Allowing each of the above wave functions to evolve only under the action of the part of the Hamiltonian (1.2) not involving the nth spin, we obtain a time-dependent basis set $\{\Psi_{n\alpha}(t)\}$. Then, we choose *time-independent* basis wave functions for the nth spin as $\{|\uparrow\rangle, |\downarrow\rangle\}$ with the quantization axis along the same μ-direction of the initial average polarization of this spin. Finally, the basis set for the whole system becomes $\{ \{|\uparrow\rangle\Psi_{n\alpha}(t)\}, \{|\downarrow\rangle\Psi_{n\alpha}(t)\} \}$.

According to the above recipe, the basis sets designed for the description of different spins are identical at $t = 0$, but then each of those sets evolves differently. The advantages of this representation will become clear after the formal structure of our treatment is developed.

In the basis designed for the nth spin, the density matrix of that spin is just the average over 2×2 blocks of the density matrix of the whole system — each block corresponds to a fixed value of index α. However, these blocks cannot yet be treated as elementary dynamical quantities, because the initial many-body density matrix (1.5) is, by itself, the result of statistical averaging, implying initial thermal contact with the environment.

Since, in our problem, there is no contact with the environment at later moments of time,

we represent the evolution of the density matrix of the whole system as the average over the evolutions of many density matrices of "pure states". Pure states are the states of the isolated spin system — each describable by a wave function. The choice of the ensemble of pure states (to be specified later) is not unique, because, provided the averaging over the pure state density matrices at $t = 0$ gives the density matrix (1.5), the result of the averaging at later moments of time must be independent of other details of this choice.

The time-dependent 2×2 density matrix of the nth spin can now be considered as an average over 2×2 time-dependent blocks, each originating from some pure state density matrix. If one of the pure state wave functions is represented by a set of coefficients $\{ \{C_{\uparrow n\alpha}(t)\}, \{C_{\downarrow n\alpha}(t)\}\}$ in the basis $\{ \{|\uparrow\rangle\Psi_{n\alpha}(t)\}, \{|\downarrow\rangle\Psi_{n\alpha}(t)\} \}$, then the elementary block participating in the averaging is

$$\begin{pmatrix} C_{\uparrow n\alpha}(t)C^*_{\uparrow n\alpha}(t) & C_{\downarrow n\alpha}(t)C^*_{\uparrow n\alpha}(t) \\ C_{\uparrow n\alpha}(t)C^*_{\downarrow n\alpha}(t) & C_{\downarrow n\alpha}(t)C^*_{\downarrow n\alpha}(t) \end{pmatrix}. \tag{2.19}$$

Each block of the form (2.19) can be described by three independent variables: $\{|C_{\uparrow n\alpha}|, |C_{\downarrow n\alpha}|, \Phi_{n\alpha}$ where $\Phi_{n\alpha}$ is the difference between the complex phases of $C_{\uparrow n\alpha}$ and $C_{\downarrow n\alpha}$. Therefore, the time evolution of each of those blocks can be mapped to a trajectory in the three-dimensional space corresponding to the above set of variables. The trajectories thus defined become the primary objects in the subsequent treatment. We shall call them "block trajectories".

In the following, when no distinction between $C_{\uparrow n\alpha}(t)$ and $C_{\downarrow n\alpha}(t)$ has to be made, we shall use the notation $C_{\uparrow(\downarrow)n\alpha}$.

We shall also use the variables $\{|C_{\uparrow n}|, |C_{\downarrow n}|, \Phi_n\}$ (the same as $\{|C_{\uparrow n\alpha}|, |C_{\downarrow n\alpha}|, \Phi_{n\alpha}\}$ but without index α), whenever we discuss one block trajectory as a representative of the statistical properties of all trajectories with different α. In particular, we introduce the probability distribution $P_n(t, |C_{\uparrow n}|, |C_{\downarrow n}|, \Phi_n)$, which implies averaging over the whole ensemble of the pure states and over all values of the index α. This probability distribution will play the same role as the probability distribution on a sphere played earlier in the case of the classical

spins.

We can now explain two advantages of the "interaction representation" basis $\{ \{|\uparrow\rangle\Psi_{n\alpha}(t)\},\ \{|\downarrow\rangle\Psi_{n\alpha}(t)\} \}$.

The first advantage is that, in this representation, interactions which do not affect the nth spin directly also do not have a direct influence on the evolution of the block trajectories — those interactions are mostly absorbed by the time dependence of $\Psi_{n\alpha}(t)$, and the time dependence of the coefficients $C_{\uparrow(\downarrow)n\alpha}(t)$ is directly controlled only by those terms in the Hamiltonian (1.2) that include the nth spin. If the wave functions $\{ \{|\uparrow\rangle\Psi_{n\alpha}(0)\},\ \{|\downarrow\rangle\Psi_{n\alpha}(0)\} \}$ were used as a permanent basis set, then the interactions between two spins very distant from the nth spin would have immediate effect on the coefficients $C_{\uparrow(\downarrow)n\alpha}$, which does not affect the final average for the nth spin but introduces irrelevant fast timescales in the behavior of those coefficients.

The second advantage of the interaction-like representation is that each of the wave functions $\Psi_{n\alpha}(t)$ can be considered as representing a generic evolution of the environment of the nth spin, and, therefore, as far as the properties of that spin are concerned, it is sensible to use one probability distribution $P_n(t, |C_{\uparrow n}|, |C_{\downarrow n}|, \Phi_n)$ to describe all block trajectories corresponding to different values of the index α.

Below we specify the initial probability distribution of the coefficients $C_{\uparrow(\downarrow)n\alpha}$ for the ensemble of many-body pure states. As we already mentioned, this distribution is only constrained by the requirement that the average of the initial pure state density matrices is equal to the density matrix $\rho(0)$ given by Eq.(1.5). We impose one additional constraint necessary for the consistency of our treatment: Namely, we require that the initial probability distribution $P_n(0, |C_{\uparrow n}|, |C_{\downarrow n}|, \Phi_n)$ in the space of block trajectories, which is derivable from the full probability distribution of the coefficients $C_{\uparrow(\downarrow)n\alpha}$, should be such that it is only slightly different from the "equilibrium" probability distribution $P_n(\infty, |C_{\uparrow n}|, |C_{\downarrow n}|, \Phi_n)$.

Since the object of our interest is the probability distribution $P_n(0, |C_{\uparrow n}|, |C_{\downarrow n}|, \Phi_n)$ rather

than the full probability distribution of the pure states, the details characterizing the latter will be given only to the extent sufficient to define the former.

The fact that the initial density matrix (1.5) is diagonal in the initial basis $\{ \{|\uparrow\rangle\Psi_{n\alpha}(0)\}, \{|\downarrow\rangle\Psi_{n\alpha}(0)\} \}$ allows us to assign equal probability to all values of the complex phases of the coefficients $C_{\uparrow(\downarrow)n\alpha}$, which implies that the probability distribution in respect to $\Phi_{n\alpha}$ is uniform for each value of α. Therefore,

$$P_n(0, |C_{\uparrow n}|, |C_{\downarrow n}|, \Phi_n) = \frac{1}{2\pi}\, p_n(|C_{\uparrow n}|, |C_{\downarrow n}|), \tag{2.20}$$

where $p_n(|C_{\uparrow n}|, |C_{\downarrow n}|)$ is the distribution of $|C_{\uparrow(\downarrow)n}|$ defined by the above equation.

The set of absolute values $\{|C_{\uparrow(\downarrow)n\alpha}|\}$ for a sample pure state can be considered as a vector in a high-dimensional space. Since $\sum_{\uparrow(\downarrow)\alpha} |C_{\uparrow(\downarrow)n\alpha}|^2 = 1$, the tip of that vector is restricted to a "quadrant" of the high-dimensional hypersphere, where each point has a non-negative projection on each axis. We define the probability of sampling on this "spherical quadrant" to be uniform, with small corrections reflecting the weak polarizations of spins. We do not define those corrections explicitly, because, as we show below, there is a simple direct way to see what the resulting distribution $p_n(|C_{\uparrow n}|, |C_{\downarrow n}|)$ must be.

Let us first obtain $p_n(|C_{\uparrow n}|, |C_{\downarrow n}|)$ in the case when there are no small corrections, which corresponds to infinite temperature. We denote such a distribution as $p_{n\infty}$.

According to the above sampling procedure, the probability distribution $p_{n\infty}(|C_{\uparrow n}|, |C_{\downarrow n}|)$ is an average over identical probability distributions for each of the coefficients $C_{\uparrow(\downarrow)n\alpha}$. The probability for any of the coefficients $C_{\uparrow(\downarrow)n\alpha}$ to have a value in the interval between y (an auxiliary variable) and $y + dy$ is proportional to the area of the thus-restricted hypersurface, which is given by $A_{(N_{\rm b}-1)}(\sqrt{1-y^2})dy/\sqrt{1-y^2}$, where $A_{N_{\rm b}-1}(\sqrt{1-y^2})$ denotes the surface area of the $(N_{\rm b}-1)$-dimensional hypersphere of radius $\sqrt{1-y^2}$; and $N_{\rm b}$ is the number of the states in the quantum basis of the entire system. Since $A_{(N_{\rm b}-1)}(\sqrt{1-y^2}) \simeq (\sqrt{1-y^2})^{(N_{\rm b}-2)}$, and $N_{\rm b}$ is supposed to be very large, the overall dependence of the probability distribution

on y should be well approximated by $\exp(-\frac{N_b}{2}y^2)$. As a result,

$$p_{n\infty}(|C_{\uparrow n}|,|C_{\downarrow n}|)=\frac{\pi}{2N_b}\exp\left[-\frac{N_b}{2}\left(|C_{\uparrow n}|^2+|C_{\downarrow n}|^2\right)\right]. \tag{2.21}$$

Predictably, the mean square deviation $\langle|C_{\uparrow(\downarrow)n}|^2\rangle$ corresponding to $p_{n\infty}(|C_{\uparrow n}|,|C_{\downarrow n}|)$ is equal to the inverse number of basis states.

When the inverse temperature β_0 appearing in Eq.(1.5) is small the initial probability distribution for the $|C_{\uparrow n}|$ should correspond to infinite temperature for "spins-up" and be Gaussian, with mean squared deviation $\langle|C_{\uparrow n}|^2\rangle$ proportional to the probability $\mathcal{P}_{n\uparrow}$ of finding "spin-up," while the distribution of $|C_{\downarrow n}|$ should also be Gaussian but with a slightly smaller mean squared deviation $\langle|C_{\downarrow n}|^2\rangle$ proportional to the probability $\mathcal{P}_{n\downarrow}$ of finding "spin-down". Both $\mathcal{P}_{n\uparrow}$ and $\mathcal{P}_{n\downarrow}$ are very close to $\frac{1}{2}$. Thus, taking into account only the leading order corrections to Eq.(2.21), we obtain

$$p_{n}(|C_{\uparrow n}|,|C_{\downarrow n}|)=\frac{\pi}{2N_b}\exp\left[-\frac{N_b}{4}\left(\frac{|C_{\uparrow n}|^2}{\mathcal{P}_{n\uparrow}}+\frac{|C_{\downarrow n}|^2}{\mathcal{P}_{n\downarrow}}\right)\right]. \tag{2.22}$$

We assume that in the course of the nonequilibrium evolution, the probability distribution $P_n(t,|C_{\uparrow n}|,|C_{\downarrow n}|,\Phi_n)$ will ultimately evolve to

$$P_n(\infty,|C_{\uparrow n}|,|C_{\downarrow n}|,\Phi_n)=\frac{1}{2\pi}p_\infty(|C_{\uparrow n}|,|C_{\downarrow n}|), \tag{2.23}$$

where p_∞ is given by Eq.(2.21).

Comparing the block trajectories in the quantum case with the trajectories of the spin vectors on a sphere in the classical case, three differences can be observed.

The first difference is that, unlike the trajectories of individual classical spins, the block trajectories introduced for the description of the nth spin in principle describe the whole system, because the coefficients $C_{\uparrow(\downarrow)n\alpha}(t)$ are taken from the many-body wave function. However, in the basis $\{\{|\uparrow\rangle\Psi_{n\alpha}(t)\},\ \{|\downarrow\rangle\Psi_{n\alpha}(t)\}\}$ designed for the nth spin, only the quantum operators of that spin have a simple time-independent form. The operators of other spins are time-dependent, and, at later times, they presumably have a very complex and

intractable form. Therefore, when the behavior of the coefficients $C_{\uparrow(\downarrow)n\alpha}(t)$ is projected onto the three dimensional space $\{|C_{\uparrow n}|, |C_{\downarrow n}|, \Phi_n\}$ — the same for all values of the index α, the information about the environment of the nth spin is lost.

The second difference is closely related to the first one. Namely, unlike the case when one sample point representing a given spin moves on a spherical surface in the course of a sample evolution of the whole system, many sample points corresponding to different blocks of the sample pure state actually move simultaneously in the space $\{|C_{\uparrow n}|, |C_{\downarrow n}|, \Phi_n\}$. Moreover, those sample points interact with each other, because the corresponding blocks are coupled by the quantum Hamiltonian. In other words, if we consider a given block trajectory constructed for the nth spin and representing the evolution of a pair of coefficients $C_{\uparrow n\alpha}(t)$ and $C_{\downarrow n\alpha}(t)$, then the immediate environment of that trajectory is characterized not only by the probability distributions $P_k(|C_{\uparrow k}|, |C_{\downarrow k}|, \Phi_k)$ of the spins that interact with the nth spin, but also by the distribution $P_n(|C_{\uparrow n}|, |C_{\downarrow n}|, \Phi_n)$ itself.

Finally, the third difference is that in comparison with the spherical surface, which is periodic in all directions and, therefore, finite, the space of variables $\{|C_{\uparrow n}|, |C_{\downarrow n}|, \Phi_n\}$ is periodically closed only in the direction of Φ_n. The situation is less straightforward along the $|C_{\uparrow n}|$ and $|C_{\downarrow n}|$-directions: Both variables are bound by zero from below, and also there is a global normalization condition $\sum_{\uparrow(\downarrow)\alpha} |C_{\uparrow(\downarrow)n\alpha}|^2 = 1$, which imposes the upper bound $|C_{\uparrow(\downarrow)n}| \leq 1$. However, the real upper bound is not 1 but a much smaller value imposed by the statistical constraint; this could already be seen from the fact that, according to both the initial (2.22) and the final (2.21) probability distributions , the typical value of the variables $|C_{\uparrow(\downarrow)n}|$ is of the order of $1/\sqrt{N_{\rm b}}$, where the number of the basis states $N_{\rm b}$ is exponentially greater than supposedly large number of spins in the system. If evolution of a pure state starts from the values of all variables $|C_{\uparrow(\downarrow)n\alpha}|$ of the order of $1/\sqrt{N_{\rm b}}$, then it is improbable that any of those variables can ever become close to 1. What is overwhelmingly probable is that any $|C_{\uparrow(\downarrow)n\alpha}(t)|$ will stay within an upper bound of the order of $1/\sqrt{N_{\rm b}}$ during a time

interval of any reasonable length.

Given all the above differences, the block trajectories still have two properties that allow us to treat them in very much the same way as in Sections 2.2 and 2.4 we treated the classical trajectories on the spherical surface. Those two properties are: (a) the mean free time of the block trajectories is given by the same one-spin interaction time τ defined by Eq.(1.3); and (b) the mean free path of the block trajectories is of the order of the size of the finite volume to which those trajectories are constrained, i.e. $\sim \pi$ along the Φ_n-direction and $\sim 1/\sqrt{N_{\rm b}}$ along the $|C_{\uparrow(\downarrow)n}|$-directions.

The reason why the one-spin interaction time characterizes the block trajectories is that, as was already mentioned, in the "interaction representation" we chose earlier, the evolution of the coefficients $C_{\uparrow(\downarrow)n\alpha}(t)$ is directly controlled by the interaction of the nth spin with its neighbors — without that interaction, the coefficients $C_{\uparrow(\downarrow)n\alpha}$ would be time-independent. Since, in general, no separation of the dynamic timescales is expected in the problem, all indirect factors affecting the evolution of the block trajectories should also be characterized by the same timescale.

The mean free paths given above originate from a simple estimate of how much the value of the individual coefficient $C_{\uparrow(\downarrow)n\alpha}$ can change over an interval of the order of τ — subject to the condition that all coefficients dynamically coupled with a given one have absolute values of the order of $1/\sqrt{N_{\rm b}}$ and arbitrary complex phases.

Now, we make the hypothesis that the block trajectories have a chaotic mixing property of the same kind as was assumed in Section 2.2 for the trajectories of the classical spins. Namely, we assume that on the scale characterized by the mean free time τ: (i) each block trajectory loses the memory of the initial position; (ii) a set of all block trajectories starting from the initial positions within an arbitrarily small subvolume of the statistically constrained part of the space of variables $\{|C_{\uparrow n}|, |C_{\downarrow n}|, \Phi_n\}$ disperses over that part in a random manner; and (iii) the statistics of the trajectory patterns of this set becomes representative of the statistics of

the whole ensemble of the block trajectories. In correspondence with the previous discussion, the term "statistically constrained" implies not too large values of variables $|C_{\uparrow(\downarrow)n\alpha}|$ in comparison with $1/\sqrt{N_{\rm b}}$.

Most of the arguments we used in Section 2.3 in order to justify *Conjecture I* were given in quite general form and apply directly to the quantum problem posed in terms of the block trajectories. The only exception is the phase space picture motivated by the properties of hyperbolic chaotic systems (Section 2.3.5). In principle, one could try to introduce a similar picture in the $2N_{\rm b}$-dimensional space representing the absolute values and the complex phases of all coefficients $C_{\uparrow(\downarrow)n\alpha}$, but we do not pursue that line. Instead, we rely on the general statement made in Section 2.3.6 that *Conjecture I* only requires that the environment which governs the evolution of a given subsystem has a continuous dynamics and a continuous probability distribution in the space of its variables. The concept of environment of a given block trajectory has been discussed earlier — it certainly satisfies the above condition.

Starting from this point, our entire treatment of the classical spin systems can be directly translated to the quantum case. Below, we discuss the quantum case only to the extent that allows us to establish a correspondence with the mathematical construction obtained in Section 2.4 for the classical case.

As in the classical case, we apply *Conjecture I* to the ensemble of the block trajectories and thus justify Eqs.(2.13,2.14), in which x_n now represents the three variables $\{\ |C_{\uparrow n}|,\ |C_{\downarrow n}|,\ \Phi_n\ \}$; and

$$f_n(t, x_n) = P_n(t, x_n) - P_n(\infty, x_n), \tag{2.24}$$

where $P_n(\infty, x_n)$ is given by Eqs.(2.23, 2.21).

It turns out that Eqs.(2.13,2.14) need not to be modified in order to take into account the fact, discussed earlier, that the environment of the block trajectories constructed for the nth spin is partially represented by their own probability distribution: The kernel $K_{nn}(x, x')$ representing the influence of the nth probability distribution on itself already exists in those

equations, though in the classical case its existence was motivated by indirect dynamical effects.

As we have already mentioned, the statistical constraint limits the evolution of the block trajectories to a finite volume. From the viewpoint of the diffusion description, that constraint implies that the diffusion coefficients and the integral kernels in Eq.(2.13) rapidly approach zero as the values of variables $|C_{\uparrow(\downarrow)n}|$ become greater than $1/\sqrt{N_{\rm b}}$.

The solution of the set of Eqs.(2.13,2.14) yields the distribution function $f_0(t, x_0)$, from which the correlation function of interest can be obtained as the average polarization of the zeroth spin, i.e.

$$G(t) \simeq \langle |C_{\uparrow 0}|^2 \rangle (t) - \langle |C_{\downarrow 0}|^2 \rangle (t). \tag{2.25}$$

For any wave vector $\boldsymbol{q}$ commensurate with the lattice periodicity, the same symmetry argument as in the classical case guarantees that the diffusion problem (2.13,2.14) corresponding to the calculation of the correlation function (1.1) can be reduced to Eq.(2.16).

Even though Eq.(2.16) now describes the block trajectories, the finite volume argument asserting the discreteness of the spectrum is still applicable, and so are the estimates given in Section 2.4. Therefore, we come to the conclusion that the asymptotic long-time behavior of $G(t)$ has the functional form (1.24) or (1.25). Such a behavior should become pronounced after the time of the order of several τ.

2.6 On the limits of the theory

The validity of the theory presented here depends critically on the validity of the long-time assumption of chaotic mixing (Sections 2.2, 2.5), and on the validity of the complementary short-time assumption which we called *Conjecture I* (Section 2.3.4). Strictly speaking, the set of assumptions also includes the recipe for constructing the diffusion description based on *Conjecture I*.

It is thus fair to summarize that, like the tip of the iceberg, the long-time prediction

(1.24,1.25) rests on a large body of assumptions. All of those assumptions are very plausible, but none of them has been tested directly. It is an open question, what is the limit of applicability of our assumptions in generic systems with an infinite number of interacting spins, or whether such a limit exists at all.

Although at first sight it might seem that *Conjecture I* is more vulnerable in comparison with the long-time assumption of chaotic mixing, the analysis presented in Section 2.3 brought us to the conclusion that this conjecture is valid as long as the assumption of chaotic mixing is properly satisfied. In principle, *Conjecture I* just represents an explicit consequence of the fact that parts (ii) and (iii) of our mixing assumptions in Sections 2.2 and 2.5 do not include a limit on how small the initial subvolume can be or how uniform the subsequent mixing of trajectories starting from that subvolume will be.

Since it is not impossible that in the idealized problem the long-time behavior (1.24,1.25) can be valid down to extremely (infinitely?) small values of $G(t)$, it is pertinent to analyze, what corrections to that behavior can appear as far as the realistic systems are concerned. Addressing the above issue, we assume that the range of applicability of *Conjecture I* is much wider than the treatment of the spin correlation functions. Therefore, the discussion will deal with an abstract relaxation process, the properties of which can be derived from *Conjecture I*.

Conjecture I requires very accurate ensemble averaging, which means that an obvious factor limiting the practical applications of this conjecture to the description of the relaxation processes is the finite number of particles in actual many-body systems. As the value of an ensemble averaged quantity becomes smaller, a larger ensemble is necessary to achieve the averaging with the necessary accuracy. Therefore, the system in question should contain a sufficiently large number of sufficiently independent subsystems which contribute to the average quantity of interest. When the required accuracy of the averaging grows, the criteria of independence of different subsystems should simultaneously become more stringent, which

means that, within a given system, a smaller number of properly uncorrelated subsystems is available for the averaging. Even a very large system can thus experience a deficit of very independent subsystems, which limits the application of extreme results based on perfect ensemble averaging to the description of real relaxation processes.

In macroscopic systems, where the number of particles is sufficient to support an extremely accurate ensemble averaging, another limiting factor can become important: it might be that the fine coarse-graining envisioned by *Conjecture I* starts probing extremely small scales, where the applicability of the physical description based on the original Hamiltonian of the problem becomes questionable. For example, if a macroscopic system is described by classical variables, then such a fundamental limit would correspond to the scale at which the quantum nature of the elementary quantities composing the system becomes important. The situation becomes even more interesting, when *Conjecture I* is applied to a quantum system. In this case, the fine coarse-graining actually probes the structure of the Hilbert space of the problem. This suggests that, in macroscopic quantum systems with a realistic number of particles, the agreement of the behavior of the ensemble averaged quantities with the predictions based on *Conjecture I* can be sensitive to processes which are fundamental even with respect to the quantum mechanics as we know it today.

2.7 Summary

In this Chapter, the treatment of spin systems was centered around *Conjecture I*, which extended a Brownian-like formalism to non-Markovian space- and timescales. If true, that conjecture is important for non-equilibrium physics in general. Another result of general interest is a novel formalism developed for the quantum systems, in order to apply the above conjecture. A potentially fundamental issue associated with *Conjecture I* is the absence of apparent limits beyond which the exact dynamics of systems with infinite numbers of particles invalidates that conjecture.

It should be emphasized, that although we presented *Conjecture I* as a natural extension of physical and mathematical experience, we used it to address the properties of fast microscopic relaxation, which are generally considered very difficult to access, and for which not much reliable experience exists. At present, our theory based on *Conjecture I* can make only one solid prediction for the fast relaxation, namely, that the functional form of the generic long-time behavior of the infinite temperature spin correlation functions (1.1) is given by Eqs.(1.24, 1.25). The underlying description, however, has a substantial explanatory power and also allows estimates to be made.

To summarize what was explained by our theory but was not explained by the theory of Borckmans and Walgraef (see Section 1.6), we now give the answers to the questions posed in Section 2.1.

Why is the long-time regime universal?

In the many-dimensional space representing all dynamical variables of the problem, the long-time regime is characterized by a probability distribution, which is *intrinsic* to a given dynamical problem and has the property that, one one hand, it is extremely complex, but, on the other hand, it develops cells of an extremely smooth structure that spread over the entire many-dimensional space.

What makes that regime different from the initial regime?

The initial probability distribution is not intrinsic to a given dynamical problem.

How should the apparent time-irreversibility of Eqs.(1.24,1.25) be reconciled with the time-reversibility of the underlying microscopic dynamics of a perfectly isolated system?

The stability properties in the many-dimensional space of dynamical variables are not identical for the forward and backward time evolutions, because some of those variables change sign under the time reversal. Therefore, the intrinsic probability distribution for the forward time evolution is similar but, in a sense opposite to the intrinsic distribution for the backward time evolution.

Why does the long-time decay have functional form (1.24,1.25)?

Conjecture I, which is motivated by the answers to the previous questions and by intuitive and empirical arguments, asserts that a kind of Markovian diffusion description can be applied to the long-time regime. Within the framework of such a description, it is important that we deal with spins, and, therefore, each lattice site is characterized by the parameter space, which has is finite volume. In the end, it is the finiteness of that volume which guarantees that the spectrum of the exponential solutions of the diffusion problem is discrete.

What mechanism is responsible for the oscillations in Eq.(1.25)?

The resulting diffusion description is non-Hermitian, which can be linked to a natural asymmetry between different mutual orientations of two spins interacting according to Hamiltonian (1.2). The eigenvalues of the non-Hermitian diffusion problem can have both real and imaginary parts. The presence of the imaginary parts leads to the oscillations.

Why are Eqs.(1.24,1.25) primarily relevant to the q-dependent correlation functions (1.1) and not to the pair correlation functions?

The long-time behavior (1.24,1.25) requires the diffusion problem to be posed in a finite volume, which, in particular, implies that, for such a problem, there should be no more than a finite number of non-equivalent lattice sites. For the diffusion problem corresponding to the q-dependent correlation functions (1.1), actually, all lattice sites are equivalent, which is the consequence of the fact that those correlation functions correspond to the irreducible representations of the group of lattice translations. For the pair correlation functions, one can only establish a ceiling for the long-time decay. That ceiling is given by the long-time decay of the q-dependent correlation function, which, in comparison with all other q-dependent correlation functions, has the smallest constant ξ entering Eq.(1.24) or (1.25).

What makes the situation at finite temperatures less transparent than at the infinite temperature?

Our theory crucially depends on the assumption of the chaotic dynamical mixing. That

assumption is less sound at finite temperatures because of the presence of equilibrium spin correlations.

Finally, we would like to mention that both the theoretical estimates and the empirical evidence show that knowledge of the long-time behavior (1.24, 1.25) has a practical value, related to the fact that this behavior becomes pronounced before the correlation functions (1.1) decay to impractically small values.

3 Approximation method

In this Chapter, we develop a method for approximating the entire class of correlation functions given by Eq.(1.1). That method is based on quite a universal kinetic model that will be introduced in Section 3.2. However, we shall start our treatment not with the model itself but with a semi-empirical analysis of various factors affecting the competition between the monotonic and the oscillatory regimes of correlation functions (1.1). That analysis should be considered as both an introduction and a model-independent supplement to the theoretical picture developed in Section 3.2.

3.1 Factors affecting the competition between the monotonic and the oscillatory regimes

The analysis to be presented in this part cannot prove by itself that the the correlation functions (1.1) should have the long-time behavior either of the form (1.24) or (1.25) — this is the subject of Chapter 2. However, it turns out, that once the functional form of the long-time behavior is established, it is not difficult to formulate semi-empirical rules that would allow one to anticipate the outcome of the competition between the monotonic and the oscillatory regimes.

First, it is necessary to mention that the behavior of the correlation functions (1.1) depends on the form of the Hamiltonian, the value of the wave vector and the choice of the spin component μ (x, y or z). A change in any one of the above three conditions can modify the behavior of the correlation functions from monotonic to oscillatory and vice versa.

We shall exemplify our analysis by the correlation functions (1.1) involving the x-components of spins (i.e. $\mu \to x$ in Eq.(1.1)). This covers all examples presented in Sections 1.5.1 and 1.5.3.

The following factors can be identified as important for discriminating between the two

regimes:

The first and the most important factor is direct correlations. This factor can be evaluated by comparing two quantities. The first of them is the second moment of $G(t)$:

$$M_2 = -\left.\frac{d^2G}{dt^2}\right|_{t=0} = \frac{1}{3}\,S(S+1)\,\sum_n [{J^y_{kn}}^2 + {J^z_{kn}}^2 - 2J^y_{kn}J^z_{kn}\cos(\boldsymbol{q}\cdot\boldsymbol{r}_{kn})]. \tag{3.1}$$

The second quantity is the second moment of the one-spin autocorrelation function

$$u(t) = \frac{\langle S^x_k(t)S^x_k(0)\rangle}{\langle S^x_k(0)S^x_k(0)\rangle}. \tag{3.2}$$

That second moment is given by

$$M_{2u} = -\left.\frac{d^2u}{dt^2}\right|_{t=0} = \frac{1}{3}\,S(S+1)\,\sum_n [{J^y_{kn}}^2 + {J^z_{kn}}^2]. \tag{3.3}$$

The inequality $M_2 < M_{2u}$ indicates that the correlation between the average polarizations of neighboring spins decreases the rate of the initial decay of $G(t)$ in comparison with $u(t)$. In this case, $G(t)$ tends to exhibit monotonic behavior. In the extreme case when $M_2 << M_{2u}$, the characteristic time of the decay of $G(t)$ is much longer than the mean free time τ. This justifies the Markovian approximation which would predict simple exponential decay.

In the opposite case, when $M_2 > M_{2u}$, the direct correlations favor oscillatory decay. It is, however, impossible to propose a Hamiltonian of form (1.2) that would lead to $M_2 >> M_{2u}$. The best one can get is $M_2 = 2M_{2u}$, which is the case for Figs.1.4(a,e,g).

The difference between M_2 and M_{2u} is due to the term $2J^y_{kn}J^z_{kn}\cos(\boldsymbol{q}\cdot\boldsymbol{r}_{kn})$ in Eq.(3.1). Therefore, the sign of this difference depends on the sign of $\cos(\boldsymbol{q}\cdot\boldsymbol{r}_{kn})$ and on the relative sign of J_y and J_z.

The above dependence on the relative sign of J^y_{kn} and J^z_{kn} is, at first sight, difficult to grasp intuitively. However, a closer examination of Hamiltonian (1.2) reveals that when J^y_{kn} and J^z_{kn} have the same sign, the x-components of two interacting spins tend to change in the opposite directions, which, in the extreme case of $J^y_{kn} = J^z_{kn}$, leads to the conservation of the x-component of the total spin. When J^y_{kn} and J^z_{kn} have the opposite signs, the x-components

of two interacting spins tend to change simultaneously in the same direction. (This factor will be explained in more detail in Section 3.2.)

The direct correlation factor alone would favor oscillatory decay in the examples shown in Figs. 1.2 and in 1.4(a,b,d,e,g), and monotonic decay in Figs.1.4(f,h). This factor would give no preference in the case shown in Fig.1.4(c). It is thus highlightened by the examples (b),(c) and (d) that there are other important factors to consider.

The second factor to be considered here is motional narrowing. In our definition, motional narrowing is associated with the fact that, generically, the lifetimes of local-fields generated by Hamiltonian (1.2) are finite. Here, we are primarily concerned only with the lifetimes of the local field components contributing to M_2 (i.e. y- and z-components).

The name "motional narrowing" originates from the limit of very short lifetimes, when a Markovian approximation applies and, as usual, justifies simple exponential decay. This situation is essentially identical to Problem B defined in our discussion of exchange narrowing (Section 1.4).

According to the Hamiltonian (1.2), the local field $\boldsymbol{h}_k$ that affects the kth spin is given by

$$\boldsymbol{h}_k = \sum_n \left[J_{kn}^x \; S_n^x \; \hat{\boldsymbol{e}}_x + J_{kn}^y \; S_n^y \; \hat{\boldsymbol{e}}_y + J_{kn}^z \; S_n^z \; \hat{\boldsymbol{e}}_z \right], \tag{3.4}$$

where $\hat{\boldsymbol{e}}_x$, $\hat{\boldsymbol{e}}_y$ and $\hat{\boldsymbol{e}}_z$ are the unit vectors in the respective directions.

The lifetime of the y-component of the local field can be estimated as $[S^2 \; \sum_n (J_{kn}^{x\;2} + J_{kn}^{z\;2})]^{-1/2}$, and the lifetime of the z-component as $[S^2 \sum_n (J_{kn}^{x\;2} + J_{kn}^{y\;2})]^{-1/2}$.

Motional narrowing does not affect the second moments of correlation functions (1.1), but it does affect the higher moments. The effect of the motional narrowing is always to shift the balance towards monotonic decay. The shorter the lifetime of the local fields, the stronger is the above trend.

The best way to expose the influence of the motional narrowing is to change J_x, because the corresponding term in the Hamiltonian does no affect either M_2 or M_{2u}. Therefore, it

does not contribute to the direct correlation effect discussed earlier. At the same time, the presence of that term reduces the lifetimes of both the y- and z-components of the local-fields.

Let consider the examples shown in Figs.1.4(b,d). In the both cases, the direct correlation effect is modest. It favors oscillatory behavior, which would be the case if $J^x_{kn} = 0$. However, the value of J^x_{kn} is sufficiently large. As a result, the motional narrowing ultimately outweighs the direct correlations, and the decay becomes monotonic.

The J^x_{kn}-term is also important for the example shown in Fig.1.4(f). Although the direct correlations in this case already favor monotonic decay, that trend would be much weaker without the J^x_{kn}-term.

The third factor to be discussed here is the indirect correlations. That factor is particularly important for the example shown in Fig.1.4(c). From the preceeding discussion, it would follow that the direct correlations give no preference in that case, but the motional narrowing factor is present, and, therefore, the correlation function should decay monotonically — in contrast to what is observed.

Under the name "indirect correlations", we refer to the correlations between spins that do not interact directly. These correlations cannot, therefore, contribute to the second moment M_2, but otherwise they are very similar to the direct correlations discussed above.

We cannot formulate a simple rule for the trend caused by the indirect correlations. We can only mention that, in general, the indirect correlations do not modify the effect of the direct correlations qualitatively. However, one has to be aware that the presence of the indirect correlations introduces a substantial uncertainty to the earlier analysis, when the polarization transfer between different spins is efficient (i.e. $|J^y_{kn}| \approx |J^z_{kn}|$), but the wave vector $\boldsymbol{q}$ is such that the effect of the direct correlations (i.e. the difference between M_2 and M_{2u}) is anomalously small. When such a coincidence occurs, as is the case for the correlation function shown in Fig.1.4(c), our experience indicates that the indirect correlations favor the oscillatory regime.

The fourth factor we would like to mention is the number of interacting neighbors. From our experience, a smaller number of interacting neighbors tends to favor the oscillatory behavior, though, typically, this effect is not very significant.

For instance, the correlation functions shown in Figs.1.4(a,e,g) differ from each other only by the dimensionality of the lattice, which means 2, 4 and 6 interacting neighbors respectively. Plots (e) and (g) are nearly identical (if the time axes are rescaled properly). However, each of them shows a somewhat smaller amplitude of the oscillations then plot (a).

The same trend is also evident for the plots (b) and (d). Again, example (b) is different from example (d) only by the smaller number of interacting neighbors. Although in both cases the decay ultimately becomes monotonic, the plot (b) shows a stronger initial drive toward oscillating behavior.

Now we would like to discuss the transition between the monotonic and oscillatory long-time regimes. For that purpose, it is helpful to bring out one of the results of Chapter 2, namely, that the long-time behavior of the correlation functions (1.1) is, actually, the sum of many exponential terms, some of which can have the monotonic form (1.24) and others can have the oscillatory form (1.25). It is then the slowest of those terms that ultimately dominates in the long-time behavior.

That notion sheds light on the way in which the transition from the monotonic to the oscillatory decay proceeds as parameters of the Hamiltonian change. The likely scenario (which is also supported by our numerical experience) is that, at the transition, the exponential decay constants of both the slowest oscillating term and the slowest monotonic term become equal to each other. Therefore, as the transition approaches, the long-time behavior of the correlation functions should be parametrized as the sum of two terms — one having form (1.24) and the other having form (1.25).

The above description implies that, when the previous analysis does not give an unambiguous prediction, a transitional situation should be suspected, which means that the

correlation function can exhibit a superposition of the two regimes during an extended initial time interval. Such a competition is, for example, present in Figs.1.4(b,d).

Concluding this part, we would like to mention that everything in the above analysis equally applies to both classical and quantum spin systems. However, the substitution of classical spins by quantum ones (especially spins 1/2) is, by itself, a factor, which, to some extent, favors the oscillatory regime.

3.2 Kinetic model of spin-spin relaxation

In this Section, we first present our model for the free induction decay problem of spins 1/2 and then generalize it to other cases.

3.2.1 Free induction decay for a lattice of spins 1/2

From the viewpoint of the general formulation given in Section 1.2, the present subsection is devoted to the case of $q = 0$ for spins 1/2. Moreover, the treatment will be limited to the form of the spin-spin interaction given by Hamiltonian (1.27) which, for convenience of discussion, we reproduce below:

$$\mathcal{H} = \sum_{k<n}[J^{\perp}_{kn}(S^x_k S^x_n + S^y_k S^y_n) + J^z_{kn} S^z_k S^z_n]. \qquad \text{(same as Eq.(1.27))}$$

As explained in Section 1.5.1, that form of interaction is the most general one for free induction decay.

In the following, we continue using the nonequilibrium formulation of our general problem (Section 1.2). In the case of free induction decay, that formulation was represented by Eq.(1.28), which we also reproduce here:

$$G(t) = \frac{m_x(t)}{m_x(0)}, \qquad \text{(same as Eq.(1.28))}$$

where we recall that $m_x(t)$ is the x-component of the small average polarization of every spin in the system, which decays from the initial value $m_x(0)$ to the equilibrium value equal to

zero. Other components of the average spin polarization remain equal to zero at all times, because, according to both the Hamiltonian and the initial probability distribution, any two opposite directions in the yz-plane are equivalent, and, therefore, there is no preferential direction in which the average spin polarization can emerge in that plane.

The general approach presented in this Section can be characterized as the extension of the framework of the Boltzmann kinetic description beyond the limit of instantaneous collisions. We thus outline that approach by comparing it with the derivation of the Boltzmann kinetic equation (BKE) [49].

The BKE can be considered as a modification of the exact equation for the system of noninteracting classical particles. In our method, we modify the exactly solvable case of the Ising-like Hamiltonian. The BKE is derived by counting particles entering and leaving small volumes of the phase space. Similarly, we analyze the averaged spin behavior in a given configuration of neighbors. (The configuration of neighbors refers to the phase space domain arising in the context of an Ising-like Hamiltonian.)

The derivation of BKE is based on the approximation of instantaneous collisions, which is not applicable to our problem. Instead, we substantiate the quantitative claim of our approach by adopting the criteria presented below.

The first criterion is that the mathematical construction of our theory has to be time reversible. This ensures that the odd powers of t are not present in the power series of $G(t)$. Since the exact expression (1.1) has the same property, the important parameters of the theory can be obtained by matching the exact moments M_2 and M_4, which must be directly evaluated from the time expansion of Eq.(1.1). Time reversibility implies abandoning simple first-order differential rate equations. Consequently, the minimal description has to be based on time-reversible second-order differential rate equations.

Among various dynamical correlations that complicate the analysis, the most important are the two-spin correlations. If an approximate calculation can accurately take the two-

spin correlations into account, then it is reasonable to expect that the contribution from the higher order correlations is more random, i.e better averageable. A criterion which at least partially guarantees that the two-spin correlations are respected is as follows:

The shape of the free induction decay obtained by the effective calculation is a function of the microscopic coefficients $J^{\perp}_{kn}$ and J^{z}_{kn}. We require that if in this function all $J^{\perp}_{kn}$ and J^{z}_{kn}, except for the coefficients describing the interaction between any given pair of spins, equal zero, then the function reproduces the exact result (1.11) for the two-spin system. In the notation of the Hamiltonian (1.27), that result can be rewritten as

$$G(t) = \cos\left[\frac{1}{2}(J^{z}_{12} - J^{\perp}_{12})t\right]. \tag{3.5}$$

We shall refer to the above requirement as the "T-criterion."

Model for the Ising case.

The free induction decay can be evaluated in a closed form in the Ising-like case when all $J^{\perp}_{kn} = 0$ (Section 1.3.1). We use the Lowe and Norberg interpretation [2] of this evaluation to initially motivate the formalism of our description.

In the Ising-like Hamiltonian (1.6), the operator of the local field, which affects the kth spin, is

$$h^{z}_{k} = \sum_{n} J^{z}_{kn} S^{z}_{n} \ . \tag{3.6}$$

Since the z-component of each spin is a constant of the motion, Eq.(3.6) implies that each spin is rotated by a constant local field created by that spin's neighbors.

If all operators S^{z}_{n} are diagonal in the basis chosen for the trace evaluation in Eq.(1.1), the contributions to the trace can be interpreted as a result of spin precessions in classical local fields. The possible values of these fields are the eigenvalues of the field operator h_k.

We introduce an index $\mathcal{C}$ to refer to the configurations of neighbors, and define a configuration as a particular set of the eigenvalues of operators S^{z}_{n} in Eq.(3.6). Let assume that

each spin interacts with N_0 neighbors that contribute to Eq.(3.6). It thus follows that there are infinitely many spins surrounded by a given configuration $\mathcal{C}$ of N_0 neighbors. Below we use the notation $\langle ... \rangle_{\mathcal{C}}$ to indicate averaging over all configurations of neighbors.

We continue using the notation $m_x(t)$ introduced in Section 1.5.1 for the average polarization of one spin. For the configuration $\mathcal{C}$, we also define $m_{\mathcal{C}x}(t)$ as the average polarization of nuclei that are surrounded by neighbors with the specified set of instantaneous spin projections on the z-axis. The initial uniform polarization implies that

$$m_{\mathcal{C}x}(0) = m_x(0) \simeq \frac{\Omega}{4k_BT}. \tag{3.7}$$

Another initial condition related to the fact that $m_{\mathcal{C}y}(0) = 0$ is

$$\left.\frac{dm_{\mathcal{C}x}(t)}{dt}\right|_{t=0} = 0\ . \tag{3.8}$$

The evolution of $m_{\mathcal{C}x}$ is governed by the equation

$$\frac{d^2m_{\mathcal{C}x}}{dt^2} = -\omega_{\mathcal{C}}^2 m_{\mathcal{C}x}, \tag{3.9}$$

where $\omega_{\mathcal{C}}$ is the precession rate in configuration $\mathcal{C}$:

$$\omega_{\mathcal{C}} = \tfrac{1}{2}\sum_n \pm J_{kn}^z. \tag{3.10}$$

Each configuration of neighbors uniquely specifies the combination of signs in Eq.(3.10).

Equations (3.9, 3.10) do not constitute any approximation. They just represent an intuitive interpretation of terms that appear in the exact expression for the RHS of Eq.(1.1).

For each configuration of neighbors, Eq.(3.9) with initial conditions (3.7, 3.8) has the following solution:

$$m_{\mathcal{C}x}(t) = m_{\mathcal{C}x}(0)cos(\omega_{\mathcal{C}}t). \tag{3.11}$$

The result of averaging $m_x(t) = \langle m_{\mathcal{C}x}(t)\rangle_{\mathcal{C}}$ should then be substituted to Eq.(1.28) which gives [2]

$$G(t) = \prod_n \cos\left(\frac{1}{2}J_{kn}^z t\right). \tag{3.12}$$

The right-hand side (RHS) of Eq.(3.12) is the Fourier transform of the discrete distribution of $\omega_{\mathcal{C}}$, which can be considered as a sum of random quantities $\pm J^z_{kn}/2$. Therefore, according to the central limit theorem, the distribution approaches Gaussian when

$$max\{|J^z_{kn}|\} << 2\sqrt{M_2}, \tag{3.13}$$

where $M_2 = \frac{1}{4}\sum_n (J^z_{kn})^2$. In this case, the RHS of Eq.(3.12) can be approximated as $\exp(-M_2\, t^2/2)$.

Model for the general case.

Apart from the Ising-like case, the configurations of neighbors of a given spin change with time. However, the primary element of our description continues to be not one spin evolving through many configurations of neighbors, but the average polarization $m_{\mathcal{C}x}(t)$ of all spins that are, at time t, surrounded by a given configuration of neighbors. In such a framework, the time evolutions of $m_{\mathcal{C}x}(t)$ for different configurations of neighbors become mutually dependent. A part of that dependence comes from the simple fact that the evolution of every spin through many configurations of neighbors results in the polarization transfer between those configurations.

The above concept of configurations of neighbors is quite similar to the concept of the spectral packets used by Shakhmuratov[39] in his time irreversible Markovian model.

Our model for the evolution of $m_{\mathcal{C}x}$ is time-reversible and based on the following generalization of Eq.(3.9):

$$\frac{d^2 m_{\mathcal{C}x}}{dt^2} = -(W^2_{\mathcal{C}+} P_{\mathcal{C}x+} - W^2_{\mathcal{C}-} P_{\mathcal{C}x-}) m_0, \tag{3.14}$$

where $P_{\mathcal{C}x+}$ and $P_{\mathcal{C}x-}$ are the probabilities that the spin projections on the x-axis are positive and negative, respectively; $W_{\mathcal{C}+}$ is the effective rate of the transition from a state where the spin is oriented positively along the x-axis to the state where the spin is oriented negatively along the same axis; $W_{\mathcal{C}-}$ is the rate of the reverse transition; $m_0 = 1/2$ is the maximum

polarization of one spin. The probabilities obey the relationships:

$$P_{\mathcal{C}x+} + P_{\mathcal{C}x-} = 1, \tag{3.15}$$

$$m_0(P_{\mathcal{C}x+} - P_{\mathcal{C}x-}) = m_{\mathcal{C}x}. \tag{3.16}$$

Equation (3.14) is not derived but postulated in the framework of our model. That equation should be considered not as representing spin precessions but rather as describing the transitions between the positive and the negative polarizations of spins along the x-axis. Keeping in mind that the transition rates are conventionally denoted by symbol W and not by symbol ω, we indicated the rate nature of Eq.(3.14), by introducing new variables $W_{\mathcal{C}+(-)}$ instead of modifying old variables $\omega_{\mathcal{C}}$. At the same time, the similarity in the appearance of the two symbols is also intentional — it indicates the close relationship between $\omega_{\mathcal{C}}$ and $W_{\mathcal{C}+(-)}$.

For the purposes of physical interpretation, the second-order rate equation (3.14) can be considered as equivalent to its first-order analog: $\frac{dm_{\mathcal{C}x}}{dt} = -(W_{\mathcal{C}+}P_{\mathcal{C}x+} - W_{\mathcal{C}-}P_{\mathcal{C}x-})m_0$. The reason why we have not used the first-order rate equation is that, earlier, we have restricted our choice to time-reversible mathematical constructions. The second-order rate equations thus provide the minimal basis for such a construction.

In general, rate models based on second-order differential equations are less popular in comparison with rate models based on first-order equations. Such a situation is, in part, due to the fact that it is more difficult to guarantee that systems of second-order rate equations do not produced exponentially growing unphysical solutions, when applied to actual physical situations. The mathematical construction resulting from our model will not have that deficiency, but at the same time it will provide us with all advantages of the time-reversible formalism.

The rates $W_{\mathcal{C}+}$ and $W_{\mathcal{C}-}$ in Eq.(3.14) characterize the net effect of all the factors discussed in Section 3.1. The asymmetry between those rates is an unusual but, at the same time, very

important physical ingredient of our model. Below we shall explain how the presence of weak polarization in the spin system in combination with two factors — the direct correlations with neighbors and the motional narrowing — can explain such an asymmetry. That explanation simultaneously gives a a new perspective to the above two factors.

The factor of direct correlations can be understood after we rewrite the two-spin Hamiltonian extracted from Eq.(1.27) as

$$\mathcal{H}_{kn} = J_{kn}^{\perp} S_k^x S_n^x + \frac{1}{4}(J_{kn}^{\perp} - J_{kn}^z)(S_k^+ S_n^+ + S_k^- S_n^-) + \frac{1}{4}(J_{kn}^{\perp} + J_{kn}^z)(S_k^+ S_n^- + S_k^- S_n^+), \quad (3.17)$$

where $S_k^+ = S_k^y + iS_k^z$, and $S_k^- = S_k^y - iS_k^z$.

The second and third terms in Eq.(3.17) lead to the double-flip of two parallel spins and the flip-flop of two antiparallel spins, respectively. If the kth spin is parallel to the average spin polarization, it is more probable that the nth spin will be parallel to the kth spin. This effectively increases the influence of the double-flip term on the kth spin and reduces the influence of the flip-flop term. If the kth spin is antiparallel to the average polarization, the opposite effect would occur. When $m_x > 0$, the double-flip correlation increases $W_{\mathcal{C}+}^2$ and reduces $W_{\mathcal{C}-}^2$ in Eq.(3.14). The flip-flop correlation leads to the opposite result.

The other factor mentioned above, motional narrowing, leads to the flux of spin polarization to and from the configuration $\mathcal{C}$. This means that the faster the time variations of the real local fields, the greater the difference between the chosen configuration of neighbors and those configurations that actually drove the spin to its current surroundings. One can conclude that spins coming to configuration $\mathcal{C}$ from other configurations tend to be slightly polarized in the direction of the average magnetization. This reduces $W_{\mathcal{C}+}^2$ and increases $W_{\mathcal{C}-}^2$, provided $m_x > 0$.

We define the average rate as

$$W_{\mathcal{C}}^2 = \frac{1}{2}(W_{\mathcal{C}+}^2 + W_{\mathcal{C}-}^2), \quad (3.18)$$

The high temperature condition guarantees that the difference between $W_{\mathcal{C}+}^2$ and $W_{\mathcal{C}-}^2$ is

small. The basic assumption of our analysis is that the leading term of this difference can be expressed as

$$\frac{1}{2}(W_{\mathcal{C}+}^2 - W_{\mathcal{C}-}^2) = \alpha\ W_{\mathcal{C}}^2\ \frac{m_x}{m_0}, \tag{3.19}$$

where α is a configuration independent parameter, which is determined by the average of all factors considered in Section 3.1. The status of assumption (3.19) is somewhat similar to the self-consistent relaxation time approximation, which is frequently adopted to solve the BKE.

The substitution of Eqs.(3.15, 3.16, 3.18, 3.19) into Eq.(3.14) yields

$$\frac{d^2 m_{\mathcal{C}x}}{dt^2} = -W_{\mathcal{C}}^2\ m_{\mathcal{C}x} - \alpha\ W_{\mathcal{C}}^2\ m_x. \tag{3.20}$$

Given the initial uniformly polarized state, the solution of Eq.(3.20) is

$$m_{\mathcal{C}x}(t) = m_{\mathcal{C}x}(0)\ cos(W_{\mathcal{C}}t) - \ \alpha \int_0^t m_x(t-t')W_{\mathcal{C}} sin(W_{\mathcal{C}}t')dt'. \tag{3.21}$$

Since $m_x(t) = \langle m_{\mathcal{C}x}(t)\rangle_{\mathcal{C}}$, the averaging of Eq.(3.21) over all configurations, together with Eq.(1.28), results in the integral equation

$$G(t) = g(t) + \alpha \int_0^t G(t-t')\frac{dg(t')}{dt'}dt', \tag{3.22}$$

where $g(t) = \langle cos(W_{\mathcal{C}}t)\rangle_{\mathcal{C}}$.

We choose $g(t)$ and α such that the second and the fourth moments obtained from Eq.(3.22) match the exact calculation. Matching the second moment gives

$$M_{2g} = \frac{M_2}{1+\alpha}, \tag{3.23}$$

where M_{2g} is defined as $-\frac{d^2 g}{dt^2}|_{t=0}$, and, in accordance with Eq.(3.1),

$$M_2 = \frac{1}{4}\ \sum_n (J_{kn}^{\perp} - J_{kn}^{z})^2. \tag{3.24}$$

Matching the fourth moment, combined with Eq.(3.23), allows α to be expressed as

$$\alpha = \frac{\frac{M_{4g}}{M_{2g}^2} - \frac{M_4}{M_2^2}}{\frac{M_4}{M_2^2} - 1}, \tag{3.25}$$

where $M_{4g} = \frac{d^4 g}{dt^4}|_{t=0} = \langle W_{\mathcal{C}}^4 \rangle_c$. We do not provide here the exact expression for the fourth moment M_4 in terms of the interaction constants $J_{kn}^{\perp}$ and J_{kn}^{z}, but that expression can be found in Ref.[10].

Eqs.(3.23,3.25) relate the shape and the scale of the acceptable distributions of $W_{\mathcal{C}}$. Namely, the shape specifies the ratio of M_{4g}/M_{2g}^2, which enters Eq.(3.25) and determines the value of α. With a known α, Eq.(3.23) gives the value of M_{2g}, which defines the scale of the distribution.

Equations (3.22,3.25) together with the recipe for the functional form of $g(t)$ is all that is needed for the calculation of $G(t)$ within the framework of our model.

Below we shall first discuss the general properties of Eq.(3.22), and only then introduce the recipe for $g(t)$. However, in order to be specific in the first half of that discussion, it is necessary to mention that, in most cases, our recipe for $g(t)$ will not be much different from Gaussian and its long-time decay will not be slower than exponential.

Properties of Eq.(3.22).

The integral equation (3.22) is known as a Volterra equation of the second kind[50]. In our case, the initial condition for that equation is $G(0) = g(0) = 1$. When $g(t)$ and α are known, Eq.(3.22) is easily solvable numerically. Our preferred method of its numerical solution is explicit integration.

The procedure of explicit integration requires choosing the time grid $\{t_i\}$, and on that time grid the value of $G(t_j)$ is obtained iteratively by substituting the previous values $G(t_i)$ $(t_i \leq t_j)$ into the integral on the RHS of Eq.(3.22). In principle the expression for $G(t_j)$ would then depend on $G(t_j)$ itself. However, the reason why the above method is very efficient is that, in our case, for each step of the above iteration procedure, the discrete term containing the unknown value of $G(t_j)$ does not contribute to the integral. That term should be multiplied by the value of the kernel $\frac{dg(t')}{dt'}$ at $t' = 0$, but that value equals zero, because

according to our recipe, $g(t)$ will always be an even function of time.

The behavior of the solutions of Eq.(3.22) are mainly controlled by the value of the parameter α. In correspondence with the empirical picture, the solutions exhibit two basic regimes: monotonic and oscillatory. The monotonic regime roughly corresponds to $-1 \leq \alpha < 0$, and the oscillatory one — to $0 < \alpha \leq \infty$.

Values of α smaller than -1 would lead to unstable, exponentially growing solutions that are not meaningful. It is impossible to obtain $\alpha < -1$ with any meaningful recipe for $g(t)$.

After $g(t)$ decays to sufficiently small values, the monotonic solutions approach the long-time functional form (1.24), and the oscillatory ones approach the long-time functional form (1.25).

In the limiting case of $\alpha = -1$, the solution of Eq.(3.22) is $G(t) = 1$. This solution does not depend on the form of $g(t)$. The limit $\alpha = -1$ can appear if one treats the $q = 0$ problem for the case of pure Heisenberg interaction. In that case, the solution $G(t) = 1$ is indeed exact, because, as we have already mentioned in Section 1.4, the correlation function (1.1) for $q = 0$ is proportional to the decay of the total spin polarization, which is conserved by the Heisenberg interaction.

When α is greater than -1, but very close to that value, the solutions of Eq.(3.22) are nearly exponential and, as usual, correspond to the situation with the separation of the timescales. In terms of Eq.(3.22), the separation of timescales means that $G(t)$ decays much slower than $g(t)$. The necessary condition for α to become close to -1 is an anomalously large value of the ratio $\frac{M_4}{M_2^2}$ that enters Eq.(3.25). The large value of that ratio is, indeed, known to be a reliable indicator of the separation of timescales in the underlying microscopic dynamics of the system[3].

The transition between the monotonic and the oscillatory solutions of Eq.(3.22) corresponds to $\alpha \approx 0$. Therefore, according to Eq.(3.22), that transition proceeds via the situation when $G(t) = g(t)$.

The above mode of transition indicates certain limitations of our model: As we have already discussed in Sections 2.4 and 3.1, the transition between the analogous two regimes for the true correlation functions of form (1.1) is likely to proceed via an extended interval of the superposition of both functional forms (1.24) and (1.25). At the same time, our recipe for $g(t)$ will not contain a possibility for such a superposition. Therefore, if formula Eq.(3.25) gives the value of α in the interval between -0.1 and 0.1, and the underlying microscopic situation is not close to any of the exactly matched limits discussed later, then the resulting approximation should be expected to be less accurate then on the average.

Finally, the last important limit is that of $\alpha \to +\infty$. For any choice of the functional form of $g(t)$ with finite moments, the limit $\alpha \to +\infty$ would lead to a purely oscillatory solution: $G(t) = \cos(t\sqrt{M_2})$. That limit guarantees the fulfillment of the T-criterion introduced earlier (see Eq.(3.5)), because the exact solution (3.5) for the system of two spins 1/2 always gives the ratio $M_4/M_2^2 = 1$, which formally leads to an infinite value of α in Eq.(3.25). That divergence does not appear in the solution of Eq.(3.22), because, according to Eq.(3.23), it is offset by the small value of M_{2g}. When the two-spin problem is considered as a limit of the many-spin problem with $J_{kn}^{\perp}, J_{kn}^{z} \to 0$, except for $J_{12}^{\perp}$ and J_{12}^{z}, the solution of Eq.(3.22) converges to the RHS of Eq.(3.5).

The observable part of $G(t)$ obtained from Eqs.(3.22, 3.23, 3.25) is weakly sensitive to the variations of the input shape of the $W_{\mathcal{C}}$ distribution. Thus relatively crude assumptions about that shape should still lead to good accuracy in the result. The choice of the shape of the $W_{\mathcal{C}}$ distribution is equivalent to the choice of the functional form of $g(t)$. Below, we shall mostly discuss the latter rather than the former.

Choice of the functional form of g(t).

We introduce our recipe for the form of $g(t)$ by considering a sequence of functional forms — from more simple to more sophisticated. At each step, we shall present the arguments

why the next level of sophistication is required. Of course, in addition to those arguments, the computational relevance of each element of the final recipe has been verified by our actual experience with the solutions of Eq.(3.22).

Since the fulfillment of the T-criterion is guaranteed, and the important many-spin correlations are taken into account by the choice of parameter α, we assume that $g(t)$ is produced by uncorrelated contributions from spin neighbors. Moreover, if the neighbors are static, which corresponds to the Ising case, we just insist that the model should reproduce the exact result (3.12). A straightforward way to achieve this is to propose a general recipe for $g(t)$ which for the purely Ising case just reproduces the RHS of Eq.(3.12). In that case, Eq.(3.25), would guarantee that $\alpha = 0$, and, therefore, according to Eq.(3.22), $G(t) = g(t)$.

In the general case of the Hamiltonian (1.27), one could proceed with a recipe, which would associate the functional form of $g(t)$ with the solution of an "optimal" Ising-like case. The definitions of the optimal Ising-like case can vary. For example, one can just take the Ising part of the Hamiltonian (1.27), or rewrite the Hamiltonian (1.27) as

$$\mathcal{H} = \sum_{k<n} [J_{kn}^{\perp} \boldsymbol{S}_k \cdot \boldsymbol{S}_n + (J_{kn}^{z} - J_{kn}^{\perp}) S_k^z S_n^z], \tag{3.26}$$

and then take the last term of the resulting expression.

We tentatively choose the latter option, which is motivated by the fact that, with such a choice, the free induction decay for the Ising problem has the same second moment as for the problem with the full Hamiltonian (3.26), and thus the solution of that Ising problem, by itself, can be considered as a "zero-order approximation" for the actual behavior of $G(t)$.

In fact, the choice between the above two options would not matter too much, if our recipe for the form of $g(t)$ did not include anything else: In the end, the resulting functional form should be renormalized as required by Eq.(3.23). As long as the ratio of $J_{kn}^{\perp}/J_{kn}^{z}$ is same for every pair of interacting spins (which is the case for every example presented in

Section 1.5), the resulting expression would still be given by

$$g(t) = \prod_n \cos\left[\frac{1}{2}(J^z_{kn} - J^\perp_{kn})\,\zeta\; t\right], \tag{3.27}$$

where ζ is the renormalization factor required by Eq.(3.23). The formula for this factor is

$$\zeta = \sqrt{\frac{1}{1+\alpha}}. \tag{3.28}$$

There are, however, several reasons, why we have made the recipe for $g(t)$ somewhat more sophisticated.

First, if the Ising-like part of the Hamiltonian only includes interaction with a finite number of neighbors, then, as follows from Eq.(3.10), the Fourier transform of the expression in the RHS of Eq.(3.12) has a discrete structure. Therefore, if that expression is used to give the functional form of $g(t)$, then sooner or later all discrete components in the frequency spectrum of $g(t)$ will get refocused, and $g(t)$ will return to its value at $t = 0$, and then such a refocusing will occur more or less periodically. According to Eq.(3.22), the return of $g(t)$ to the initial value will result in the follow-up rebouncing of $G(t)$, which seems to be rather unphysical provided the correction to the Ising term in the Hamiltonian (3.26) is not too small.

Such a complication is, apparently, very realistic for problems with a small number of interacting neighbors, but, even for a larger number of the direct couplings (eg. the magnetic dipolar interaction discussed in Section 1.5.1), the discreteness of the Ising spectrum can also result in a spurious response of $G(t)$.

The resulting difficulty can be summarized by stating that the solution of the "optimal" Ising problem exerts an excessive influence on the solution of the full problem. That influence is very dramatic at longer times, but it also affects the initial behavior of $G(t)$ to the extent that it reduces the accuracy of our approximation.

In order to deal with such a complication we recall that, in our model, the values of the rates $W_\mathcal{C}$ reflect not only the direct influence of neighbors on a given spin but also

the polarization flux between different configurations of neighbors. The later is caused by the fact that, in general, the lifetimes of the local fields produced by the Ising term in the Hamiltonian are finite. Therefore, the discrete Ising spectrum for $W_{\mathcal{C}}$ can and should be "washed out" by the effect of finite lifetimes.

The proper scale for that lifetime effect is given by the second moment

$$M_{2\varphi} = - \left. \frac{d^2\varphi(t)}{dt^2} \right|_{t=0}, \tag{3.29}$$

where

$$\varphi(t) = \frac{\langle h_k^z(t) h_k^z(0) \rangle}{\langle h_k^z(0) h_k^z(0) \rangle} \tag{3.30}$$

is the correlation function of the local field

$$h_k^z = \sum_n (J_{kn}^z - J_{kn}^{\perp}) S_n^z \tag{3.31}$$

produced by the Ising term in the Hamiltonian (3.26).

A simple way to allow for the lifetime factor is to replace every line in the discrete Ising spectrum by a Gaussian having the second moment M_{2phi}, which amounts to making the convolution between that spectrum and the Gaussian. As a result, in the time domain, $g(t)$ becomes a product of a Gaussian and the RHS of Eq.(3.27):

$$g(t) = exp\left[-\frac{1}{2} M_{2\varphi} (\zeta t)^2\right] \prod_n \cos\left[\frac{1}{2}(J_{kn}^z - J_{kn}^{\perp})\zeta t\right], \tag{3.32}$$

where the new renormalization factor required by Eq.(3.23) is

$$\zeta = \sqrt{\frac{M_2}{(1+\alpha)(M_2 + M_{2\varphi})}}. \tag{3.33}$$

When the timescale represented by $M_{2\varphi}$ is added to the recipe for $g(t)$, our earlier specification of the optimal Ising Hamiltonian becomes more important. Should we choose the optimal Ising term as $\sum_{k<n} J_{kn}^z S_k^z S_n^z$, the ratio of the characteristic times for the Gaussian and for the product of cosines would be different in Eq.(3.32).

The introduction of the lifetime factor entails an additional detail that should be added to our recipe. Namely, in looking for the "optimal" Ising case we should not restrict ourselves only to the $S_k^z S_n^z$ terms in the Hamiltonian. For example, the Hamiltonian (1.27) can be decomposed as

$$\mathcal{H} = \sum_{k<n} [J_{kn}^{\perp} S_k^x S_n^x + J_{kn}^z (S_k^y S_n^y + S_k^z S_n^z) + (J_{kn}^{\perp} - J_{kn}^z) S_k^y S_n^y], \tag{3.34}$$

and the last $S_k^y S_n^y$ term of that expression thus can also be treated as a candidate for being the optimal Ising case. As our previous choice, the above $S_k^y S_n^y$ term alone would lead to the correct second moment of $G(t)$

In order to optimize the orientation of the Ising term, we compare the lifetimes of the local fields created by each possible alternative and then choose the orientation that gives the longest lifetime. As a measure of the lifetime factor, we use the quantity analogous to $M_{2\varphi}$ but defined for each orientation appropriately.

Below we continue using the $S_k^z S_n^z$ form of the optimal Ising Hamiltonian only in order to be specific.

In the general case, it is impossible to separate the lifetime effect from the rest of the problem. Therefore, the treatment of that effect on the basis of Eq.(3.32) can be qualified as adequate enough, in the sense that it is as crude as the concept of the lifetime itself.

However, in the limit of the exchange narrowing, Problem B (Section 1.4), the concept of of the local field fluctuations is well justified, and the result for $G(t)$ is known to be given by Eq.(1.20). Although that problem requires two spin species, it is, otherwise, a direct analog of the free induction decay problem.

Therefore, we would like to introduce the last modification of the recipe for $g(t)$ to incorporate formula (1.20) as the exact limit of our model. Again, as with the Ising case, the way we do that is to modify the formula for $g(t)$ in such a way that in the limit of Problem B, $g(t)$ becomes equal to the RHS of Eq.(1.20).

We thus need a formula for $g(t)$ that interpolates between Eq.(3.27), for the purely Ising case, and the RHS of Eq.(1.20) for the case of fast fluctuations of the Ising local fields. The difficulty in constructing such a formula is that, in the limit of the fast fluctuations, Eq.(1.21) contains no residue of the Ising spectrum except for its second moment. It is, therefore, not straightforward to propose how, in the frequency domain, the discrete Ising structure appears from the narrow peaked Lorentzian shape corresponding to Eq.(1.20).

We constructed our formula by analogy with a simple problem of a spin that can precess with two possible values of frequency $+\omega_0$ and $-\omega_0$ under condition that the frequency fluctuates between the two values. The fluctuations are described by a random Markovian process with rate γ. (See Appendix F in Ref.[48] and also Ref.[51])

That problem is explicitly time irreversible and thus cannot appear as a formal limit of our general problem. However, the qualitative structure of its solution appears to be very relevant to our search for the interpolation between the static and the fast fluctuating cases.

For $\gamma < \omega_0$, that solution has the form of damped oscillations of the form $\exp(-\gamma t)$ $\cos(t\sqrt{\omega_0^2 - \gamma^2} - \phi)$. For $\gamma > \omega_0$ the oscillations disappear — they turn into the sum of two monotonic exponential decays with the constants $\gamma \pm \sqrt{\gamma^2 - \omega_0^2}$. In the limit $\gamma \gg \omega_0$, the slowest of the above two terms dominates the decay, and the constant of that decay reproduces the one given by Eq.(1.21) (provided $\varphi(t) = \exp(-2\gamma t)$ and $M_2 = \omega_0^2$ are substituted into that equation).

By analogy with the above problem, we assume that (i) for $M_{2\varphi} < M_2$, the functional form of $g(t)$ should be more similar to the one given by Eq.(3.32); (ii) the equality $M_{2\varphi} = M_2$ represents the critical situation when any residue of the discrete Ising spectrum should disappear; and (iii) for $M_{2\varphi} > M_2$, $g(t)$ should be of the form of the RHS of Eq.(1.20).

The above qualitative picture finds its specific realization in the final version of our recipe for $g(t)$. Below, we formulate that final recipe in its full detail, which requires reintroducing certain elements that have been discussed earlier.

First we identify the optimal Ising term. That term alone should give the same second moment (3.24) as the full Hamiltonian gives. The preferred axis of that term should correspond to the longest-living local fields. The lifetimes of the local fields should be judged by the value of $M_{2\varphi}$ defined by Eq.(3.29), where $\varphi(t)$ is the correlation function of the local fields created by the Ising term. (If the Ising term has a form other than $S_k^z S_n^z$, then Eqs.(3.30, 3.31) should be modified accordingly.)

Let assume that the z axis is, indeed, the preferred one for the optimal Ising term and decompose the full Hamiltonian (1.27) as

$$\mathcal{H} = \tilde{\mathcal{H}} + \sum_{k<n} \tilde{J}_{kn}^z S_k^z S_n^z. \tag{3.35}$$

In the above equation, the $\tilde{J}_{kn}^z$ are the coefficients of the optimal Ising term, and $\tilde{\mathcal{H}}$ is the rest of the full Hamiltonian.

We also reintroduce $M_{2\varphi}$ as the second moment of the correlation function

$$\varphi(t) = \frac{\langle \tilde{h}_k^z(t) \tilde{h}_k^z(0) \rangle}{\langle \tilde{h}_k^z(0) \tilde{h}_k^z(0) \rangle}, \tag{3.36}$$

where

$$\tilde{h}_k^z = \sum_n \tilde{J}_{kn}^z S_n^z. \tag{3.37}$$

Our recipe for $g(t)$ can now be expressed as follows:

For $M_{2\varphi} \leq M_2$,

$$g(t) = \exp\left[-\frac{M_{2\varphi}}{2} (\zeta_0\, t)^2\right] \prod_n \cos\left[\frac{1}{2} \tilde{J}_{kn}^z\, \zeta_0\, \zeta_a\, t\right], \tag{3.38}$$

where the renormalization factors are

$$\zeta_0 = \sqrt{\frac{1}{1+\alpha}}, \tag{3.39}$$

$$\zeta_a = \sqrt{1 - \frac{M_{2\varphi}}{M_2}}. \tag{3.40}$$

For $M_{2\varphi} > M_2$,

$$g(t) = \exp\left[-M_2\, {\zeta_0}^2 \int_0^t (t - t')\, \varphi(\zeta_0\, \zeta_b\, t')\, dt'\right], \tag{3.41}$$

where ζ_0 is still given by Eq.(3.39), and

$$\zeta_b = \sqrt{\frac{M_{2\varphi}}{M_2} - 1}. \tag{3.42}$$

When $M_{2\varphi} = M_2$, both Eq.(3.38) and Eq.(3.41) give a perfect Gaussian:

$$g(t) = \exp\left[-\frac{M_2}{2}\,(\zeta_0\, t)^2\right]. \tag{3.43}$$

After identifying the optimal Ising problem, the resulting mathematical construction should be used as follows:

It is, necessary, first, obtain the values of theoretical parameters M_2, M_4, $M_{2\varphi}$ and ζ_a or ζ_b. Formulas for $M_{2\varphi}$, ζ_a and ζ_b are given by Eqs.(3.29), (3.40) and (3.42), and the values of M_2 and M_4 should be obtained by the direct evaluation of the time derivatives of the RHS of Eq.(1.1).

The values of the parameters ζ_0 and α and the form of $g(t)$ should then be determined self-consistently. First, it is necessary to substitute $\zeta_0 = 1$ in Eq.(3.38) or (3.41) and, from the resulting expression for $g(t)$ compute the ratio $\dfrac{M_{4g}}{M_{2g}^2}$. That ratio does not actually depend on ζ_0 but, at the same time, allows α to be computed using formula (3.25). After that, the true value of ζ_0 should be determined by formula (3.39), and that value should be substituted into Eq.(3.38) or (3.41) to obtain the final form of $g(t)$.

Despite the numerous details of our recipe, the form of $g(t)$ corresponding to a typical situation remains close to Gaussian. The main influence of those details on the solution of Eq.(3.22) comes through the ratio M_{4g}/M_{2g}^2 which enters formula (3.25) for the parameter α.

The above recipe allows one practical simplification. Namely, when the problem is not too close to the limit of Eq.(1.20), it makes very little difference for the solution of Eq.(3.22), if, in Eq.(3.41), instead of the form of $\varphi(t)$ given by Eq.(3.36, one uses just a Gaussian with the same second moment. In most cases, all we need to know accurately about $\varphi(t)$ is just its second moment $M_{2\varphi}$, which affects the ratio of M_{4g}/M_{2g}^2, and therefore affects the value

of α given by Eq.(3.25). Of course, otherwise, the calculation of $\varphi(t)$ would be the hardest part of our entire approximation.

It turns out that, for all examples considered in this work, $M_{2\varphi}$ is either equal exactly to or very closely approximated by the second moment of the pair correlation function $\langle S_n^z(t) S_n^z(0) \rangle$. (We still keep the convention that the z axis corresponds to the preferred axis for the optimal Ising term.) In other words, we will evaluate $M_{2\varphi}$ on the basis of the formula

$$M_{2\varphi} = -\frac{1}{\langle S_n^z(0) S_n^z(0) \rangle} \, \frac{d^2}{dt^2} \, \langle S_n^z(0) S_n^z(0) \rangle. \tag{3.44}$$

However, one should keep in mind that the above simplification is not always adequate. In particular, an example where formula (3.44) would not work is given by the infinite-range Ising problem discussed in the end of Section 1.3.1. In that case, the comparison of the value of $M_{2\varphi}$ obtained from the original definition (3.29, 3.36) with the value of $M_{2\varphi}$ given by Eq.(3.44) would reveal that the full Ising field (3.37) lives infinitely longer than the individual z-components of spins.

The exact solution (1.8) of the above mentioned long-range Ising problem has form (1.8). For the infinite lattice, the product in the RHS of Eq.(1.8) includes an infinite number of cosines with frequencies $J_I/2$, which implies that the RHS of Eq.(1.8) can be perfectly approximated by a Gaussian. At the same time, our model with the original definition (3.29, 3.36) for $M_{2\varphi}$ gives $\dfrac{M_{2\varphi}}{M_2} \to 0$, when the lattice size is increased to infinity. In that limit, $g(t)$ given by formula (3.38) will reproduce the exact solution, and so will $G(t)$.

Finally, another exact limit that was matched by the final form of our recipe for $g(t)$ is the one represented by Eq.(1.15) for the spin 1/2 XX chain. The correlation function given by that equation is purely Gaussian. It turns out that when our recipe is applied to the setup underlying Eq.(1.15), the prescription for $g(t)$ would be the one given by Eq.(3.43), i.e. also purely Gaussian.

3.2.2 Other cases

The generalization of the free induction decay treatment to other cases is quite straightforward. In fact, the approximation scheme that emerged from that treatment (i.e. Eqs(3.22, 3.25, 3.38-3.41)) has already been formulated in Section 3.2.1 in an entirely general fashion.

We recall that, from the viewpoint of the general formulation given in Section 1.2, the setup considered in the context of the free induction decay was that of $q = 0$, spins $1/2$ and the Hamiltonian (1.27). Below we shall discuss the generalizations in the following order: (i) beyond the Hamiltonian (1.27); (ii) beyond spins $1/2$; and (iii) beyond $q = 0$.

The first generalization is simple:

Neither the mathematical construction developed in Section 3.2.1 nor its justification needs any adjustment when, instead of the form given by Eq.(1.27), the Hamiltonian of the problem has the more general form (1.2).

We would only like to mention that for the general form of the Hamiltonian, the formulation of the T-criterion should be linked to Eq.(1.11) instead of Eq.(3.5).

Beyond spins $1/2$, it is only necessary to replace the product in Eq.(3.38) with the more general solution (1.7) of the Ising problem. Thus, for $M_{2\varphi} \leq M_2$, Eq.(3.38) in the recipe for $g(t)$ is replaced by

$$g(t) = \exp\left[-\frac{M_{2\varphi}}{2}\,(\zeta_0\, t)^2\right] \prod_n \frac{\sin\left[(S+\frac{1}{2})J^z_{kn}\,\zeta_0\,\zeta_a\,t\right]}{(2S+1)\sin\left[\frac{1}{2}J^z_{kn}\,\zeta_0\,\zeta_a\,t\right]} \tag{3.45}$$

where the renormalization factors ζ_0 and ζ_a are still given by Eqs.(3.39, 3.40).

For $M_{2\varphi} \leq M_2$, the recipe (3.41) for the form of $g(t)$ remains applicable to all values of spins.

In this work, besides spins $1/2$, we only consider classical spins, for which the Ising solution is given by Eq.(1.9), and correspondingly, the specific form of Eq.(3.45) is the

following:

$$g(t) = \exp\left[-\frac{M_{2\varphi}}{2}\,(\zeta_0\; t)^2\right]\;\prod_n\;\frac{\sin\left(SJ^z_{kn}\;\zeta_0\;\zeta_a\;t\right)}{SJ^z_{kn}\;\zeta_0\;\zeta_a\;t}. \tag{3.46}$$

The only difference for spins greater than 1/2 is that the T-criterion is not relevant anymore, which mean that the resulting construction does not match the solution of the two-spin problem exactly.

It would, of course, be desirable to keep the T-criterion intact. However, we abandoned it because, the solution of the two-spin problem for spins greater than 1/2 does not have a simple analytic form, and, therefore, that solution cannot be easily incorporated as an exact limit.

The generalization beyond $q = 0$ is very easy to formulate. Namely, the mathematical construction for $q = 0$ applies to any $\boldsymbol{q}$ corresponding to a wavelength commensurate with the lattice periodicity. No corrections are required.

It is, however, necessary to explain that generalization.

First, we note that the entire recipe in Section 3.2.1 is formulated in terms of the moments, which could be computed for any $\boldsymbol{q}$. That recipe also requires matching several exact limits. However, in each of those limits, the exact solutions are identical for every value of $\boldsymbol{q}$.

From the viewpoint of the justification of the underlying model, a crucial role is played by assumption (3.19), which is supposed to reflect the direct correlations as the most important factor.

We recall that asymmetry between the rates $W_{\mathcal{C}+}$ and $W_{\mathcal{C}-}$ entering Eq.(3.14) is, to a large extent, associated with the direct correlation effects caused by the presence of average spin polarization of the neighbors of each spin.

For $q = 0$, the average polarization m_x is obviously the same for each lattice site. That fact allowed us to express the average polarization of neighbors of a given spin through the average polarization of that spin itself and thus close the system of equations.

One can easily see from the examples presented in Fig. 1.1 that not all average spin polarizations are equal to each other for $q \neq 0$.

It thus might seem reasonable to proceed in the following way: (i) divide the lattice into groups of sites having the same average polarization; (ii) label each such group by the value of the index i; (iii) for each group, introduce variables $m_{\mathcal{C}xi}$, m_{xi}, $W_{\mathcal{C}i+}$ and $W_{\mathcal{C}i-}$ analogous to the $m_{\mathcal{C}x}$ and m_x, $W_{\mathcal{C}+}$ and $W_{\mathcal{C}-}$ defined in Section 3.2.1; (iv) rewrite Eq.(3.19) for each group of spins separately, and correct the RHS of that equation to account for the correlations between spins belonging to different groups, i.e.

$$\frac{1}{2}(W_{\mathcal{C}i+}^2 - W_{\mathcal{C}i-}^2) = W_{\mathcal{C}i}^2 \sum_j \alpha_{ij} \frac{m_{xj}}{m_0}, \tag{3.47}$$

where the newly-introduced matrix α_{ij} is the analog of the parameter α in Eq.(3.19).

The new assumption (3.47) would lead to a system of coupled integral equations. Apart for the cross terms, each of those integral equations would look similar to Eq.(3.22).

Such a generalization can, indeed, be necessary for situations with two or more physically nonequivalent spin species — for example, electronic and nuclear spins, or two kinds of nuclear spins with different gyromagnetic ratios — i.e. situations, when the form of the Hamiltonian rather than the presence of a non-zero wave vector discriminates between different spins.

However, in this work we address only problems with one kind of spin species and only with initial conditions (1.5) that correspond to a modulated structure $\cos(\boldsymbol{q} \cdot \boldsymbol{r}_n)$ commensurate with the lattice periodicity. In that case, the relationship (3.47) is reduced back to the form (3.19).

Such a simplification is a consequence of the fact that the modulation $\cos(\boldsymbol{q} \cdot \boldsymbol{r}_n)$ is the real part of $\exp(i\ \boldsymbol{q} \cdot \boldsymbol{r}_n)$, which is an irreducible representation of the group of lattice translations. The argument here is entirely analogous to the one given in Section 2.4 in order to justify Eq.(2.15):

In order, for assumption (3.19) to be restored, it is necessary have the condition when

$$m_{xi}(t) = k_{ji} m_{xj}(t), \tag{3.48}$$

where k_{ji} are the time independent proportionality coefficients.

In that case, Eq.(3.47) can be transformed back to the form

$$\frac{1}{2}(W^2_{\mathcal{C}i+} - W^2_{\mathcal{C}i-}) = \alpha \; W^2_{\mathcal{C}i} \; \frac{m_{xi}}{m_0}, \tag{3.49}$$

where

$$\alpha = \sum_j k_{ij} \alpha_{ij}. \tag{3.50}$$

The time independence of the proportionality coefficients is assured by the fact that the modulation of the average spin polarizations initially having form $\cos(\boldsymbol{q} \cdot \boldsymbol{r}_n)$ can change its amplitude but not its shape — the change in its shape would imply an emerging contributions from other irreducible representations (not present at $t = 0$), but this cannot happen in the linear response regime when the Hamiltonian of the problem satisfies the translational symmetry of the lattice.

Concluding the discussion of the problems with $q \neq 0$, we should mention that the T-criterion that has already been abandoned for $S > 1/2$, is also not meaningful for spin 1/2 problems with the values of q other than 0 or π (or their higher dimensional analogs), because only the above values of q can be defined for the "two-spin lattice" (see Section 1.3.2).

3.2.3 Comparison with the empirical data

We now apply the approximation developed in Sections 3.2.1 and 3.2.2, to the systems considered in Section 1.5. The comparison between the results of our approximate calculations and the empirical data is presented in Figs. 3.1, 3.2 and 3.3. For each situation presented, the values of the two important parameters characterizing the approximate calculations, namely, $\frac{M_{2\varphi}}{M_2}$ and α are given in Table 3.1.

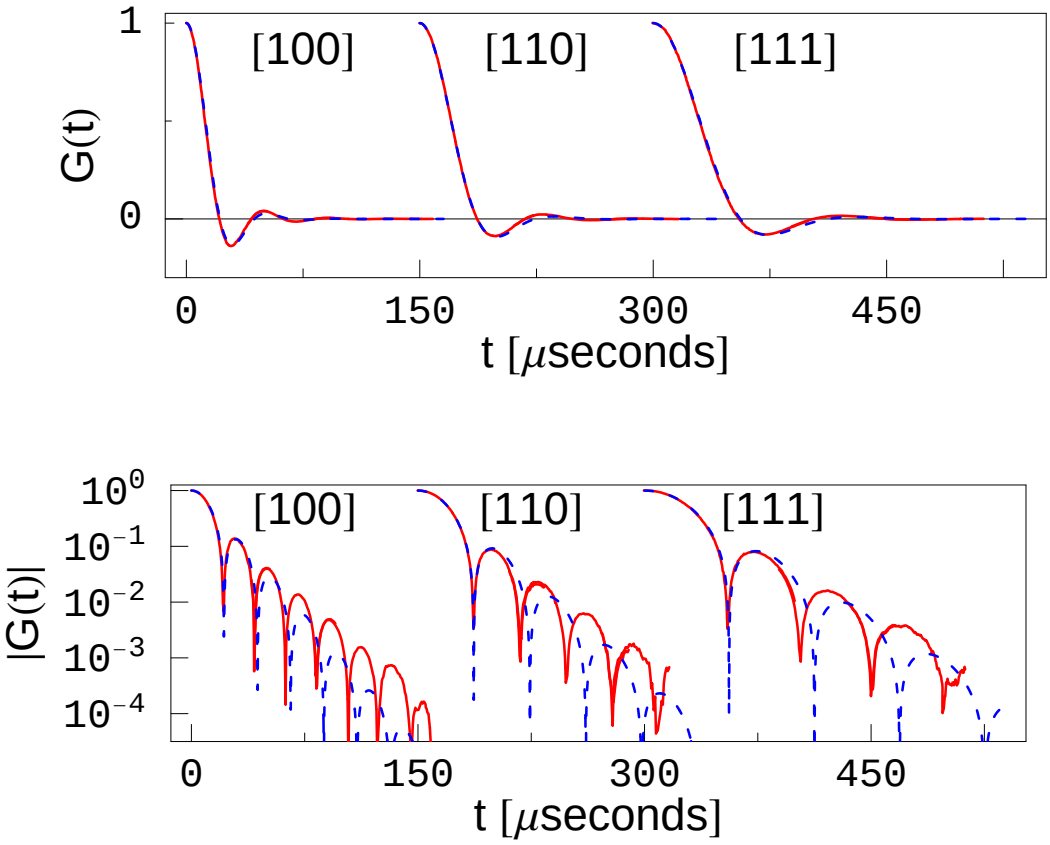

Figure 3.1: Free induction decay in CaF_2. The top and bottom frames contain identical pieces of data presented on direct(non-logarithmic) and on logarithmic scales respectively. The solid red lines represent the experimental data of Engelsberg and Lowe [20]. The blue dashed lines represent the solutions of Eq.(3.22). Each plot is labeled by the direction of the external magnetic field. The time origins of the [110] and [111] plots are shifted by 150 and 300 microseconds respectively.

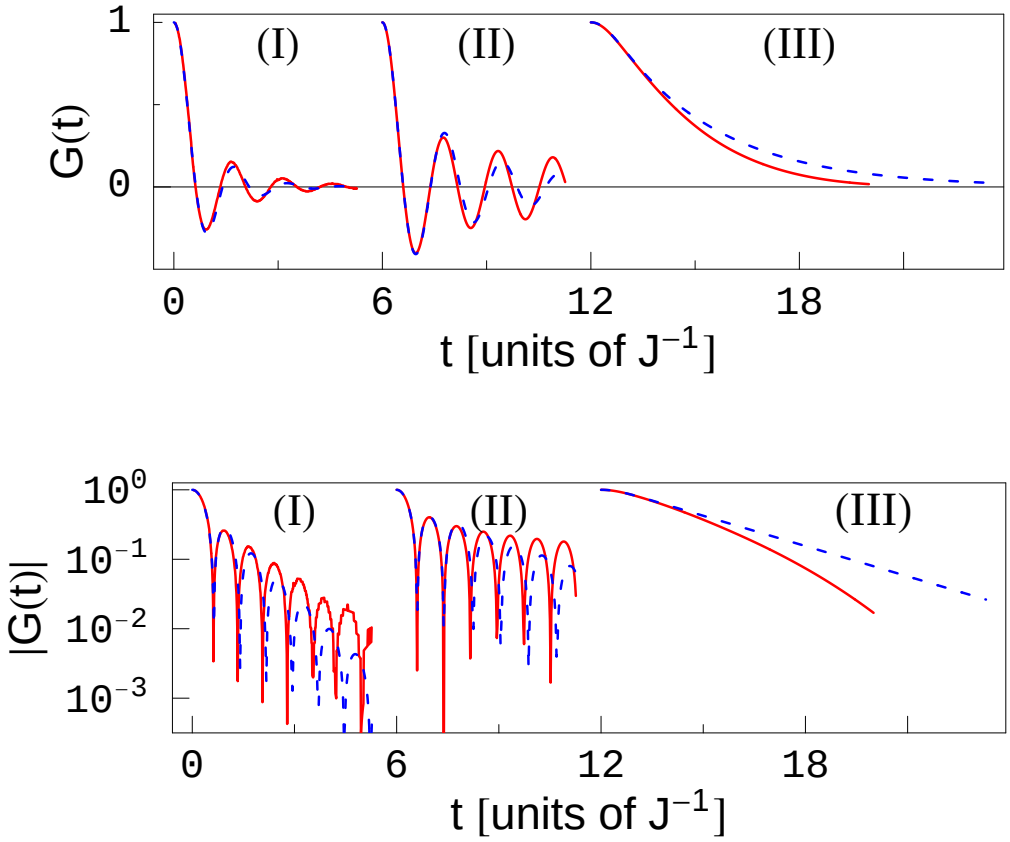

Figure 3.2: Intermediate structure factors for the spin 1/2 XXZ chains. The top and bottom sets of plots contain identical pieces of data presented on direct(non-logarithmic) and on logarithmic scales respectively. The solid red lines represent (I) the numerical result of Fabricius *et al.*[13]; (II) the analytical result given by Eq.(1.14); (III) an unpublished numerical result of K. Fabricius[54] The dashed blue lines represent the solutions of Eq.(3.22). Each of those correlation functions is characterized by the following parameters entering Eqs.(1.1, 1.2): $J^x_{n,n+1} = J^y_{n,n+1} = J$, where J is an auxiliary variable. Other parameters are: (I) $J^z_{n,n+1} = J$, $q = \pi$, any value of μ; (II) $J^z_{n,n+1} = 0$, $q = \pi$, $\mu \to z$; (III) $J^z_{n,n+1} = 0.5J$, $q = 0$, $\mu \to x$. The time origins of plots (II) and (III) are shifted by 6 and 12 time units respectively.

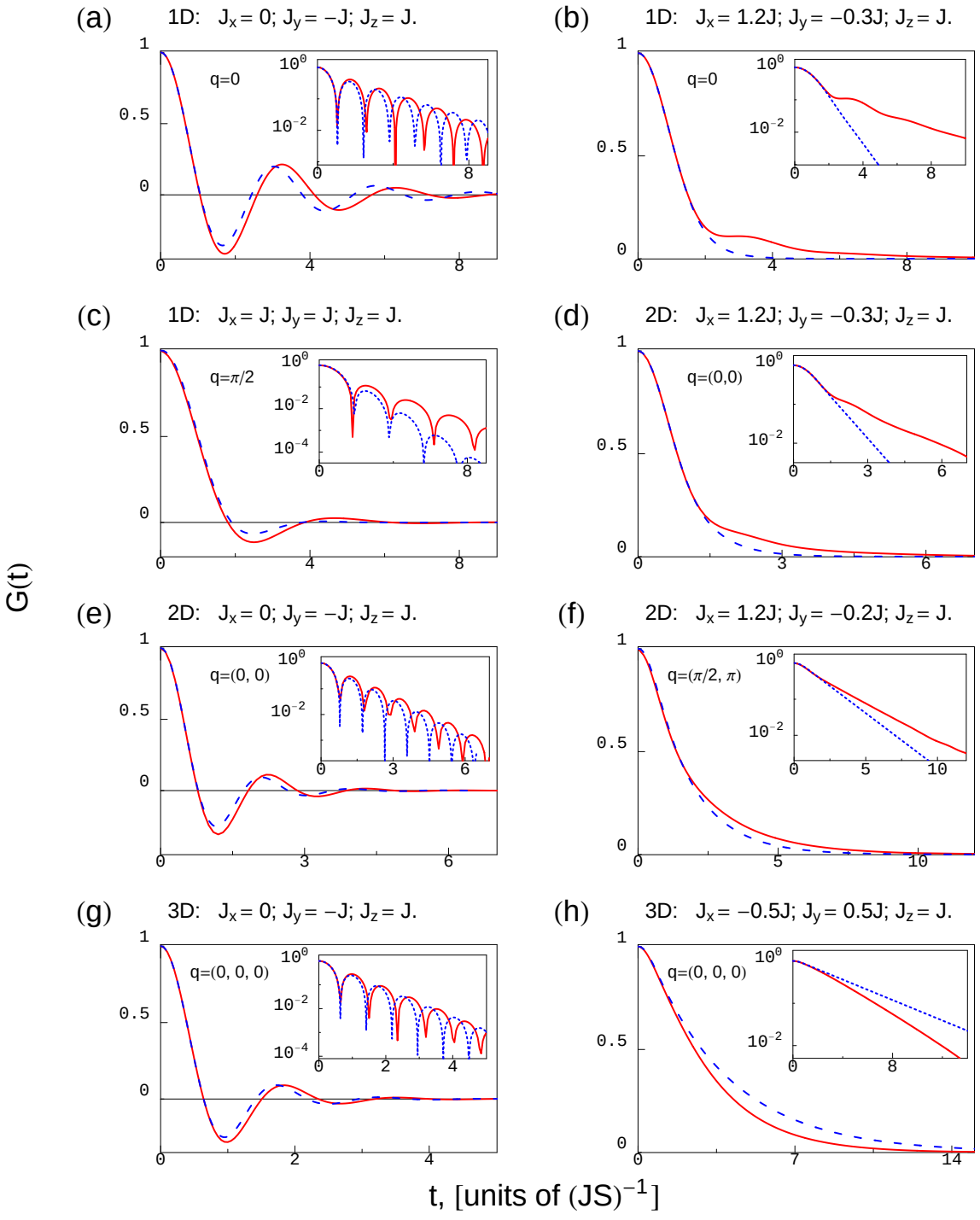

Figure 3.3: Correlation functions of the form (1.1) with the Hamiltonian (1.30) for a 1D chain, 2D square lattice, and 3D cubic lattice of classical spins. The solid red lines represent the results of our simulations. The dashed blue lines represent the solutions of Eq.(3.22).

	Figure 3.1			Figure 3.2		
	[100]	[110]	[111]	(I)	(II)	(III)
$\frac{M_{2\varphi}}{M_2}$	0.22	0.22	0.22	0.5	0.25	5.0
α	0.56	0.43	0.42	1.33	1.86	-0.33

Figure 3.3

	(a)	(b)	(c)	(d)	(e)	(f)	(g)	(h)
$\frac{M_{2\varphi}}{M_2}$	0.25	0.91	1.0	0.91	0.25	1.76	0.25	2.0
α	1.77	-0.086	0.34	-0.24	1.24	-0.46	1.28	-0.72

Table 3.1: The parameters $M_{2\varphi}/M_2$ and α characterizing the approximate calculations presented in Figs. 3.1, 3.2 and 3.3.

The data presented in Figs. 3.1 and 3.3 have already been shown in Figs. 1.2 and 1.4 respectively. The content of Fig. 3.2 is analogous to Fig. 1.3. However, only the situations (I) in each of the two figures are the same.

Situation (II) in Fig. 3.2, actually, corresponds to the analytically solvable limit of Eq.(1.14) — the only limit from Section 1.3 that has not been matched exactly within our approximation scheme.

The situation in Fig. 3.2(III) corresponds to the monotonic regime, which was missing in Fig. 1.3. The numerical result shown in that figure was not exhibited in Section 1.5.2, because that result is not entirely free from finite size effects[54], which prevents us from forming a judgment about its long-time behavior. However, for the purposes of the present Chapter, the difference between our approximation and that numerical result is noticeably greater than the numerical uncertainty associated with finite size effects.

In our calculations, we used a Gaussian form for $\varphi(t)$ with the second moment $M_{2\varphi}$ obtained from Eq.(3.44).

The difference between Eq.(3.44) and the full definition of $M_{2\varphi}$ given by Eqs.(3.29, 3.36) can arise only when spins contributing to the local field (3.37) interact directly with each other.

In the case of free induction decay in CaF_2, the use of Eq.(3.44) instead of the definition (3.29, 3.36) is justified by the fact that the coefficients of the truncated magnetic dipolar interaction (1.29) have both positive and negative signs, which nearly cancels the difference between Eq.(3.44) and the full definition (3.29, 3.36).

For the rest of the situations considered in Section 1.5, Eq.(3.44) is equivalent to the full definition (3.29, 3.36), because for a given lattice site the nearest neighbors creating the local field (3.37) simply do not interact with each other directly.

To compute the values of the parameter α given by Eq.(3.25) we used the values of the theoretical ratios $\frac{M_4}{M_2^2}$ obtained or derived from the following sources: for the free induction

decay in CaF_2 — Ref.[52]; for spin 1/2 chains — Refs.[53] and [10]; and, for the classical spins — from our own simulations.

For the calculation of the free induction decay in CaF_2, it was necessary to use expression (3.38) for the form of $g(t)$. In that case, the product in the RHS of Eq.(3.38) includes an infinite number of cosines, which reflects the infinite range of the magnetic dipolar interaction. Evaluating that product, we individually included 20 cosines with the interaction constants making the largest contribution to M_{2g}, and approximated the product of other cosines by a Gaussian exponent which adds the remaining contribution to M_{2g}.

3.2.4 Summary and discussion

In this Section, we have developed a kinetic model for the approximate calculations of the correlation functions (1.1) The justification of that model is quite conservative, in the sense that the model does not rely on any number extracted from empirical knowledge of the correlation functions (1.1) unless that knowledge comes from analytically solvable limits.

In that sense, the potential of the interpolation approach proposed in Section 1.7 has not yet been fully realized. That approach calls for adjusting an approximation scheme directly to the whole body of empirical knowledge. At present, development of such a scheme is the theoretical project we are pursuing. However, the model presented in this Section can be considered as the first step toward the full realization of that approach, because it can be considered as providing an interpolation between the exact limits of the problem.

In fact, all exact results mentioned in Section 1.3 (with the exception of Eq.(1.14) have been incorporated in the formalism of our model. Based on physical arguments, the mathematical structure of the model extended the above exactly solvable cases in the space of all possible interaction coefficients of the interaction Hamiltonian (1.2). Given also the fact that the values of the first four derivatives of $G(t)$ at $t = 0$ obtained from Eq.(3.22) coincide with the exact theoretical values, it was reasonable to expect that, in most cases, the solution

of Eq.(3.22) approximates the observable part of the correlation functions (1.1) with good accuracy. The accuracy was mainly limited by the adequacy of assumption (3.19).

The numerous tests of our model revealed that, indeed, it provides a consistently good approximation for the correlation functions (1.1). The worst performance of the model is associated with the test shown in Fig.(3.3)(b). However, an important fact about that test is that such a poor performance could be anticipated theoretically as corresponding to the transitional regime between the oscillatory and the monotonic behavior. We strongly suspect that such a regime poses the ultimate challenge to any approximation scheme.

Conceptually, the model presented in this Section falls in line with other approximation methods discussed in Section 1.6. Namely, with this model, we try to approximate the correlation functions (1.1) by using knowledge of the first few exact moments of the true correlation function and also some additional formal manipulations and physical arguments.

However, it is still difficult to compare the present model with other works, because, in several aspects, it certainly stands apart. In particular, none of the alternative theoretical schemes discussed in Section 1.6 has been tested as extensively as this model; no other scheme has matched that many exact limits, and none of those schemes has attempted to consider the case of large non-zero wave vectors in Eq.(1.1) on the same footing as the case of $q = 0$.

Therefore, the definitive comparison of our approximation method with others should be postponed until other methods undergo similar extensive tests. As we have discussed in Section 1.6, the merits of an approximation scheme should not be judged solely on the basis of its performance with respect to the free induction decay experiments in CaF_2[20]. As far as those experiments are concerned the present model appears to be as good as most of others. A more important question is: How will other schemes perform beyond the CaF_2 setup?

It is nevertheless possible to comment on the conceptual similarities and differences be-

tween our model and several of other methods.

The approximation based on our model is formally comparable to the original treatment of Lowe and Norberg [2] (Section 1.6), in the sense that it starts from the Ising-like Hamiltonian, matches the second and the fourth moments, and does not involve adjustments to experimental data. Moreover, the T-criterion for spins 1/2 introduced in this Section is also satisfied in the Lowe and Norberg calculation.

There are, however, four features of our method that distinguish it from the method of Lowe and Norberg. Namely, (i) our method guarantees the correct form of the long-time behavior given by Eqs.(1.24, 1.25); (ii) the model we use is based on physical arguments, which give better control over the calculation; (iii) the mathematical construction of our model matches more exact limits, and, finally, (iv) that mathematical construction appears to be more simple computationally.

The mathematical structure of our approximation scheme can also be compared with that of the memory function approach represented by Eq.(1.33). At first sight, it might seem that the status of function $g(t)$ in Eq.(3.22) is similar to that of the memory function $F(t)$ in Eq.(1.33).

To some extent, the above observation is correct. However, there is an important difference between $g(t)$ and $F(t)$:

The recipe for the functional form of $g(t)$ has been motivated by matching several exact limits in the situations, when, in Eq.(3.22), $\alpha = 0$, and, therefore, function $g(t)$ is, by itself, the solution of the whole problem (i.e. $G(t) = g(t)$).

By contrast, the memory function $F(t)$ can never be equated with a meaningful correlation function. In principle, the form of $F(t)$ can still be adjusted, so that the solution of Eq.(1.33) matches any of the exact limits. However, the resulting form of $F(t)$ will, in general, be very non-intuitive. To the best of our knowledge, the project of matching many exact limits within one general recipe for the form of $F(t)$ has not been attempted so far.

We would like to point out specifically, that the nearly Gaussian form of $g(t)$ comes naturally from the exact limits that have been matched. At the same time, we are not aware of any example in which the Gaussian assumption for $F(t)$ would result in the exact solution of the problem.

The next approximation scheme to be compared with our model is that of Becker, Plefka and Sauermann (BPS)[34]. We have already mentioned in Section 1.6 that those authors have come up with the same integral equation as we did, i.e. Eq.(3.22). However, in Eq.(3.22), they used formulas for $g(t)$ and α that are different from Eqs.(3.38, 3.41, 3.25).

In particular, BPS obtained the value of parameter α not from matching the fourth moment M_4 (as we did) but from a certain manipulations with the interaction coefficients. In comparison with the the BPS recipe, our recipe for determining the values of α is better defined and better generalizable.

The BPS expression for $g(t)$ corresponds to Eq.(3.27), which is to be compared with our final recipe given by Eqs.(3.38, 3.41). It was explained in the discussion following Eq.(3.27) that the recipe for $g(t)$ given by Eq.(3.27) and used by BPS has certain unphysical features, which are eliminated in the final version of our recipe (Eqs.(3.38, 3.41)). That final version also matches more exact limits.

The improvements in our recipes for $g(t)$ and α in comparison with the recipes of BPS became possible because we obtained Eq.(3.22) from a physical model instead of a formal manipulation and thus had a broader picture of that result and were less constrained in our choice of the ingredients entering Eq.(3.22). With the recipes of BPS, Eq.(3.22) could not be applied to many problems beyond the free induction decay in CaF_2. In particular, the scheme of BPS could not be applied to the case of spin 1/2 chains considered in this thesis.

Finally, we shall discuss yet another alternative approximation scheme — the one proposed by Lundin and Makarenko[37],[38].

On the basis of a treatment of the free induction decay problem with the truncated

magnetic dipolar interaction (1.29), the above authors obtained an integral equation which is reminiscent of Eq.(3.22) but with a different integral term:

$$G(t) = \tilde{g}(t) - \tilde{\alpha} M_2 \int_0^t \tilde{g}(t-t') \int_0^{t'} \tilde{g}(t'-t'') G(t'') dt'', \tag{3.51}$$

where the function $\tilde{g}(t)$ and the parameter $\tilde{\alpha}$ are analogous to those that enter Eq.(3.22).

The recipe of Lundin[38] for $\tilde{g}(t)$ and $\tilde{\alpha}$ entering Eq.(3.51) does not match the fourth moment moment of $G(t)$ but can be easily amended to do so. His recipe for $\tilde{g}(t)$ is similar to the one given by Eq.(3.27. That recipe can also be amended to satisfy as many exact limits as our scheme does. It remains then to be seen how well Eq.(3.51) will perform.

Our preference for Eq.(3.22) is mainly related to the fact that we find it difficult to generalize the physical picture underlying Eq.(3.51) beyond the situation considered by Lundin and Makarenko.

References

[1] E. Balcar and S. W. Lovesey, *Theory of Magnetic Neutron and Photon Scattering* (Clarendon, Oxford, 1981).

[2] I. J. Lowe and R. E. Norberg, Phys. Rev. **107**, 46 (1957).

[3] A. Abragam, *Principles of Nuclear Magnetism* (Clarendon Press, Oxford, 1961), Chap. IV.

[4] N. Bloembergen, Physica **15**, 386 (1949).

[5] K. Fabricius and B. M. McCoy, Phys Rev B **57**, 8340 (1998).

[6] B. V. Fine, Phys. Rev. Lett. **79**, 4673 (1997).

[7] G. O. Berim, J. Stolze, H. Leshke, XXth IUPAP International Conference on Statistical Physics, Paris, 1998 (http://www-spht.cea.fr/SPhT/spht/statphys/textes /T1629.html).

[8] B. V. Fine, cond-mat/9911230.

[9] B. V. Fine, cond-mat/9911229.

[10] J. H. Van Vleck, Phys. Rev. **74**, 1168 (1948).

[11] E. Lieb, T. Schultz, and D. Mattis, Ann. Phys. (N.Y.) **16**, 407 (1961).

[12] S. Katsura, Phys. Rev. **127**, 1508 (1962).

[13] K. Fabricius, U. Löw, J. Stolze, Phys. Rev. B **55**, 5833 (1997).

[14] Th. Niemeijer, Physica **36**, 377 (1967).

[15] S. Katsura, T. Horiguchi, and M. Suzuki, Physica **46**, 67 (1970).

[16] P. W. Anderson, P. R. Weiss, Rev. Mod. Phys. **25**, 269 (1953).

[17] J. E. Guley, D. Hone, D. J. Scalapino, B. G. Silbernagel, Phys. Rev. B **1**, 1020 (1970).

[18] J. E. Guley, B. G. Silbernagel, V. Jaccarino, J. Appl. Phys. **40**, 1318, (1969).

[19] B. Cowan, *Nuclear Magnetic Resonance and Relaxation* (Cambridge University Press, 1997)

[20] M. Engelsberg and I. J. Lowe, Phys. Rev. B **10**, 822 (1974).

[21] G. Müller, Phys. Rev. Lett. **60**, 2785 (1988).

[22] R. W. Gerling and D. P. Landau, Phys. Rev. Lett. **63**, 812 (1989); G. Müller, Phys. Rev. Lett. **63**, 813 (1989); R. W. Gerling and D. P. Landau, Phys. Rev. B **42**, 8214 (1990).

[23] A. Bonfim and O. F. Reiter, Phys. Rev. Lett. **69**, 367 (1992).

[24] F. Bloch, Phys. Rev. **70**, 460 (1946).

[25] N. Bloembergen, E. M. Purcell, and R. V. Pound, Phys. Rev. **73**, 679 (1948).

[26] J. A. Tjon, Phys. Rev. **143**, 259 (1966).

[27] G. W. Parker and F. Lado, Phys. Rev. B **8**, 3081 (1973).

[28] P. Borckmans and D. Walgraef, Phys. Rev. **167**, 282 (1968).

[29] P. Borckmans and D. Walgraef, Phys. Rev. Lett. **21**, 1516 (1968).

[30] I. Prigogine, *Non-Equilibrium Statistical Mechanics* (Interscience Publishers, New York 1962).

[31] P. Résibois and M. De Leener, Phys. Rev. **151**, 305 (1966).

[32] M. Engelsberg and N.-C. Chao, Phys. Rev. B **12**, 5043 (1975).

[33] J. Jensen, Phys. Rev. B **52**, 9611 (1995).

[34] K. W. Becker, T. Plefka and G. Sauermann, J. Phys. C **9**, 4041 (1976).

[35] J. P. Hansen and I. R. McDonald, *Theory of simple liquids* (Academic Press, London, 1986).

[36] A. A. Lundin and B. N. Provotorov, Zh. Eksp. Teor. Fiz. **70**, 2201 (1976) [Sov. Phys. JETP **43**, 1149 (1976)].

[37] A. A. Lundin and A. V. Makarenko, Zh. Eksp. Teor. Fiz. **87**, 999 (1984) [Sov. Phys. JETP **60**, 570 (1984)].

[38] A. A. Lundin, Zh. Eksp. Teor. Fiz. **102**, 352 (1992) [Sov. Phys. JETP **75**, 187 (1992)].

[39] R. N. Shakhmuratov, J. Phys. Condens. Matter **3**, 8683 (1991).

[40] Such a comment is especially relevant in the light of recent controversy related to the investigations of microscopic chaos by P. Gaspard *et al*, Nature **394**, 865 (1998). See: P. Grassberger and T. Schreiber, cond-mat/9906311; C. P. Dettmann, E. G. D. Cohen, H. van Beijeren, chao-dyn/9904041.

[41] P. Gaspard, *Chaos, scattering and statistical mechanics* (Cambridge University Press, Cambridge, 1998).

[42] N. S. Krylov, *Works on the Foundations of Statistical Physics*, (Princeton University Press, Princeton, 1979)

[43] L. Onsager, Phys. Rev. **37**, 405 (1931); **38**, 2265 (1931).

[44] R. Kubo, M. Toda, N. Hashitsume, *Statistical Physics II: Nonequilibrium Statistical Mechanics*, 2nd ed. (Springer-Verlag, Berlin, 1991).

[45] The possibility of such a transformation is the consequence of the fact that the origin of the time axis can be arbitrarily shifted by some value t_0 without changing the correlation function of the equilibrium fluctuations. The transformation proceeds as follows:

$$\begin{aligned}\left\langle \tfrac{d^2X(t)}{dt^2} X(0) \right\rangle &= \left\langle \tfrac{d^2X(t+t_0)}{dt^2} X(t_0) \right\rangle \\ &= \left\langle \tfrac{d^2X(t+t_0)}{dt_0^2} X(t_0) \right\rangle \\ &= -\left\langle \tfrac{dX(t+t_0)}{dt_0} \tfrac{dX(t_0)}{dt_0} \right\rangle + \tfrac{d}{dt_0} \left\langle \tfrac{dX(t+t_0)}{dt_0} X(t_0) \right\rangle ,\end{aligned}$$

In equilibrium, the second term obtained above must be equal to zero, and the first term is obviously equal to $-\langle \dot{X}(t)\dot{X}(0)\rangle$.

[46] A. Einstein, Ann. Physik **17**, 549 (1905).

[47] The NMR technique known as "magic echo" actually demonstrates that the spin dynamics can be experimentally reversed well into the regime describable by Eq.(1.25), and the initial value of $G(t)$ can be recovered. See W.-K. Rhim, A. Pines, J. S. Waugh, Phys. Rev. B **3**, 684 (1971); and also Chapter 8 of Ref.[48].

[48] C. P. Slichter, *Principles of Magnetic Resonance*, 3rd ed. (Springer, Berlin, 1990).

[49] E.M. Lifshits and L.P. Pitaevskii, *Physical Kinetics* (Pergamon Press, Oxford, 1981).

[50] P. M. Morse and H. Feshbach, *Methods of Theoretical Physics* (McGraw-Hill, New York, 1953).

[51] H. S. Gutowsky, D. W. McCall and C. P. Slichter, J. Chem. Phys. **21**, 279 (1953).

[52] G. W. Canters and C. S. Johnson, Jr., J. Mag. Resonance 6, 1 (1972).

[53] M. Böhm and H. Leschke, J. Phys. A, **25**, 1043 (1992).

[54] This piece of numerical data has been provided to the author by K. Fabricius. It represents the result of numerical diagonalization for the chain containing 16 spins 1/2. At the end of the time interval shown in Fig. 3.2, the above result deviates slightly from the numerical result for the chain of 14 spins, which implies the presence of small finite size effects.

Vita

Boris Veniaminovich Fine was born in Chelyabinsk, Russia, on February 8, 1971. He graduated from high school #31 in Chelyabinsk. In 1987, Mr. Fine enrolled in the Physics Department at Tomsk State University. In 1989, he was transferred to the Department of General and Applied Physics at Moscow Institute of Physics and Technology (MIPT). Mr. Fine graduated, Summa Cum Laude, from MIPT in July of 1994 with an M.S. in Physics. In August of 1994, he enrolled in the Physics Ph.D. program at the University of Arizona, Tucson.

Mr. Fine entered the Physics Ph.D. program at University of Illinois at Urbana-Champaign in January 1995, after being transferred from the University of Arizona. From January 1995 to August 2000, Mr. Fine was a Teaching Assistant for the following courses: Physics 111, 225, 415, 417, 489 and 498MMP. Alternating with the teaching assistantship, he held a Research Assistant position with Prof. A.J. Leggett.

In 1997, Mr. Fine received the Prize for the best student poster presentation at the 25th Midwest Solid State Theory Symposium at Argonne. In 1998, he was a recipient of the Jordan Asketh Fellowship from the Physics Department of the University of Illinois at Urbana-Champaign. Mr. Fine was also awarded the Harry Drickamer Research Fellowship from the University of Illinois for the academic year 1998-99.